



Spatial Patterns in Meta-Food-Webs: A Colonization-Extinction Model Approach

Von der Fakultät für Mathematik und Naturwissenschaften der
Carl von Ossietzky Universität Oldenburg zur Erlangung des
Grades und Titels eines

Doktors der Naturwissenschaften (Dr. rer. nat.)

angenommene Dissertation

von Herrn Kai Uwe von Prillwitz
geboren am 03.11.1989 in Kevelaer

Erstgutachter: Prof. Dr. Bernd Blasius
Zweitgutachter: Prof. Dr. Thilo Gross
Tag der Disputation: 09.01.2020

Zusammenfassung

Obwohl ökologische Gemeinschaften von Natur aus im physikalischen Raum existieren, vernachlässigten erste ökologische Modelle diese räumliche Natur. Einige Resultate dieser Modelle legen nahe, dass Artengemeinschaften nur aus wenigen Arten bestehen und Nahrungsnetze so simpel wie möglich sein sollten. Dies steht im Widerspruch zum großen Artenreichtum und zu komplexen Nahrungsnetzen, die in der Realität beobachtet werden können. Ökologische Modelle in einen räumlichen Kontext einzubetten, kann dabei helfen diesen Widerspruch aufzulösen. Das heißt, dass die räumliche Ausbreitung von Artengemeinschaften zum Beispiel dazu führen kann, dass mehr Arten koexistieren können, als in einem nicht-räumlichen Modell. Dazu reicht es grundsätzlich aus, den Raum nur sehr indirekt in ökologische Modelle einzubeziehen und dabei die tatsächliche Struktur des Raumes beziehungsweise die Anordnung von Teilhabitaten komplett zu vernachlässigen. Diese räumliche Struktur kann Modellresultate jedoch signifikant beeinflussen und im Extremfall sogar über das Überleben oder Aussterben einer Art entscheiden. Gerade im Kontext der fortschreitenden, menschenverursachten Zerstörung und Fragmentierung von Lebensräumen, gewinnt die explizite räumliche Struktur der verbleibenden Lebensräume an Bedeutung.

Von einem rein akademischen Standpunkt aus betrachtet, kann die Einbeziehung der räumlichen Struktur nicht nur dazu verwendet werden ihren Einfluss auf Modellergebnisse zu untersuchen, sondern diese Ergebnisse können auch räumlich aufgelöst werden. Letzteres heißt, dass räumliche Muster ökologischer Größen, wie etwa der Länge von Nahrungsketten oder der Anwesenheit einzelner Arten, beschrieben werden können. In dieser Arbeit geht es genau um diese doppelte Rolle der räumlichen Struktur in ökologischen Modellen. Dazu kombinieren wir ein bestehendes Modell zur Beschreibung von Meta-Nahrungsnetzen mit expliziten, räumlichen Habitaten, untersuchen räumliche Muster von Nahrungskettenlängen und der Präsenz einzelner Arten, und erklären die beobachteten Muster mithilfe der räumlichen Habitatstruktur.

Das verwendete Meta-Nahrungsnetzmodell basiert auf dem Zusammenspiel von Kolonisierungen und dem lokalen Aussterben der Arten. Lokal müssen die Arten zudem Einschränkungen durch ihre trophischen Beziehungen genügen. Im Detail bedeutet dies, dass ein Räuber zum Überleben die Anwesenheit einer passenden Beuteart benötigt, und dass nur ein Räuber pro Beuteart überleben kann (Konkurrenzausschlussprinzip zwischen verschiedenen Räubern für eine gemeinsame Beute). Die Dynamik des Modells kann sowohl durch (näherungsweise) Differentialgleichungen sowie durch stochastische Simulationen beschrieben und gelöst

werden. Wir gelangen in dieser Arbeit zu den folgenden drei Hauptresultaten:

1. Wenn das Gesamthabitat eine regelmäßige, gitterähnliche Struktur aufweist, und das zugrundeliegende Nahrungsnetz eine einfache Nahrungskette ist, ist die erwartete Nahrungskettenlänge im Zentrum des Habitats maximal und nimmt zum Rand hin ab, obwohl das Modell keine anderen, räumlich variierenden Umweltfaktoren miteinbezieht. Das Resultat kann als Erweiterung des sogenannten *mid-domain effects* für den Artenreichtum zu einem *mid-domain effect* für die Nahrungskettenlänge betrachtet werden.
2. Wir verallgemeinern das obige Resultat auf Habitats, die durch unregelmäßige Zufallsnetzwerke beschrieben werden und beobachten, dass die Nahrungskettenlänge mit der *Zentralität* der Habitatfragmente zunimmt. Das Konzept der Zentralität dient grundsätzlich dazu die ‘Wichtigkeit’ oder ‘Verbundenheit’ eines Netzwerkknotens (in unserem Kontext eines Habitatfragments) zu charakterisieren, und zu diesem Zweck existiert eine Vielzahl an sogenannten *Zentralitätsmaßen*. Wir führen ein weiteres Zentralitätsmaß ein, das in unseren Studien eine stärkere Korrelation zur Nahrungskettenlänge aufweist als alle anderen ebenfalls betrachteten Zentralitätsmaße.
3. Die Konkurrenz zwischen einem spezialisierten Räuber und mehreren omnivoren Räufern für teilweise gemeinsame Beutearten führt zu einer Aufteilung des Habitats in räumliche Nischen. In einem regelmäßigen, gitterähnlichen Habitat ist der spezialisierte Räuber im Zentrum des Habitats besonders präsent, während die omnivoren Räuber sukzessive zu den Rändern gedrängt werden. Wir zeigen, dass die Entstehung dieser räumlichen Nischen auch für Arten in einer reinen Konkurrenzgemeinschaft stattfindet.

All diese Resultate haben gemeinsam, dass sie allein durch das Zusammenspiel der räumlichen Dynamik, in einem beschränkten Habitat mit expliziter räumlicher Struktur, und der Interaktion der Arten untereinander entstehen. Dies steht im Kontrast zu vielen anderen ökologischen Studien, die ökologische Größen (und deren räumliche Muster) wie etwa Populationsgrößen, Artenreichtum und Nahrungskettenlänge durch andere Umweltfaktoren (und deren räumliche Variation) wie etwa Temperatur, Lichteinfall und Ressourcenangebot erklären. Unsere Resultate verdeutlichen, dass, unabhängig von solchen (variierenden) Umwelteinflüssen, allein die räumliche Position innerhalb eines größeren Habitats ein bestimmender Faktor für solche ökologischen Größen sein kann.

Abstract

Species communities are naturally embedded into space, yet early ecological models describing species dynamics neglect this spatial context. Results of these models indicate that species communities and food webs should be small and simple. This is in contrast to the observation that real communities and food webs are often large and complex. Incorporating space into ecological models can help resolve this contradiction. For example, in a spatial model species can regionally coexist even if they competitively exclude each other locally, which would prevent their coexistence in a non-spatial model. Early models of spatial ecology incorporated space in an implicit way, meaning that habitats had no explicit spatial structure. This spatial structure can, however, influence model results, in the extreme case deciding over the persistence of a species, and is particularly interesting in the context of ongoing human-caused habitat destruction and fragmentation.

More theoretically, when including the explicit spatial structure in an ecological model one can not only investigate how the spatial structure influences model results, but one can also spatially resolve these results and thus investigate emergent spatial patterns of ecological quantities like food chain length or the presence of individual species. It is exactly this twofold role of the spatial structure that we are concerned with in this thesis. More specifically, we here combine an established meta-food-web model with spatially explicit habitat networks, investigate spatial patterns of food chain length as well as of individual species, and explain the observed patterns by the spatial structure of the habitat.

The used meta-food-web model is based on colonization-extinction dynamics, and the species are locally restricted by their trophic relations. Precisely, on a given habitat patch a predator needs a prey to persist and only one predator can persist on one prey. The latter amounts to the local application of the competitive exclusion principle between different predators for a common prey. The model dynamics can be described and solved either via (approximate) differential equations or stochastic simulations. Our three main results are as follows:

1. On regular, lattice-like habitats, and when the underlying food web is a simple chain, the expected food chain length is maximal in the center of the habitat and decreases towards the boundaries even in the absence of environmental gradients. This amounts to the extension of the *mid-domain effect* for species richness to a mid-domain effect for food chain length.
2. We generalize this result to non-regular, random habitat networks and find that food chain length increases with the *centrality* of a patch. The concept

of centrality is generally used to describe in some sense the ‘importance’ or ‘connectedness’ of a patch within a network, and there exist many different so-called *centrality measures*. We introduce a new centrality measure and find that in our study this new measure is more strongly correlated to food chain length than all other considered centrality measures.

3. We find that the competition for common prey between a specialist predator and several omnivores leads to a spatial niche partitioning between these species. The specialist predator dominates the mid-domain of a regular, lattice-like habitat while more omnivorous species are driven successively towards the boundary. We show that this spatial niche partitioning can also be found for species in a purely competitive community.

All these results have in common that they are solely caused by the interplay between the spatial dynamics on structured, constrained habitats and the species interactions. This is in contrast to many other ecological studies that consider environmental factors like temperature, light, and resource availability (and their spatial variations) as determinants of (spatial patterns of) ecological quantities like species abundances, species richness, or food chain length. Our results demonstrate that even in the absence of spatially varying environmental conditions the mere position of a patch within a larger habitat might be an important determinant of such ecological quantities on the given patch.

About this thesis

The main part of this thesis (Part II) consists of three research chapters that are written in the form of scientific articles. The first research chapter (Chapter 5: Mid-domain effect for food chain length) was co-authored by my supervisor Prof. Dr. Bernd Blasius, and, at the time of submitting this thesis, has been submitted to a scientific journal. Concerning the contributions to Chapter 5: Bernd Blasius conceived the study, I implemented the model and performed the study, and both of us prepared the manuscript. For the other research chapters and the rest of the thesis no co-authors were involved. The reason for using *we* instead of *I* in these parts of the thesis as well is to include the reader.

Contents

I	Introduction	5
1	Background, scope, and outline	7
2	Networks	8
2.1	Introduction to network theory	9
2.1.1	Definition and basics	9
2.1.2	Representations of networks	10
2.1.3	Degree distribution and other network properties	12
2.2	Spatial networks	14
2.2.1	Lattices	14
2.2.2	Random geometric graphs (RGGs)	16
2.2.3	Erdős-Rényi random graphs (ER graphs)	17
2.2.4	Scale free graphs (SF graphs)	17
2.3	Food webs	18
3	From metapopulations to meta-food-webs	21
3.1	Levins' metapopulation approach	21
3.2	Tilman's competing metacommunities	23
3.3	The meta-food-web model by Pillai et al	24
3.3.1	General model	24
3.3.2	Food chains	25
3.3.3	Omnivory	27
3.4	Making the models spatially explicit	28
3.4.1	Generalizing the differential equations	28
3.4.2	Solving the differential equations	29
3.4.3	Stochastic approach via Gillespie algorithm	30
3.5	Equivalence to an epidemic model	32
4	Objectives of research chapters	35

II	Research Chapters	37
5	Mid-domain effect for food chain length	39
5.1	Introduction	40
5.2	Methods	42
5.3	Results	44
5.4	Discussion	52
5.A	Appendix 1: Snapshot of a stochastic simulation in a one-dimensional habitat	57
5.B	Appendix 2: Food chain length and edge length vs colonization range	58
6	Food chain length and the SIS centrality	59
6.1	Introduction	60
6.2	Methods	61
6.3	The SIS centrality	65
6.4	Predicting food chain length	66
6.5	Discussion	74
6.A	Appendix 1: Computational effort for calculating centrality measures	77
6.B	Appendix 2: Dependence of fit parameters on graph type and connectivity	78
7	Spatial niche partitioning in food webs	79
7.1	Introduction	80
7.2	Methods	81
7.3	Results	84
7.4	Discussion	94
III	Final discussion	99
8	Joint discussion of research chapters	101
8.1	Summary and common message of research chapters	101
8.2	Simplifying model assumptions	102

<i>CONTENTS</i>	3
9 Future work	105
9.1 The fourth research chapter	105
9.2 Focusing on purely competitive communities	106
Appendix	107
A Equations for general meta-food-webs	109

Part I
Introduction

1 Background, scope, and outline

One of the prime goals of ecology is to understand the assembly and persistence of complex ecosystems. In contrast to the high biodiversity of many real systems, early ecological principles seem to suggest rather limited diversity. The *competitive exclusion principle*, for example, states that two directly competing species cannot coexist (Grinnell, 1904; Volterra, 1931; Lotka, 1932; Gause, 1932, 1934; Hardin, 1960). Competitive exclusion can be avoided if species have, for example, different limiting resources, feeding habits, or abiotic preferences, that is, if they occupy different *ecological niches* (Grinnell, 1917; Elton, 1927; Hutchinson, 1957; MacArthur and Levins, 1967; Leibold, 1995; Pocheville, 2015). Alternatively, *neutral theory* can explain the assembly of diverse communities by dispersal even if species are competitively equivalent (Hubbell, 2001; Bell, 2001). Similarly, colonization-extinction dynamics of a metacommunity can lead to the regional coexistence of an in principle arbitrary number of competitors, if weaker competitors are better colonizers (Tilman, 1994). Thus, spatial dynamics are likely to play a crucial role in the assembly and persistence of diverse communities. For this, a habitat does not need to be spatially heterogeneous, favoring different species at different locations, but the mere embedding of the system in a spatial context, combined with simple spatial dynamics, is sufficient.

A similar story can be told about trophically interacting communities. Again, early theory predicts that small food webs with few and weak interactions should be the most stable ones (Gardner and Ashby, 1970; May, 1972, 1973), while in reality large and complex food webs are observed (Warren, 1989; Martinez, 1991; Polis, 1991; Havens, 1992; Goldwasser and Roughgarden, 1993). One part of the solution to this apparent contradiction is again to incorporate space into food web models. Spatial dynamics can, for example, have stabilizing effects on predator-prey interactions (Hassell et al., 1991; de Roos et al., 1998; Holt, 2002; McCann et al., 2005), lead to the emergence of complex food webs on a regional scale even if locally only food chains are allowed (Pillai et al., 2010, 2011), and promote the persistence of complex food webs (Gravel et al., 2011a; Mougi and Kondoh, 2015).

Many spatial models, in particular the metacommunity and meta-food-web models by Tilman (1994) and Pillai et al. (2010), do not require an explicit spatial structure. In these models it is sufficient that space is incorporated via a habitat that is divided into many patches all of which are connected to each other. In reality, however, habitats always have an explicit spatial structure,

and there are good reasons to take this structure into account. For example, when working on biodiversity conservation strategies one is faced not only with habitat destruction but also with ongoing habitat fragmentation caused by deforestation, agricultural use, urbanization, road constructions, and other anthropogenic influences (Skole and Tucker, 1993; Vitousek et al., 1997; Broadbent et al., 2008). For finding proper conservation strategies it is thus necessary to investigate the effects of this fragmentation (Saunders et al., 1991; Komonen et al., 2000; Hiebeler, 2000; Fahrig, 2003; Liao et al., 2017b).

From a more theoretical point of view, incorporating the explicit spatial structure into ecological models can be important for two reasons. First, the spatial structure can affect the results of model dynamics, for example food chain length results in a meta-food-web model, and second, the structure allows to spatially resolve these results and thus make spatial patterns visible. In combination, these two aspects mean that by using spatially explicit models one can investigate the effects of the spatial structure on resulting spatial patterns of interesting ecological quantities. This is exactly the scope of this thesis. More precisely, in this thesis we model the dynamics of spatially explicit meta-food-webs in the food web framework by Pillai et al. (2010), look for spatial patterns of food chain length and distributions of individual species, and link these patterns to the spatial structure of the habitat.

The rest of the thesis is structured as follows: Since both food webs and spatially explicit habitats can be represented as networks, we begin with an introduction to network theory in Chapter 2. In Chapter 3 we sketch the development from the metapopulation concept by Levins (1969) to the meta-food-web model by Pillai et al. (2010) and show how to implement spatial networks into these models. In Chapter 4, at the end of the introductory Part I, we briefly foreshadow the research chapters and explain how they are related to each other. Part II is the main body of this thesis and consists of the three research chapters: *Mid-domain effect for food chain length* (Chapter 5), *Food chain length and the SIS centrality* (Chapter 6), and *Spatial niche partitioning in food webs* (Chapter 7). In Part III we conclude the thesis with a final discussion bringing together the results of all research chapters.

2 Networks

In this thesis we consider the spatial dynamics of species forming a food web. Both space (habitats) and food webs can be represented as networks, thus sharing the same theoretical framework. As a consequence, understanding the basics of network theory is helpful for understanding this thesis. But also beyond this thesis, networks are ubiquitous in science and in the real world. Examples of networks, or where networks can be applied, are the internet, social networks, protein interaction networks, electrical power grids, transportation networks, disease spreading, and brain modelling, to name only a few. Studying networks is thus interesting from a more general point of view and being able to work with networks can open access to many applications.

2.1 Introduction to network theory

Here we introduce some basic concepts and terminology of network theory that are used throughout the thesis. Since the food webs that we consider in this thesis are rather small, the theory is mainly required for the spatial (habitat) networks. Additional concepts are introduced when needed. Recommendable books for further reading into the theory of networks and its applications are *Networks: An Introduction* by Newman (2010) and *Network Science* by Barabási (2016). Large parts of this introduction are based on the first book.

Note that we sometimes also refer to networks as *graphs*. While the two terms are often used interchangeably, the term ‘graph’ actually refers to the mathematical concept while the term ‘network’ is typically used when graphs are applied to real world systems.

2.1.1 Definition and basics

A network consists of *nodes* (or *vertices*) representing certain units and *links* (or *edges*) indicating possible interaction between pairs of nodes. In a food web, for example, the nodes represent species and the links encode the feeding relations between them, thus telling us who eats whom. In a food web links are typically *directed* since one species is the predator and the other one is the prey. If both species can prey on each other, two oppositely directed links can be placed between them. If the interaction between the

nodes is symmetric, an *undirected* link is used. In principle it is also possible to have multiple undirected links between two nodes, either indicating different types of interaction, or for a more convenient mathematical treatment of certain network models. If a network has only (un)directed links we call the whole network (un)directed. In an undirected network we also refer to two connected nodes as *neighbours*. So-called *self links* indicate the possibility of a node affecting itself. In our example of a food web a self link represents *cannibalism*. Finally, one distinguishes between *weighted* and *unweighted* networks. In an unweighted network all links have the same strength (which may not be specified at all or simply be set to unity) while in weighted networks different links may have different strengths. **In this thesis we consider only unweighted networks without self links or multiple links. Food webs are directed while spatial networks are undirected.** In the following we typically denote the number of nodes of a network by N .

2.1.2 Representations of networks

Fig. 2.1 (left) shows a graphical visualization of a simple undirected, unweighted network. While such a graphical visualization may be the most natural representation of a network, it is not very helpful from a mathematical point of view or when we want to use the network in a computer program. One way to formally describe a network is to write down its *adjacency matrix*. The adjacency matrix is an $N \times N$ square matrix whose elements encode the links between the nodes. If there is no link from node i to node j then $A_{ij} = 0$. In an unweighted network the presence of a link is indicated by $A_{ij} = 1$. Other values of A_{ij} may be used to indicate weights or multiple links from i to j . The adjacency matrix of an undirected network is symmetric, that is, $A_{ij} = A_{ji}$. For a network without self links all diagonal elements satisfy $A_{ii} = 0$. The adjacency matrix of the network from Fig. 2.1 reads

$$A = \begin{pmatrix} 0 & 1 & 1 & 0 & 1 \\ 1 & 0 & 0 & 0 & 1 \\ 1 & 0 & 0 & 0 & 1 \\ 0 & 0 & 0 & 0 & 1 \\ 1 & 1 & 1 & 1 & 0 \end{pmatrix}. \quad (2.1)$$

Adjacency matrices are easy to implement in a computer program and, amongst others, tasks like checking if two nodes are connected as well as adding or removing a link can be performed quickly on adjacency matrices.

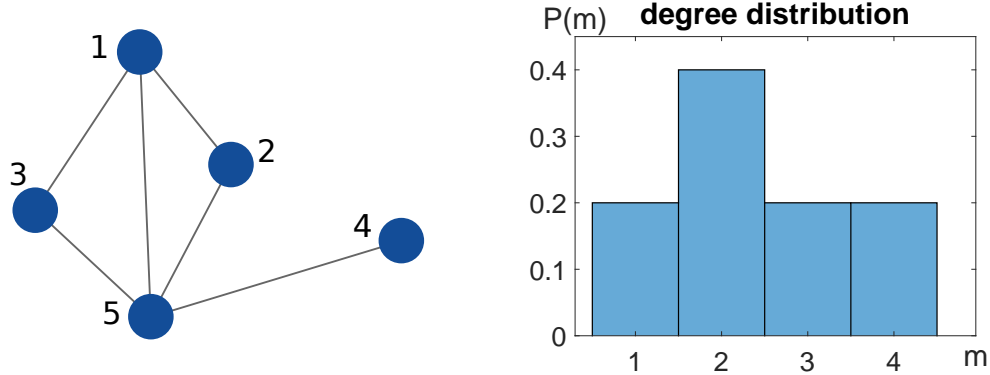


Figure 2.1: **Left:** visualization of a simple undirected, unweighted network consisting of $N = 5$ nodes. **Right:** corresponding degree distribution showing the frequencies, or empirical probabilities, $P(m)$, of all occurring degrees, m , in the network.

Some other tasks, however, can be performed faster using other representations of the network. For example, finding all neighbours of a node requires checking all matrix elements in one row or column. In addition, if a network is sparse, that is, if it has a rather small number of realized links compared to all possible links, the adjacency matrix consists mainly of zeros, meaning that it occupies unnecessarily much memory on a computer. As a solution to this latter problem many programming languages offer sparse matrix representations that require much less memory.

An alternative representation of a network is the *adjacency list*. For each node i the adjacency list contains all neighbours j of i . For a directed network one can define two lists by using either all outgoing links from node i or all ingoing links into node i . For the network from Fig. 2.1 the adjacency list reads,

node	1	2	3	4	5
neighbours	2, 3, 5	1, 5	1, 5	5	1, 2, 3, 4

We also write it more compactly as $E = \{[2, 3, 5], [1, 5], [1, 5], [5], [1, 2, 3, 4]\}$, where the i_{th} element of the outer list $\{\cdot\}$ is the list of all neighbours of node i . Tasks like finding all neighbours of a node can be achieved much faster when using an adjacency list compared to an adjacency matrix, since with an adjacency list one simply has to read the part of the list corresponding to the node of interest. Other tasks, like checking if two nodes share a link, require more time. For sparse networks the adjacency list requires much less

memory than the adjacency matrix. The choice between adjacency matrix and adjacency list should thus be made depending on the size and ‘sparseness’ of the network as well as on the tasks that one wants to perform on the network.

2.1.3 Degree distribution and other network properties

The number of neighbours of a node is called its *degree*, m . The degree can be considered a simple measure for the ‘connectedness’ of the node within the network. For directed networks one can define both an *in-degree* and an *out-degree*. In a food web in-degree and out-degree of a species correspond to the number of its prey and predator species, respectively.

In particular when dealing with large networks, nodes are often grouped according to their degree and the whole network is then described by its *degree distribution*. Formally, the degree distribution is the distribution of frequencies, or empirical probabilities, $P(m)$, of all degrees in the network. As an example, the histogram in the right plot of Fig. 2.1 shows the degree distribution of the simple network from the left plot in the same figure. One of five nodes has degree $m = 1$, meaning that degree 1 occurs with frequency $P(1) = 0.2$. The same is true for degrees $m = 3$ and $m = 4$. Degree $m = 2$ appears twice, resulting in the frequency $P(2) = 0.4$. For some types of (large) random networks, the networks happen to have mathematically well known degree distributions, for example a Poisson distribution.

One advantage of describing a large network by its degree distribution is that this description is much more compact (and thus less memory intensive) than using a description of the full network, for example via its adjacency matrix. The degree distribution also makes some structure of the network visible that one may not be able to see when looking at a graphical visualization of the network or at its adjacency matrix. Even though the degree distribution does not uniquely identify a network, networks with the same, or similar, degree distribution are often also similar with respect to other properties. This is, however, not always the case, as we see in Section 2.2 (comparison between RGGs and ER graphs). Since the degree distribution does not tell us which node connects to which other nodes a lot of the structure of the network may be lost. Properties that are not captured by the degree distribution are for example *degree correlations*, *network diameter*, and *component* structure.

Degree correlations describe the property that nodes with large (small) degree tend to have neighbours that have themselves large (small) de-

gree. This can happen when the links are not distributed entirely at random between the nodes.

Network diameter: A *path* between two nodes X and Y is a connected sequence of links with the first link starting at node X and the last link ending at node Y . The number of links lying on the path is the corresponding *path length*. There may be many paths with different path lengths between two nodes. One can define the *distance* between two nodes as the length of the shortest path between the nodes. The network diameter, D , is then the largest distance, that is, the longest shortest path in the network. The diameter of the network from Fig. 2.1 is $D = 2$, which is the shortest path length between nodes 1, 2, or 3 and node 4 as well as between nodes 2 and 3. The network diameter typically increases with the network size, N . Many network models and many real networks show a scaling behaviour like $D \sim \log N$, meaning that even in very large networks distances between any two nodes are extremely small. This property is characteristic for so-called *small-world networks*. For example, social networks typically show the small-world property, indicating that everyone knows everyone via a small number of acquaintances.

A component of a network is a maximal set of connected nodes. This means that there exists a path between any two nodes of the component and that there exists no path between any node from within the component to any node not belonging to the component. A node with degree $m = 0$ cannot belong to any larger component and is thus a component for itself. While the existence of these single-node components can be identified by looking at the degree distribution, the degree distribution contains no information on the structure of larger components. Two nodes of degree $m = 1$, for example, could form a small two-node component but they could also be part of a larger component. In general, many networks consist of several components, but in the research chapters of this thesis we only consider networks that consist of a single component. For food webs this makes sense since species that are not connected to the main web would most likely not be considered as being part of that web at all. For our spatial networks this means that they describe a single (potentially very large) habitat without isolated areas.

2.2 Spatial networks

In the literature the term ‘spatial network’ is often used to refer to networks that are embedded in (often two-dimensional) Euclidean space. This means that patches have coordinates and that links are (much) more likely to occur between patches that are closer together in terms of their Euclidean distance (Barthélemy, 2011; Antonioni and Tomassini, 2012; Barter and Gross, 2017). Here, we explicitly refer to such networks as *spatially embedded* and more generally use the term ‘spatial network’ to refer to any network that we interpret to represent a habitat consisting of *patches* (the nodes) between which species can disperse (along the links between nodes).

Spatially embedded networks are, amongst others, characterized by long paths between patches, which means that they are not small-world but rather large-world networks. We consider spatially embedded networks as more realistic to describe habitats with (natural) species dispersal. Networks without spatial embedding are mainly interesting from a theoretical point of view and for the purpose of generality. When necessary, we will always specify whether or not a spatial network is spatially embedded.

Note that we stated before that the spatial networks we consider here are unweighted, undirected and without self links or multiple links. These properties are not necessarily true for all networks describing a habitat. The undirectedness, for example, implies symmetric dispersal between patches, which may be unsuitable for networks representing, for example, riverine landscapes. Similarly, it may be more realistic to use weighted networks since, assuming a spatial embedding, the rate of dispersal between patches might depend on their distance.

Overall, we consider four different types of spatial networks in this thesis, two with, and two without spatial embedding. The four types are introduced below and an example of each network type is shown in Fig. 2.2.

2.2.1 Lattices

A d -dimensional lattice is a network of regularly arranged patches placed in d -dimensional space, for example on the integer coordinates of a d -dimensional coordinate system. In that case adjacent patches along one of the coordinate axes have distance 1 and only patches within that distance share a link. Lattices are thus spatially embedded. In the research chapters we also consider lattices with long-range interactions, that means, that we connect all patches within some Euclidean distance $r \geq 1$. Even though the classical

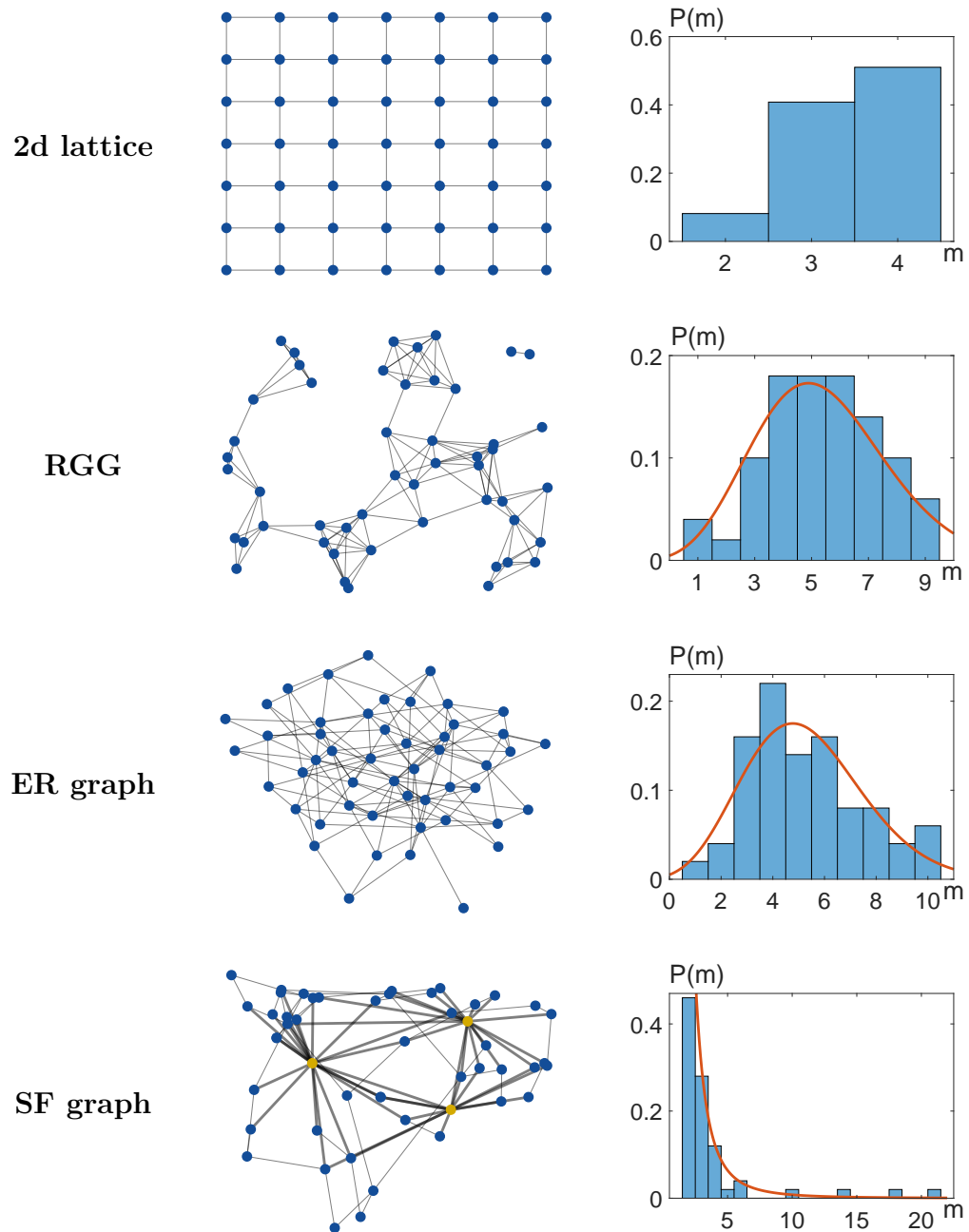


Figure 2.2: Visual representations of different networks and corresponding degree distributions. The red lines plotted over the degree distributions of the RGG, ER graph, and SF graph show the analytical forms of the degree distributions for large network sizes (see main text). The highlighted nodes in the visual representation of the SF graph are the hubs, where we here define a hub as a node with degree three times larger than the mean degree.

lattice structure (of the links) is then lost, the regular arrangement of patches is still intact, and since we use the Euclidean distance to connect patches, a long-range lattice is still spatially embedded. Lattices have large diameter, scaling as $D \sim N^{\frac{1}{d}}$. Thus, as expected for spatially embedded networks, lattices do not show the small-world property. If one wants to avoid boundary effects on a finite-size lattice, opposite boundaries of the lattice can be connected. In this case one also speaks of *periodic boundary conditions*. The top row of Fig. 2.2 shows a small, classical two-dimensional lattice with hard boundaries.

2.2.2 Random geometric graphs (RGGs)

Here we consider two-dimensional RGGs that are generated by first randomly distributing N patches in a square of area A , and then connecting all pairs of patches that fall within some Euclidean distance, r , to each other. As lattices, RGGs are thus spatially embedded. RGGs have a binomial degree distribution, $P(m) = p^m (1-p)^{N-m-1} \binom{N-1}{m}$, where $p = \frac{\pi r^2}{A}$ is the probability that two patches are connected. This can be seen as follows: Two patches are connected if one falls within the circle of radius r around the other one. This circle has area πr^2 and covers a fraction of $\frac{\pi r^2}{A}$ of the full space in which the RGG is embedded. Since the coordinates of all patches are drawn independently of each other, $\frac{\pi r^2}{A}$ is thus the probability that any pair of patches is connected. Note that this argument assumes periodic boundary conditions, since otherwise the circles around some nodes might be cut off. The probability that a patch is connected to m other patches, each with probability p , and not connected to the remaining $N-m-1$ patches, each with probability $1-p$, is then given by the binomial expression provided above. In fact, any random graph for which all pairs of patches are connected with the same probability, p , has binomial degree distribution. For large networks, $N \rightarrow \infty$, with fixed mean degree, $\langle m \rangle = \text{const}$, the binomial degree distribution becomes a Poisson distribution, $P(m) = \frac{\lambda^m e^{-\lambda}}{m!}$, with Poisson parameter $\lambda = \langle m \rangle$ (Dall and Christensen, 2002; Newman, 2010).

Since the circles defining the neighbourhoods of adjacent patches overlap, RGGs have strong degree correlations (Antonioni and Tomassini, 2012). For fixed mean degree the diameter of (two-dimensional) RGGs scales as $D \sim \sqrt{N}$ (Friedrich et al., 2013). As expected for spatially embedded networks, RGGs do thus not show the small-world property, but are characterized by long paths between patches.

2.2.3 Erdős-Rényi random graphs (ER graphs)

ER graphs, named after the Hungarian mathematicians Paul Erdős and Alfréd Rényi (Erdős and Rényi, 1959, 1960, 1961), are ‘ordinary’ random graphs defined by the number of patches, N , and the link-probability, p , between any pair of patches. Instead of the probability p one can alternatively specify the number of links and then distribute all links randomly between the patches. Completely analogous to RGGs, ER graphs have binomial degree distribution, $P(m) = p^m (1-p)^{N-m-1} \binom{N-1}{m}$, which for $N \rightarrow \infty$ and $\langle m \rangle = \text{const}$ becomes a Poisson distribution, $P(m) = \frac{\lambda^m e^{-\lambda}}{m!}$, with Poisson parameter $\lambda = \langle m \rangle$. For a given mean degree, RGGs and ER graphs thus have the same degree distribution. In contrast to RGGs, however, ER graphs are not spatially embedded and they show no degree correlations. This is the case since the patches of an ER graph have no natural coordinates and since links are entirely random. Instead, ER graphs are small-world networks with diameter scaling as $D \sim \log N$ (Newman, 2010). ER graphs and RGGs thus serve as a great example demonstrating that the degree distribution does not always sufficiently describe a network, and that in fact many network properties are not captured by the degree distribution.

2.2.4 Scale free graphs (SF graphs)

SF graphs are characterized by their degree distribution that follows a power law, $P(m) \sim m^{-\gamma}$, typically with $\gamma > 2$. This degree distribution implies that the vast majority of nodes has very small degree but that there are also a few patches with extraordinarily large degree. These large-degree nodes are also called *hubs* and they lead to a strong connectedness of the network implying very short path lengths. SF graphs with $2 < \gamma < 3$ can even be considered as ‘ultra small-world networks’, since they have a diameter scaling as $D \sim \log \log N$. For $\gamma > 3$ one finds the usual small-world behaviour, $D \sim \log N$ and for $\gamma = 3$ the scaling lies in between, $D \sim \frac{\log N}{\log \log N}$ (Bollobás and Riordan, 2004; Barabási, 2016). The degree distributions of many real world networks, like the internet or social networks, can be well approximated by power laws (Barabási, 2016).

One specific family of SF graphs can be generated by the so-called Barabási-Albert (BA) model (Albert and Barabási, 2002) that is based on two main ideas: growth and *preferential attachment* (the latter is also known as the ‘rich get richer principle’). Starting with a small, initial network of only a few

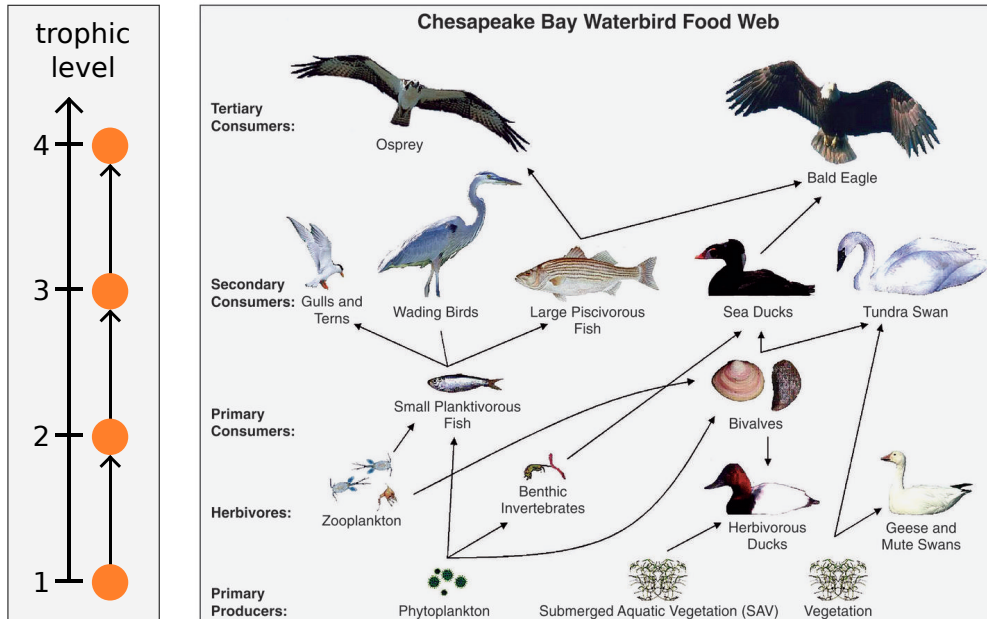


Figure 2.3: **Left:** abstract scheme of a simple food chain of $S = 4$ species. **Right:** graphical illustration of a more complex food web (credit: U.S. Geological Survey, illustration by Tim Auer).

patches, the algorithm adds at each iteration one additional node (growth) and connects this node to a fixed number of already existing nodes. The targets of the links are chosen according to their current degrees, assigning higher selection-probabilities to nodes with already large degrees (preferential attachment). To be precise, a node i is selected as the target for a new link with probability $\text{Prob}(i) = \frac{m_i}{\sum_j m_j}$, where j goes over all existing patches in the network. This mechanism eventually leads to the emergence of hubs and to a power law degree distribution with $\gamma = 3$. The described SF graphs are not spatially embedded since their nodes have no natural coordinates and since the assignment of links is not based on Euclidean distances.

2.3 Food webs

Food webs are directed networks with species as nodes and trophic interactions (feeding relations) as links. We follow the convention that links point from prey to predator, thus in the direction of energy flow. It is in principle possible to weight links according to the frequencies of the feeding relations

or the amount of flowing energy. However, as stated at the end of Section 2.1.1, in this thesis we consider only unweighted food webs. In the context of food webs we refer to the network size, that is, the number of species by S . This allows a clear and simple distinction from the size of the spatial network for which we use our standard network size label, N .

The arguably simplest food web structure, and a structure of exceptional importance for this thesis, is the food chain (see Fig. 2.3, left). The basal species of the chain is assumed to persist on some resource that is not explicitly modelled. Each additional species is a *specialist* consumer that preys exclusively on the species directly below. The food chain length can be defined either as the number of species in the chain, S , or as the number of feeding links, $S - 1$.

Species in a food web are often characterized by their *trophic levels*. In a simple food chain the trophic level takes only integer values and increases along the chain, starting with trophic level 1 for the basal species. In more complex food webs species can also have non-integer trophic levels (Levine, 1980; Williams and Martinez, 2004) which happens if a predator feeds on species from different trophic levels. We refer to such species as *omnivores* and more generally to any species that feeds on more than one prey as *generalists*. For an example of a real and more complex food web see Fig. 2.3 (right).

3 From metapopulations to meta-food-webs

In all research chapters of this thesis we use essentially the same spatially explicit meta-food-web model. In this chapter we introduce the meta-food-web approach step by step, starting with a metapopulation model of a single species, continuing with a metacommunity model of several competing species, and finally coming to a meta-food-web model of trophically interacting species. The presented models are spatially implicit, which means that the underlying habitat is not a spatial network (in the sense of Section 2.2) but that the habitat can instead be understood as consisting of many patches that are fully connected to each other (also referred to as ‘fully mixed space’ or just ‘mixed space’). In an additional step we show how to make the models spatially explicit, i. e., how to place them on spatial networks. Note that modelling communities of interacting species on spatial networks falls under the concept of multilayer networks, a field that has recently attracted more and more attention (De Domenico et al., 2013; Lee et al., 2015; Pilosof et al., 2017). Finally, we point out the equivalence of the presented metapopulation model and a model from the field of epidemics, describing the spread of an infection through a population of, for example, human individuals. The latter is well understood even in the case of an explicit network structure between the individuals.

3.1 Levins’ metapopulation approach

Levins (1969) modelled the dynamics of a pest that regionally attacks a crop, with the aim to find an optimal strategy to control the pest and thus protect the crop. The model can equivalently be used to describe the spatial dynamics of any single species. In Levins’ model a large habitat consists of many patches each of which can sustain a local population of the species. The term ‘metapopulation’ refers to the collection of all these local populations. On a given patch, the species is either present or absent while local population sizes (or abundances) are not part of the model (see left plot of Fig. 3.1). The quantity of interest in the model is the fraction of patches, p , that are occupied by the species. This fraction can change by two processes, colonizations and extinctions, which is why we also refer to the model dynamics as *colonization-extinction dynamics*.

- In a colonization event an occupied source patch sends colonizers to an empty target patch. After the colonization both patches are occupied,

that is, the population does not abandon the source patch. The rate of colonizations increases both with the fraction of occupied patches, p , from which colonizers are sent, as well as with the fraction of empty patches, $1 - p$, that can be colonized. With an additional colonization parameter, c' , the rate of change of p due to colonizations is thus $c'p(1 - p)$. Note that we here denote the colonization rate by c' since we reserve the letter c for the slightly differently defined colonization rate in the spatially explicit case.

- In an extinction event a local population dies out, leaving a formerly occupied patch empty. The rate of extinctions increases with the fraction of occupied patches, p , and the local extinction rate, e , leading to the contribution $-ep$ to the rate of change of p .

In our notation, the full differential equation at the heart of Levins' metapopulation model thus reads,

$$\frac{dp}{dt} = c'p(1 - p) - ep. \quad (3.1)$$

A steady state of the system, p^* such that $\frac{dp}{dt}|_{p=p^*} = 0$, is characterized by an equilibrium between colonizations and extinctions. While for $p^* = 0$ the species is regionally extinct, the more interesting solution is,

$$p^* = 1 - \frac{e}{c'}. \quad (3.2)$$

One can make two important observations concerning this solution:

1. For $e > c'$ one finds $p^* < 0$ which in reality translates to $p^* = 0$. The system thus has a *persistence threshold*, $c'_t = e$, such that the population can persist only if $c' > c'_t$.
2. Even when the species persists, the fraction of occupied patches always satisfies $p^* < 1$, except for the degenerate cases $e = 0$ or $c' \rightarrow \infty$. A 'mortal' species is thus never able to occupy the full habitat.

Both of these observations play an important role for the regional coexistence of several competitors, treated in the next section.

Note 1: The lack of local population dynamics implies the assumption that the local dynamics happen on a much faster time scale than the regional dynamics between the patches.

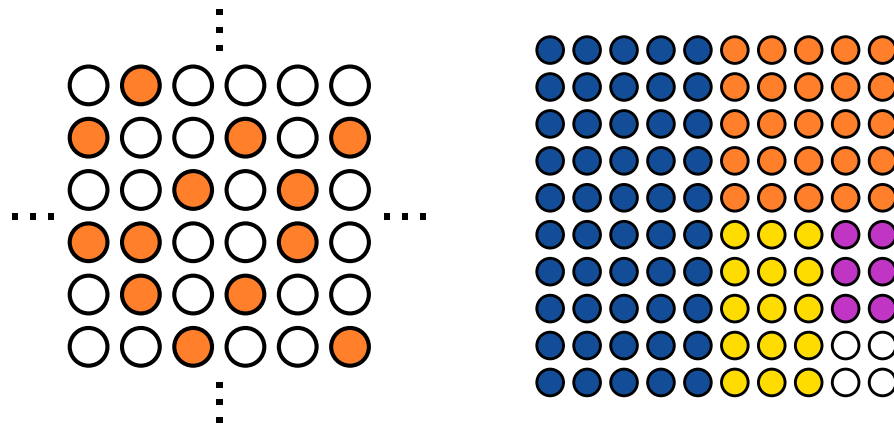


Figure 3.1: **Left:** Snapshot of a metapopulation according to Levins (1969). The habitat consists of many patches (drawn as circles) which are either occupied by the species (orange) or empty (white). No links between patches are drawn to illustrate the lack of spatial structure. The pattern of occupied patches has thus no meaning. **Right:** Illustration of the equilibrium of a metacommunity according to Tilman (1994) with regional coexistence of four competitors (represented by the different colors). A large fraction of patches is occupied by the strongest competitor. Inferior competitors can persist on the patches left empty by superior competitors. As in the left plot, the habitat is spatially implicit and the pattern of the patches has no meaning.

Note 2: Since colonizations are possible between all patches (\rightarrow fully mixed space), there is no explicit spatial structure (\rightarrow the model is spatially implicit).

3.2 Tilman's competing metacommunities

Tilman (1994) applied Levins' metapopulation approach to a community of competing species. Assuming competitive exclusion on individual patches and a strict competition hierarchy of the species, Tilman showed that in principle an arbitrary number of species can regionally coexist. This coexistence requires a *competition-colonization trade-off*, meaning that weaker competitors have to be stronger colonizers. If we define the competition hierarchy such that species with lower label k are stronger local competitors, then the necessary, opposed colonization hierarchy is $c'_1 < c'_2 < \dots < c'_k$.

Mathematically, the differential equation for the fraction of patches occupied

by species k reads,

$$\frac{dp^{(k)}}{dt} = c'_k p^{(k)} \left(1 - \sum_{j=1}^k p^{(j)} \right) - ep^{(k)} - p^{(k)} \sum_{j=1}^{k-1} c'_j p^{(j)}. \quad (3.3)$$

Since the strongest local competitor is unperturbed by any other species, Eq. 3.3 reduces for $k = 1$ to Levins' metapopulation equation (Eq. 3.1). All additional species are, however, negatively affected by any superior local competitor in two ways:

1. The effective rate of colonizations for species k is reduced since not only patches that are already occupied by species k itself are unsuitable colonization targets, but patches that are occupied by any locally superior competitor, $j < k$, cannot be colonized either (first term on the right hand side of Eq. 3.3).
2. The effective rate of extinctions is increased due to competitive displacement by a locally superior competitor (third term on the right hand side of Eq. 3.3).

Essentially, a weaker competitor must be able to persist on the patches left empty by the superior competitors and to endure the additional thread of extinction due to competitive displacement (note that we assumed the same 'intrinsic extinction rate', e , for all species; see second term on the right hand side of Eq. 3.3). This is only possible if the colonization rate, c'_k , of the weaker competitor is large enough. Tilman (1994) provided analytical expressions for the persistence thresholds of all species, in terms of the colonization rates c'_k , and found, as expected from the previous arguments, that the threshold increases with k . This leads to a more precise formulation of the competition-colonization trade-off mentioned above, and implies the necessary but not sufficient condition $c'_1 < c'_2 < \dots < c'_k$. Tilman also provided expressions for the equilibrium fractions of occupied patches of all species. The right plot of Fig. 3.1 illustrates the regional coexistence of four species in Tilman's metacommunity model.

3.3 The meta-food-web model by Pillai et al

3.3.1 General model

Pillai et al. (2010, 2011) introduced a generalization of the metacommunity approach to trophically interacting communities and showed how space can

lead to the emergence of complex food webs. The model is based on three main assumptions:

1. A predator can persist only on patches on which at least one of its prey species is present.
2. On individual patches the competitive exclusion principle holds. For a food web this means that locally only one predator can persist on one prey species. As a consequence, all local food webs are simple food chains. More complex food webs can only emerge on the regional scale when there are different realized food chains on different patches.
3. For a common prey species, a specialist predator is a stronger local competitor than a generalist or an omnivore.

Application of the competitive exclusion principle means that space is the only factor that promotes the (regional) persistence of complex food webs. If one furthermore chooses the same colonization and extinction rates for all species, there can be no classical competition-colonization trade-off as in the Tilman model (see Section 3.2). Coexistence of several predators for the same prey species is even in this case possible if, for example, one of the predators is a specialist while the other one is an omnivore that can feed on an additional species (Pillai et al., 2011; Böhme and Gross, 2012; Barter and Gross, 2017). The interactions of an omnivore and the competing specialist species are illustrated in Fig. 3.2. For the same omnivore web, Fig. 3.3 illustrates the model on a simple spatial network.

In the following subsections we present and explain the differential equations for species in a food chain and for the omnivore from Fig. 3.2. The equations for arbitrary food webs are complicated and therefore discussed in Appendix A. Note that we assume the above mentioned case that all species have the same colonization rate, c' , and extinction rate, e . These rates do also not depend on the prey on which a generalist predator feeds. Likewise, we assume that a predator does not affect the extinction rate of its prey, that is, we neglect all top-down effects. Pillai et al. (2010) considered the fully general case.

3.3.2 Food chains

For species in a food chain the metapopulation equation by Levins (Eq. 3.1) has to be modified to incorporate the fact that a predator needs its prey to

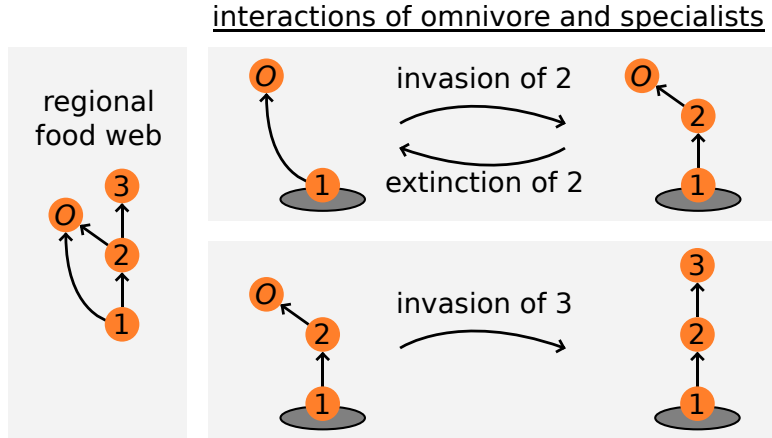


Figure 3.2: We consider a regional omnivore web (see also Pillai et al., 2011; Böhme and Gross, 2012; Barter and Gross, 2017) which is a food chain of three species extended by an omnivore that can feed on the basal species 1 and on the intermediate specialist species 2. If species 2 invades a patch on which the omnivore feeds on species 1, species 2 outcompetes the omnivore at feeding on species 1 but the omnivore can still persist by switching prey on species 2. Conversely, if on a patch with species 1, 2, and the omnivore the intermediate species 2 goes extinct, the omnivore can switch back feeding on species 1 and can thus still persist. If, however, the omnivore feeds on species 2 and then the top specialist predator species 3 invades, the omnivore is also outcompeted at feeding on species 2 and is thus competitively excluded from the patch.

persist. Since we assume no top-down effects, the equations for species in a food chain are also valid for species 1, 2 and 3 from Fig. 3.2. The differential equations for the fractions of patches occupied by these species read,

$$\frac{dp^{(k)}}{dt} = c'p^{(k)}(p^{(k-1)} - p^{(k)}) - kep^{(k)}, \quad (3.4)$$

where $p^{(0)} = 1$, meaning that all patches are habitable. For the basal species, $k = 1$, Eq. 3.4 reduces to Levins' metapopulation equation (Eq. 3.1). For species at higher trophic levels, $k \geq 2$, there are two modifications: (1) Not all patches on which species k is absent can be colonized but only those on which its prey species $k - 1$ is present. Since the set of patches occupied by species k is a subset of patches occupied by species $k - 1$, the fraction of patches that are suitable colonization targets for species k is $(p^{(k-1)} - p^{(k)})$. (2) The extinction rate is increased due to bottom-up extinctions, that is, species k cannot only go extinct by its own intrinsic extinction but also if

it loses its prey. This happens if any species further down the chain goes extinct. Since all species have the same extinction rate, e , and since species k can only be affected by a bottom-up extinction on patches on which it is present itself, its extinction rate is effectively multiplied by a factor of k .

3.3.3 Omnivory

The situation becomes more complex for species that are not part of a simple food chain, for example, the omnivore from Fig. 3.2. Pillai et al. (2010) argue that it is necessary to track the fractions of patches occupied by the feeding links, which we write as $(1, O)$ and $(2, O)$, instead of the species itself (for species in a food chain this makes no difference as they have only a single feeding link). In addition to the bottom-up effects experienced by the species in a food chain, the omnivore can also be competitively displaced and it can switch prey between species 1 and 2, as described in Fig. 3.2. This leads to additional terms in the differential equations (see also supplemental material of Pillai et al., 2011),

$$\frac{dp^{(1,O)}}{dt} = c'p^{(O)} \left(p^{(1)} - p^{(2)} - p^{(1,O)} \right) + ep^{(2,O)} - 2ep^{(1,O)} - c'p^{(2)}p^{(1,O)}, \quad (3.5)$$

$$\frac{dp^{(2,O)}}{dt} = c'p^{(O)} \left(p^{(2)} - p^{(3)} - p^{(2,O)} \right) + c'p^{(2)}p^{(1,O)} - 3ep^{(2,O)} - c'p^{(3)}p^{(2,O)}, \quad (3.6)$$

where $p^{(O)} = p^{(1,O)} + p^{(2,O)}$ is the fraction of all patches occupied by the omnivore. We briefly discuss the terms on the right hand side of Eq. 3.5 (in the given order): (1) The occupancy of the feeding link $(1, O)$ can increase when the omnivore colonizes a patch on which species 1 is present but species 2 and the omnivore itself are absent. The absence of species 2 implies that the omnivore, if it was present, would feed on species 1. The fraction of patches suitable for colonization is thus $(p^{(1)} - p^{(2)} - p^{(1,O)})$. Colonizers can be sent from any patch on which the omnivore is present, regardless of its prey. (2) The occupancy of $(1, O)$ can also increase due to prey-switching of the omnivore if species 2 goes extinct on patches on which the omnivore currently feeds on species 2. The occupancy of $(1, O)$ decreases if (3) the omnivore or species 1 goes extinct, or (4) when species 2 invades a $(1, O)$ patch which leads to prey-switching of the omnivore from species 1 to species 2. Eq. 3.6 can be understood by similar arguments.

3.4 Making the models spatially explicit

3.4.1 Generalizing the differential equations

Note: For equations analogous to our Eqs. 3.7 and 3.8 in the context of ‘epidemics on networks’ with further calculations, approximations, and discussion see also Newman (2010).

In the spatially explicit models we are not primarily interested in the fraction of occupied patches but in the occupancies of individual patches. Considering only a single species and labelling patches $i = 1, \dots, N$ we can define the indicator variable $X_i \in \{0, 1\}$ that tells us if patch i is occupied ($X_i = 1$) or empty ($X_i = 0$). We are typically interested in the *occupation probability*, $\langle X_i \rangle$, of each patch i . The spatially explicit version of Levins’ metapopulation equation (Eq. 3.1) then reads,

$$\frac{d \langle X_i \rangle}{dt} = c \sum_{j=1}^N A_{ij} \langle \bar{X}_i X_j \rangle - e \langle X_i \rangle. \quad (3.7)$$

The first term on the right hand side of Eq. 3.7 is as usual the colonization term. Patch i can be colonized from any neighbouring patch ($\sum_{j=1}^N A_{ij} \dots$) where A is the adjacency matrix of the spatial network with $A_{ij} = 1$ if patches i and j are connected (see Section 2.1.2 for the introduction of the adjacency matrix). The colonization from neighbour j to patch i is only possible if patch i is currently empty (indicated by $\bar{X}_i = 1 - X_i$) and if patch j is currently occupied (X_j). The joint probability of these two events is $\langle \bar{X}_i X_j \rangle$. \bar{X}_i and X_j are in general correlated since the species disperses through the network step by step. A patch is thus more likely to be occupied if its neighbours are occupied as well. We refer to these correlations as *neighbour correlations*. The stronger the network is connected the easier is the dispersal and the weaker are the neighbour correlations (for fully mixed space there will be no correlations left). Due to the neighbour correlations, that is, the appearance of the pairwise term $\langle \bar{X}_i X_j \rangle$, Eq. 3.7 cannot be solved. One can in principle write down an equation for $\langle \bar{X}_i X_j \rangle$ as well, but this equation would involve tri-partite terms and so on (Newman, 2010). At some point the equations have to be ‘closed’ which requires an approximation. The simplest approximation neglects all neighbour correlations, $\langle \bar{X}_i X_j \rangle = \langle \bar{X}_i \rangle \langle X_j \rangle$, and thus regards the occupancies of neighbouring patches i and j as independent.

In this case we can write Eq. 3.7 as,

$$\frac{du_i}{dt} = c(1 - u_i) \sum_{j=1}^N A_{ij}u_j - eu_i, \quad (3.8)$$

where we used the notation $\langle X_i \rangle = u_i$ for the occupation probability and similarly $\langle \bar{X}_i \rangle = 1 - u_i$. Eq. 3.8 now strongly resembles the spatially implicit metapopulation Eq. 3.1 with the following three differences:

1. Eq. 3.8 is a differential equation for the occupation probability of a single patch while Eq. 3.1 is an equation for the fraction of occupied patches. As one consequence the spatially explicit system is described by N coupled equations, instead of one single equation. The fraction of occupied patches can be calculated by averaging the occupation probabilities of all patches.
2. The colonization term is expanded by the sum over all neighbours, $\sum_{j=1}^N A_{ij}u_j$, incorporating the structure of the spatial network.
3. Instead of the global colonization rate c' , we now use the *per-neighbour colonization rate* c . For fully mixed space we would find $c' = (N - 1)c$, since in this case any patch is neighbours with all other $N - 1$ patches.

Note that aside from point (1), which applies to the equation as a whole, there are no changes to the extinction term. The extinction rate, e , is the same as before as well. All changes can straightforwardly be applied to all other metacommunity and meta-food-web equations. For example, the equations for the species in a food chain (Eq. 3.4) become,

$$\frac{du_i^{(k)}}{dt} = c \left(u_i^{(k-1)} - u_i^{(k)} \right) \sum_{j=1}^N A_{ij}u_j^{(k)} - keu_i^{(k)}. \quad (3.9)$$

3.4.2 Solving the differential equations

The differential equations can in principle be solved by numerical integration. Since we are not interested in the full time evolution of the occupation probabilities but only in the equilibrium solution, we instead use a faster, iterative method to calculate the equilibrium. In the following, we describe this method applied to the system of equations for species in a food chain given by Eq. 3.9. The generalization to more complex food webs is straightforward

and is briefly addressed below. To demand equilibrium we set the derivative on the left hand side of Eq. 3.9 to zero. Next, we rearrange the equation such that the occupation probability governed by the specific equation, $u_i^{(k)}$, is isolated on the left hand side,

$$u_i^{(k)} = \frac{u_i^{(k-1)} \sum_{j=1}^N A_{ij} u_j^{(k)}}{k_c^e + \sum_{j=1}^N A_{ij} u_j^{(k)}}. \quad (3.10)$$

Eq. 3.10 is an expression for the equilibrium occupation probability of species k on patch i . This equilibrium occupation probability depends on the equilibrium occupation probabilities of the same species on other patches, $u_j^{(k)}$, and of the prey species on the same patch, $u_i^{(k-1)}$. Since the equations for species $k = 1$ depend on no other species ($u_i^{(0)} = 1$) one can start by solving the equations for $k = 1$, then for $k = 2$, and so on. For given k the equations have to be solved simultaneously for all patches. This is done by starting with an initial guess for $u_i^{(k)}$ for all i and using Eq. 3.10 as an iteration rule. This means that the initial guess is inserted into the right hand side of Eq. 3.10 which is then evaluated to obtain a refined guess for the $u_i^{(k)}$ (output on the left hand side). The new $u_i^{(k)}$ values are inserted into the right hand side again and again until the values converge.

For more complex food webs, like the omnivore web from Fig. 3.2, it is necessary to solve the equations for the occupation probabilities of all trophic links belonging to one species simultaneously. We can already see in the spatially implicit version of the omnivore equations (Eqs. 3.5 and 3.6) that the two equations are indeed coupled. In principle one can also solve all equations, that is, the equations for all species/links and all patches simultaneously. This would in particular be necessary if we allowed top-down effects which would destroy the hierarchical structure of the equations already for species in a food chain.

Note that since $A_{ii} = 0$, $u_i^{(k)}$ does not appear on the right hand side of Eq. 3.10. The iterative method would, however, also work if $u_i^{(k)}$ could not be perfectly isolated on the left hand side.

3.4.3 Stochastic approach via Gillespie algorithm

Instead of numerically solving the differential equations from Section 3.4.1 we can alternatively run the dynamics of any of the models (metapopulation, -community, or -food-web; spatially implicit or explicit) via stochastic sim-

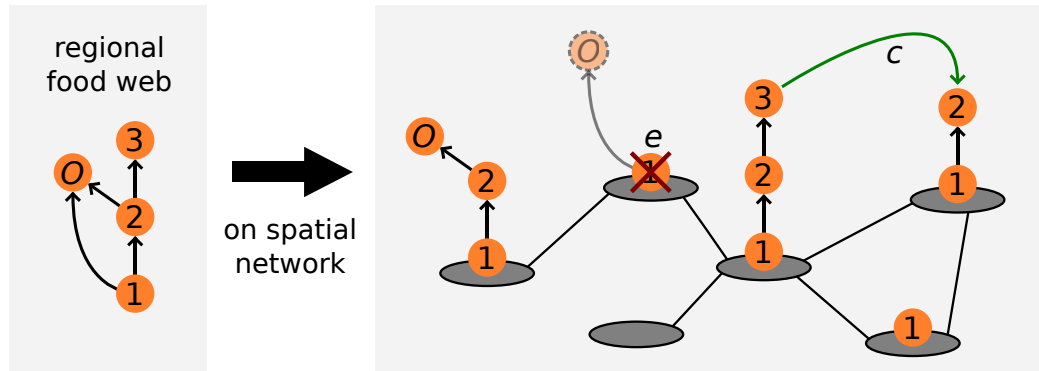


Figure 3.3: Illustration of the omnivore web from Fig. 3.2 put on a spatial network. Each patch shows one of the possible local food chain configurations that are allowed when following the rules by Pillai et al. (2010, 2011). Colonizations (associated rate c) are only possible if the involved patches share a link and if the persistence requirements of the colonizing species are met on the target patch (e.g. presence of prey). Extinctions (associated rate e) are purely local events and occur entirely at random. Predators have no effects on a prey's extinction rate (no top-down effects) but the extinction of the prey induces the bottom-up extinction of all species above, unless a predator can switch feeding on another still persisting prey.

ulations. To this end we use the Gillespie algorithm (Gillespie, 1977) which simulates the model dynamics step by step, one colonization or extinction event after another. Given the current state of the system (occupation status of all species on all patches; see also Fig. 3.3) the algorithm requires us to list all possible processes and to associate a rate with each of them. In practice, we associate one rate $w_i^{(k)}$ with each patch-species pair as follows:

Extinction event If species k is present on patch i , we use the extinction rate, $w_i^{(k)} = e$.

Colonization event If species k is absent from patch i , we check whether or not all other colonization requirements are met (presence of a prey and absence of all locally superior competitors):

- If the requirements are not met, the rate is $w_i^{(k)} = 0$ since the colonization is not allowed.
- If all requirements are satisfied, the rate is $w_i^{(k)} = n_i^{(k)} \cdot c$ where $n_i^{(k)}$ is the number of neighbours of patch i occupied by species k .

The rate $n_i^{(k)} \cdot c$ can be understood as the incoming colonization rate of species k towards patch i .

Next, all rates are normalized by their sum, $\lambda = \sum_{i,k} w_i^{(k)}$, to obtain a probability distribution that is used to randomly draw one process that is then executed. Possible competitive displacements, bottom-up extinctions or other triggered food web rearrangements are executed at the same time as the primary process. The time that passes until a chosen process is executed, is drawn from an exponential distribution with rate parameter λ . The Gillespie algorithm thus creates a trajectory of the system's state in continuous time. This also allows us to calculate the fraction of time any patch i is occupied by any species k , which is the equivalent of the occupation probability $u_i^{(k)}$ introduced in Section 3.4.1.

The Gillespie algorithm can be sped up by not recalculating all rates $w_i^{(k)}$ after each step. Only the rates for the patch on which the last process was executed, and for neighbouring patches, have to be recalculated. To go through all neighbours of a patch it is faster to use the adjacency list representation of the spatial network rather than the adjacency matrix (see Section 2.1.2).

The main advantage of the stochastic approach via the Gillespie algorithm, compared to the differential equation approach, is that it automatically incorporates all neighbour correlations (see Section 3.4.1). If we are not certain that neighbour correlations can be neglected, and if we want the result (i.e., the occupation probabilities) to be as precise as possible, it is better to use the stochastic simulations and run the algorithm for a very large number of steps, potentially repeating the simulations several times.

Note that while the model and the corresponding differential equations developed by Pillai et al. (2010) are spatially implicit, Pillai et al. (2011) also conducted spatially explicit stochastic simulations of their model.

3.5 Equivalence to an epidemic model

Epidemic models describe, for example, the spread of an infection through a host population. In one specific, simple epidemic model individuals can be either susceptible or infected. The latter individuals can spread the infection to susceptible ones, but can also recover from the infection and become susceptible again (no immunity or death). Each individual thus runs through a 'susceptible \rightarrow infected \rightarrow susceptible \rightarrow ...' cycle, which is why the model

is also called *SIS model*. The SIS model is equivalent to Levins' metapopulation approach from Section 3.1. The infection is the analog of the species and the host population is the analog of space. Spreading the infection and recovering are the equivalents of colonizations and extinctions, respectively. The SIS model (as well as other epidemic models) can also be either implicit or explicit with respect to the structure of the host population. In the implicit case the population is fully mixed, meaning that any individual is equally likely to have contact with any other individual. In the explicit case a network encodes which individuals can come in contact with each other.

One central goal when modelling the spread of epidemics is to find the *epidemic threshold* (e.g. in terms of infection and recovery rate) below which the infection cannot spread and persist. For an epidemic on a network this threshold can be calculated from the adjacency matrix as well as from the degree distribution of the network (Newman, 2010). On stronger connected networks the spread of the infection is typically easier, implying that these networks have smaller epidemic thresholds. For typical scale-free graphs the epidemic threshold is even zero, which can be important, for example, for computer viruses spreading through the internet (Pastor-Satorras and Vespignani, 2001a,b).

Like the metapopulation approach can be generalized to metacommunities or meta-food-webs, epidemic models can be generalized to several interacting infections (Newman, 2005; Ahn and Jeong, 2006; Newman and Ferrario, 2013; Zhao et al., 2014; Azimi-Tafreshi, 2016). Possible interactions are cross-immunities or that one infection (like HIV) makes an individual more susceptible to other infections.

4 Objectives of research chapters

In Chapter 1 we stated that “in this thesis we model the dynamics of spatially explicit meta-food-webs in the food web framework by Pillai et al. (2010), look for spatial patterns of food chain length and distributions of individual species, and link these patterns to the spatial structure of the habitat.” The objectives and the model setups of the individual research chapters, presented in Part II, are briefly outlined below. The relation between the research chapters is also illustrated in Fig. 4.1.

Chapter 5: Mid-domain effect for food chain length The objective of this research chapter is to investigate how the boundaries of a habitat affect the spatial pattern of food chain length in the habitat. We are in particular interested in how the food chain length changes from the center of the habitat towards the boundaries. To this end we model the dynamics of simple food chains placed on lattice-like spatial networks with hard boundaries.

Chapter 6: Food chain length and the SIS centrality In this research chapter we change the model setup from the previous research chapter by considering habitats represented by random networks. To describe spatial patterns on such networks, the concept of boundary and center has to be replaced by the concept of so-called *centrality measures*, that in some sense quantify the ‘importance’ or ‘connectedness’ of patches within the habitat network. The objective is to relate the food chain length on patches to the centrality values of the patches. To this end we also introduce a new centrality measure.

Chapter 7: Spatial niche partitioning in food webs In this research chapter we change the model setup from the first research chapter by adding omnivores to the food chain. The first objective is to investigate how the spatial pattern of food chain length found in the first research chapter changes due to the presence of omnivores. The second objective is to investigate the individual spatial patterns of a specialist predator and of increasingly omnivorous species. We compare these latter results with spatial patterns found for species in a purely competitive community.

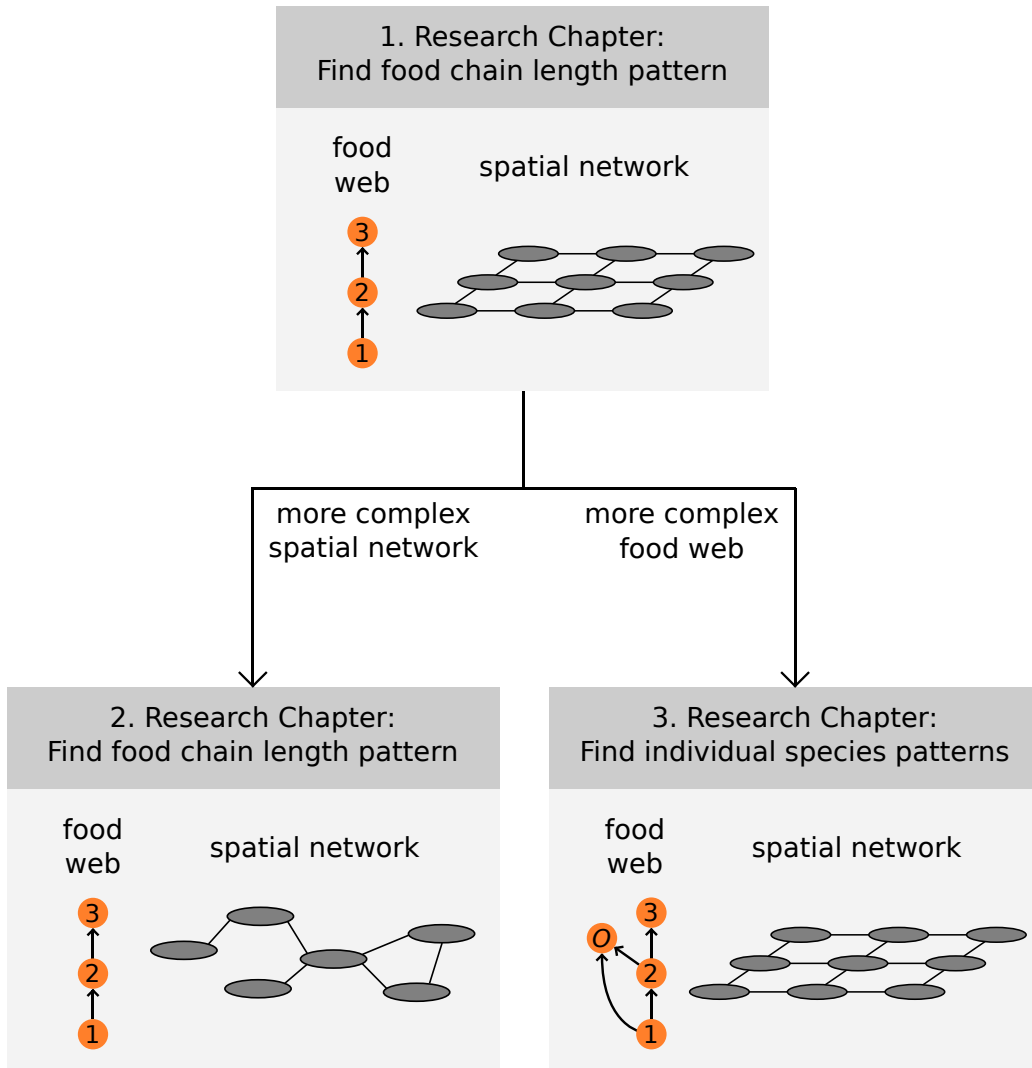


Figure 4.1: Relation between the research chapters: In the first chapter a simple food chain is placed on a lattice-like spatial network. In the second and third research chapters we consider generalizations of this setup into different directions. In the second research chapter we still consider simple food chains but the spatial network is random instead of lattice-like, while in the third research chapter we consider more complex food webs, in particular including omnivores, but keep the simple lattice-like networks.

Part II
Research Chapters

5 Mid-domain effect for food chain length

Mid-domain effect for food chain length in a colonization-extinction model

Kai von Prillwitz¹, Bernd Blasius^{1,2}

¹Institute for Chemistry and Biology of the Marine Environment,
University of Oldenburg, Germany

²Helmholtz Institute for Functional Marine Biodiversity at the University
of Oldenburg, Germany

Keywords metacommunity, spatially explicit, patch-dynamic model, spatial networks, food web

Abstract The mid-domain effect states that in a spatially bounded domain species richness tends to decrease from the center towards the boundary, thus producing a peak or plateau of species richness in the middle of the domain even in the absence of any environmental gradient. This effect has been frequently used to describe geographic richness gradients of trophically similar species, but how it scales across different trophic levels is poorly understood. Here, we study the role of geometric constraints for the formation of spatial gradients in trophically structured metacommunities. We model colonization-extinction dynamics of a simple food chain on a network of habitat patches embedded in a one- or two-dimensional domain. In a spatially homogeneous or mixed system we find that the food chain length increases with the square root of the ratio of colonization and extinction rates. In a spatially bounded domain we find that the patch occupancy decreases towards the edge of the domain for all species of the food web, but this spatial gradient varies with the trophic level. As a consequence, the average food chain length peaks in the center and declines towards the boundaries of the domain, thereby extending the notion of a mid-domain effect from species richness to food chain length. This effect already arises in a one-dimensional domain, but it is most pronounced at the headlands in a two-dimensional domain. As the mid-domain effect for food chain length is caused solely by spatial boundaries and requires no other environmental heterogeneity it can be considered a null expectation for geographic patterns in spatially extended food webs.

5.1 Introduction

The mechanisms underlying biogeographic patterns of species diversity and community structure are among the most studied and debated questions in ecology (Lomolino et al., 2017). One prominent example is the area effect, where an increasing habitat size leads to an increasing number of coexisting species (MacArthur and Wilson, 1967; Holt, 1993). Spatial diversity patterns are also related to geographic constraints. According to the so-called mid-domain effect (MDE) in a spatial domain restricted by ‘hard boundaries’, species richness tends to peak at the center of the domain and declines towards the boundaries (Colwell and Hurtt, 1994). ‘Hard boundaries’ could be realized, for example, by continental edges or mountaintops for terrestrial species, shorelines for aquatic species, or any other large-scale dispersal barriers. The MDE occurs even in the absence of other environmental gradients and is thus solely caused by spatial constraints.

The MDE is expected to occur by simple theoretic reasoning: Assuming a random distribution of species ranges within a bounded domain, in general more ranges should overlap near the middle of the domain than at the edges, producing a peak or plateau of species richness towards the center. In a large number of empirical and theoretical investigations the effect has been firmly validated and established as a null model for gradients in species richness (Willig and Lyons, 1998; Colwell and Lees, 2000; Bokma et al., 2001; Jetz and Rahbek, 2001; Grytnes, 2003; Connolly, 2005). While the MDE was traditionally formulated for one-dimensional habitats, like latitudinal (Colwell and Hurtt, 1994), elevational (Kessler, 2001;

Grytnes and Vetaas, 2002) and bathymetric (Pineda and Caswell, 1998) gradients or river courses (Dunn et al., 2006), two-dimensional extensions have been developed as well (Jetz and Rahbek, 2001; Bokma et al., 2001). Despite its seminal role of describing species richness gradients, not much is known about how the MDE scales across trophic layers - rising the question for theoretical approaches to study spatially structured trophic communities.

One prominent classic approach to theoretically capture the dynamics and patterns of spatial communities is provided by the metapopulation framework (Levins, 1969; Hanski and Gilpin, 1991). The underlying principle is that an ensemble of local populations can be described by the dynamic balance between colonization of empty patches from occupied ones and local extinction of occupied patches, allowing a species to persist regionally despite the possibility of local extinctions. By augmenting this approach to metacommunities, Tilman (1994) showed that a potentially infinite number of competitors can regionally coexist, even if locally one superior competitor drives all other species to extinction. The precise spatial structure can affect species diversity in a metacommunity, as was shown in microcosm experiments on river-like spatial networks and lattice structures (Carrara et al., 2012, 2013). Thereby, the network structure affects patterns of population densities (Altermatt and Fronhofer, 2018).

In a pioneering series of studies Holt (1993, 1996, 2002) demonstrated that space can have similar effects in trophically interacting communities. In particular he could show that in meta-food-webs species richness and food chain length should increase with increasing habi-

tat size. Subsequently, metapopulation models based on colonization-extinction dynamics were developed to study the consequences of habitat destruction at different trophic levels (Bascompte and Solé, 1998; Melián and Bascompte, 2002). In another series of studies Liao et al. (2017a,b,c) showed that habitat loss and fragmentation can have different effects on meta-food-webs and that, in particular, an intermediate level of fragmentation, compared to a strongly connected remaining habitat, can promote food web persistence. While these models treated only simple few-species food web motifs, recently, this approach was extended to include a larger number of species (Pillai et al., 2010, 2011; Calcagno et al., 2011; Gravel et al., 2011a,b). These studies showed that complex food webs can emerge at the regional scale even if locally only simple food chains are allowed. Based on these models Barter and Gross (2016, 2017) highlighted the importance of the specific spatial structure of the habitat, for example by explicitly embedding meta-food-webs in space in the form of random geometric graphs.

Many of these metacommunity studies that incorporate both trophic interactions and spatial structures are interested only in regional results, such as overall persistence or constraints on food web structure (Amarasekare, 2008; Calcagno et al., 2011). In contrast, explicit spatial patterns of food web properties, such as spatial profiles of food chain length, and the contribution of spatial effects to their emergence, have rarely been considered or even quantified. This is astonishing, as food chain length is a central character of ecological communities and quantifies the number of feeding links between resources and top predators (Post, 2002). Food chain length has classically been related to either dy-

namic constraints, where longer food chains become unstable and are particularly more vulnerable to perturbation, or to energetic constraints, where due to imperfect transfer of energy and resources a diminishing amount of energy is available to support higher trophic levels. Beside these two factors, the role of spatial constraints is increasingly recognized as a major determinant of food chain length (Post, 2002). The main reasoning is that a larger area or ecosystem size should be available to support higher trophic levels and top predators. Nevertheless, model studies that predict spatial patterns of food chain length are still missing. In particular, to our knowledge, the MDE has never been formulated for food chain length.

In this paper we study the role of geometric constraints for the formation of spatial gradients in trophically structured metacommunities. To this end, we develop a stochastic patch occupancy model including both trophic and explicit spatial structures. The model describes the colonization-extinction dynamics of a simple food chain on a network of habitat patches embedded in a one- or two-dimensional domain. By resolving results to individual patches, this setup allows us to investigate spatial patterns of food chain length, and to assess the role of the spatial constraints for the formation of these patterns. We intentionally choose a very simple model to ensure that we do not confound spatial effects with effects caused by more complicated food web dynamics. By combination of direct stochastic simulations and analytic treatment in an ODE model we calculate patch occupancies, persistence thresholds, and food chain length. Thereby we consider different spatial scenarios: First, we study a spatially homogeneous or mixed system and are able to show that

food chain length increases with the square root of the ratio of colonization and extinction rates. Next, we study the influence of hard boundaries in one- and two-dimensional domains. We find that the patch occupancy decreases towards the edge of the domain for all species of the food web, even though this spatial decrease varies with the trophic level. As a consequence, we find that the average food chain length peaks in the center and declines towards the boundaries of a spatial domain - demonstrating a clear mid-domain effect of food chain length. This effect already arises in a one-dimensional domain, but it is most pronounced at the headlands in a two-dimensional domain. Our findings exemplify the role of geometric constraints for the formation of spatial gradients in trophically structured communities.

5.2 Methods

Model setup

We develop a stochastic patch occupancy model to describe the colonization-extinction dynamics of a trophically structured community on an explicit spatial network of habitat patches (Fig. 5.1). Thereby we follow Pillai et al. (2010, 2011), Gravel et al. (2011a), and Barter and Gross (2016, 2017) but restrict the trophic structure to a simple food chain. We assume that the network is embedded in a one- or two-dimensional domain. For any given patch, $i = 1, \dots, N$, all patches within spatial distance up to the colonization range r are considered its neighbours, allowing colonizations between the patches. In the one-dimensional case, a patch that is not too close to any boundary has r neighbours to the left and r neighbours

to the right. In the two-dimensional case r is the radius of a circle. The colonization range influences the spatial structure as experienced by the species. The species in the food chain are labelled according to their trophic level by $k = 1, \dots, S$ and we refer to the species at trophic level k simply by ‘species k ’. In each patch we track the presence and absence of all species. We call patches where species k is present *k-occupied*, and where it is absent *k-empty*. A *k-empty* patch can be colonized by species k with colonization rate c per *k-occupied* neighbour, but only if its prey species $k-1$ is present on the target patch. If a patch is *k-occupied* species k can go extinct with extinction rate e . In this case, all species higher up the chain go extinct as well at the same time instance. The basal species 1 suffers no such bottom-up extinction and has access to the full network. Furthermore, we neglect top-down extinction effects. Ecologically this means that we assume that a predator does not over-exploit its prey and thereby increases its extinction risk.

For simplicity, we assume that the colonization rate c , the extinction rate e , and the colonization range r are the same for all species (i.e., being independent of the trophic level). This is not only a convenient simplification but also prevents confounding effects caused by differences between the species that go beyond their trophic positions. In all cases we set the extinction rate to $e = 1$. This implies no loss of generality but simply fixes the time scale. Note that for a single species ($S = 1$) the model is equivalent to a susceptible-infected-susceptible (SIS) model from epidemics on networks (Pastor-Satorras and Vespignani, 2001a; Newman, 2010).

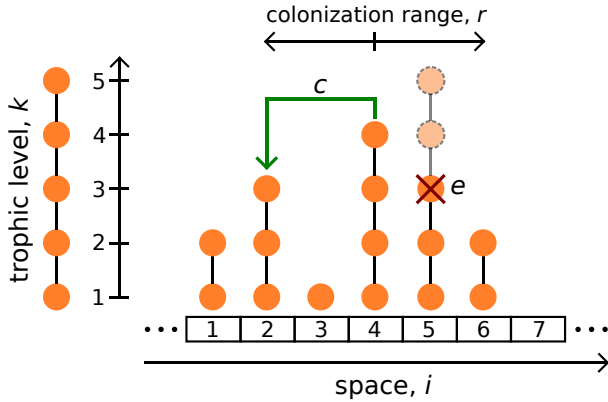


Figure 5.1: Conceptual diagram of the colonization-extinction model of a food chain on a network of habitat patches. Species (shown as orange circles) are aligned vertically according to their trophic level $k = 1, \dots, S$. Habitat patches (shown as rectangles) at spatial positions $i = 1, \dots, N$ are aligned horizontally. All species that are present in a patch at this time point are indicated vertically above the corresponding rectangle. These species must form a contiguous chain starting at the lowest trophic level $k = 1$ (trophic interactions indicated as black vertical lines connecting the circles). Species can colonize neighbouring patches within a colonization range r (black horizontal arrows). The green arrow indicates an exemplary colonization event of species 4 from patch 4 to patch 2. The dark red cross indicates a possible extinction event of species 3 in patch 5 and the subsequent bottom-up extinctions of species 4 and 5 (light orange shading). Parameter values: $S = 5$ and $r = 2$.

Stochastic approach

We use two different approaches to analyze the model. First, applying a stochastic approach we run the model based on direct stochastic simulations. Thereby we use the Gillespie algorithm (Gillespie, 1977) which simulates the dynamics step by step, one colonization or extinction event at a time. Bottom-up extinctions are executed simultaneously with the pri-

mary extinction. The algorithm also provides the time that passes between any two processes and thus produces a proper trajectory of the whole system. Quantities like food chain length or occupation probability of any species on any patch are calculated as time averages. When we are interested in these quantities resolved to single patches we let the algorithm run for $100\,000 \cdot S \cdot N$ steps and calculate the time average over the last 90% of steps. When we are interested in spatial averages, which converge much faster, we let the system run for $100\,000 \cdot S$ steps and, in addition to the spatial average, calculate the time average over the last 10% of steps. As initial conditions we usually start with each patch having a probability of 0.5 to be occupied by the whole food chain. Using intensive numerical simulations we have verified that our results on the equilibrium state are independent to variations of initial conditions, simulation and transient times, and averaging procedures.

Differential equation (ODE) approach

Second, we employ a differential equation (ODE) approach to solve our model. Thereby, we model the occupation probability, $u_i^{(k)}$, of species k on patch i in form of the following set of ordinary differential equations

$$\frac{du_i^{(k)}}{dt} = c \left(u_i^{(k-1)} - u_i^{(k)} \right) \sum_j A_{ij} u_j^{(k)} - ke u_i^{(k)}. \quad (5.1)$$

Here, A is the adjacency matrix of the spatial network with $A_{ij} = 1$ if patches i and j are connected and $A_{ij} = 0$ otherwise. The second summand on the right hand side of Eq. 5.1 describes

the extinction of occupied patches (the factor k is necessary to include bottom-up extinctions). The first summand describes the colonization of empty patches and is given as the product of two terms. The first term $(u_i^{(k-1)} - u_i^{(k)})$ is the probability that species k is currently not present on patch i , but its required prey species $k - 1$ is present. In the equation for the basal species ($k = 1$) we set $u_i^{(0)} = 1$ meaning that the basal species has access to any patch of the network. The second term $\sum_j A_{ij} u_j^{(k)}$ is the expected number of k -occupied neighbours of patch i , taking into account that colonizers can only come from these patches. Eq. 5.1 uses the approximation that these two quantities are independent. In reality, the probability that one patch is currently empty and that a given neighbour of this patch is currently occupied can be correlated (Newman, 2010). Thus, we should expect the ODE model (Eq. 5.1) to give only an approximation of the full dynamics and we therefore always compare the solution to Eq. 5.1 with direct simulations of the stochastic model to verify the accuracy of this approximation.

Calculation of food chain length

Given our model, the food chain length L_i on patch i can be obtained by simply counting the number of trophic levels. In the stochastic implementation of the model we calculate this quantity directly for every patch and time instance, which then needs to be sufficiently averaged over time. In terms of the ODE model (Eq. 5.1) and occupation probabilities $u_i^{(k)}$ we calculate food chain length as the weighted sum of all possible food chain lengths (Holt, 1993,

1996)

$$\begin{aligned} L_i &= \sum_{k=1}^S k (u_i^{(k)} - u_i^{(k+1)}) \\ &= \sum_{k=1}^S u_i^{(k)}. \end{aligned} \quad (5.2)$$

On the right hand side of the first line in Eq. 5.2 $u_i^{(k)} - u_i^{(k+1)}$ is the probability to find exactly the first k species, which follows from the hierarchical structure of the species. The food chain length is thus simply the sum of the occupation probabilities of all species in the food chain (Holt, 1993, 1996).

5.3 Results

Patch occupancy and food chain length in a spatially homogeneous system

As a benchmark for the subsequent sections, we start by investigating a one-dimensional system with periodic boundary conditions. In this case, all patches of the lattice have the same number of neighbours, so that, after an initial transient, all patches will be equivalent for all times and the system becomes spatially homogeneous. In this case the index i in Eq. 5.1 can be dropped and $\sum_j A_{ij}$ simply becomes a factor corresponding to the number of neighbours per patch, $n(r)$. For the one-dimensional lattice we have $n(r) = 2r$. With these changes, Eq. 5.1 becomes,

$$\frac{du^{(k)}}{dt} = C (u^{(k-1)} - u^{(k)}) u^{(k)} - ke u^{(k)}, \quad (5.3)$$

where we have defined the total colonization rate $C = n(r)c$. The probability $u^{(k)}$ is now not only the probability that any given patch is k -occupied, but simultaneously it is the expected

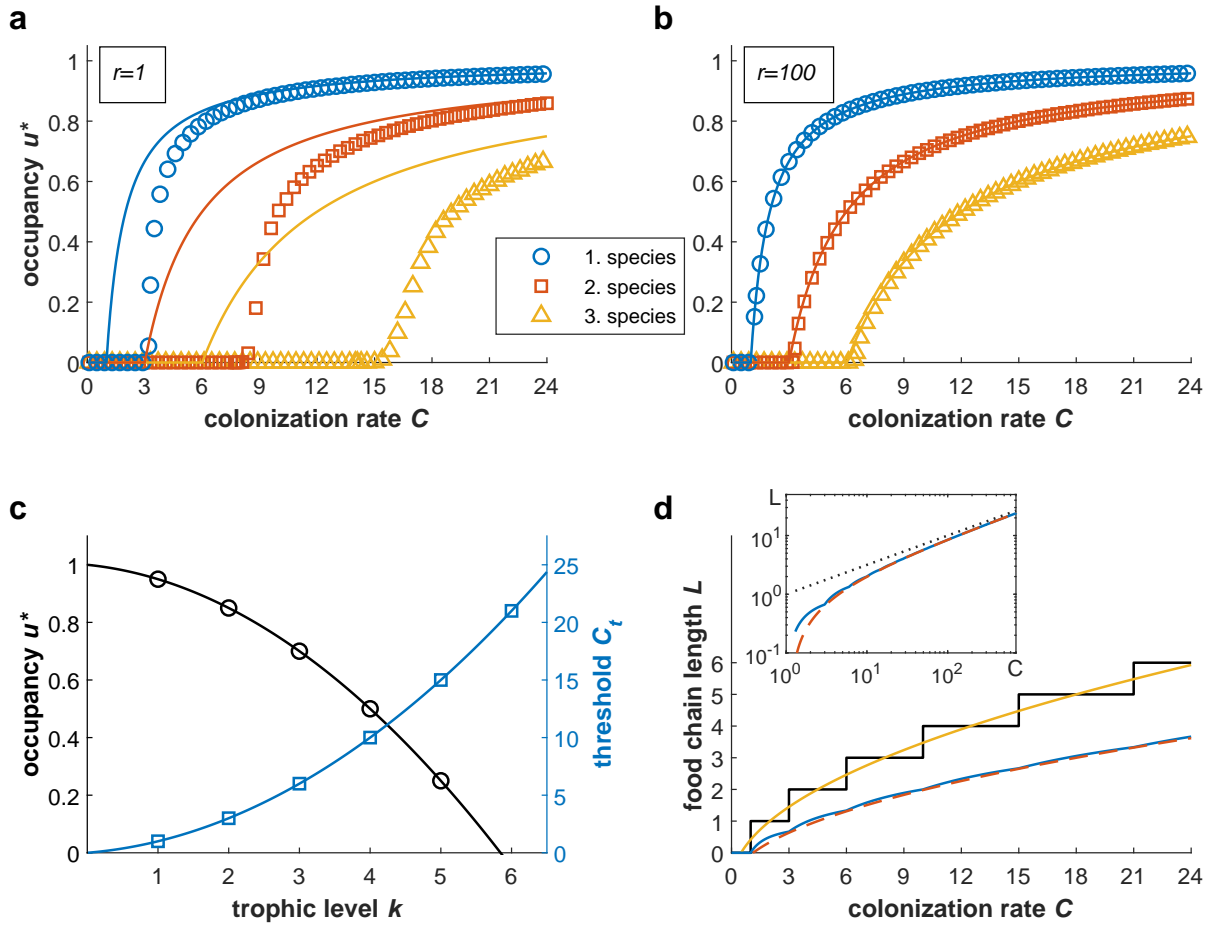


Figure 5.2: Patch occupancy and food chain length in a one-dimensional lattice with periodic boundaries. **a, b)** Equilibrium occupancies $u^{(k)*}$ of a three-species food chain as a function of the total colonization rate $C = 2rc$ for $r = 1$ (**a**) and $r = 100$ (**b**). Solid lines: analytical results obtained by Eq. 5.4; discrete marker: stochastic simulation results, averaged over 50 repetitions for each value of r and C . **c)** Stationary solution to the ODE model Eq. 5.3 for larger food chains. Black line: equilibrium occupancy u^* as function of the trophic level k for $C = 20$, following the quadratic decrease from Eq. 5.4. Blue line: persistence threshold C_t as function of the trophic level k , following the quadratic increase from Eq. 5.5. **d)** Dependence of food chain length on the total colonization rate C . Maximal possible trophic level k_{\max} : exact result from Eq. 5.6 (black) and approximation $k_{\max} \approx \sqrt{2C/e} - 1$ (yellow). Average food chain length L : exact result from Eqs. 5.2 and 5.4 (blue) and approximation by Eq. 5.7 (red). The inset shows the dependency of L on C on a double logarithmic plot. To guide the eye, the black dotted line shows a power law $L \sim C^{0.5}$. Parameter values: $e = 1$ and $N = 1000$ patches.

fraction of k -occupied patches. For the basal species Eq. 5.3 is essentially the same as the metapopulation equation introduced by Levins (1969). Note, that due to neglecting spatial correlations the equations for a closed lattice are the same as those for mixed space (Pillai et al., 2010; Calcagno et al., 2011; Gravel et al., 2011a).

Setting the right hand side of Eq. 5.3 to zero we find that the k -th species has an equilibrium occupation probability of $u^{(k)*} = u^{(k-1)*} - k(e/C)$ (Pillai et al., 2011). This can be solved to

$$u^{(k)*} = 1 - \frac{e}{2C}k(k+1), \quad (5.4)$$

where negative values can be considered as equivalent to zero. As expected, species at lower trophic levels have higher occupation probabilities. This is shown in Fig. 5.2 (a, b) for a food chain with $S = 3$ species, where we plot the expected fraction of occupied patches, $u^{(k)*}$, for each species as function of the total colonization rate C . Since for fixed $C = 2rc$, the occupation probability $u^{(k)*}$ does not depend on r , we obtain the same analytical results for $r = 1$ and $r = 100$. This is in striking contrast to direct simulations of the stochastic processes (marked symbols in Fig. 5.2 a, b). While for $r = 100$ the analytical results from Eq. 5.4 coincide well with the stochastic simulation, for $r = 1$ the analytical results strongly overestimate the occupation probabilities. For a given species, this discrepancy between analytical and stochastic calculations decreases with increasing colonization rate and both approaches practically coincide for $r \geq 100$.

For both colonization ranges, for the stochastic as well as the ODE approach, and for all species, we observe a transition from a regime

in which the species is extinct, $u^{(k)*} = 0$, to a regime in which $u^{(k)*} > 0$. The critical value $C_t^{(k)}$ at which this transition occurs, the *persistence threshold* of species k , increases with the trophic level. As seen from the stochastic simulation results in Fig. 5.2 (a, b), the persistence thresholds are larger for $r = 1$ than for $r = 100$. For example, $C_{t,r=1}^{(1)} = 3.2$, $C_{t,r=1}^{(2)} = 8.1$ and $C_{t,r=1}^{(3)} = 14.9$ compared to $C_{t,r=100}^{(1)} = 1.2$, $C_{t,r=100}^{(2)} = 3.2$ and $C_{t,r=100}^{(3)} = 6.4$. Again, for sufficiently large colonization range the persistence thresholds obtained by direct simulation coincide with that from the ODE model.

By setting Eq. 5.4 to zero, we can calculate the persistence thresholds in analytic form, showing that the $C_t^{(k)}$ increase quadratically with the trophic level

$$C_t^{(k)} = \frac{ek(k+1)}{2}. \quad (5.5)$$

This is shown in Fig. 5.2 (c). For example, the sixth species in the food chain would be able to persist for a colonization rate of $C/e > 21$. Thus, with further increase of C an arbitrarily long food chain theoretically becomes possible. As further shown in Fig. 5.2 (c), the quadratic increase of the persistence threshold with k goes together with a quadratic decrease of the equilibrium occupancy. Thus, for $C = 20$ five species would be able to persist, while the occupation probability of the sixth species would be negative and thus zero. For a given value of the colonization rate only a finite number of species can survive, even when potentially allowing an infinite number of species.

Finally, in Fig. 5.2 (d) we investigate the dependence of the food chain length on the colonization rate C . By setting Eq. 5.4 to zero and solving for k instead of C we obtain the maximal

trophic level, k_{\max} , found in the system as

$$k_{\max} = \text{floor} \left(-\frac{1}{2} + \sqrt{\frac{1}{4} + 2\frac{C}{e}} \right), \quad (5.6)$$

which increases as $k_{\max} \approx \sqrt{2C/e} - 1$ for large C . This maximal possible length of a food chain in the system is larger than the average food chain length, L , because locally species continuously go extinct, yielding a reduction of the average food chain (blue line in Fig. 5.2 d). Using Eq. 5.2 and summing up the terms in Eq. 5.4 from $k = 1$ to the upper bound $k_{\max} \approx \sqrt{2C/e} - 1$, we can approximate the average food chain length as

$$L \approx \frac{2}{3} \sqrt{\frac{2C}{e}} - 1. \quad (5.7)$$

Thus, the average food chain length roughly scales with the square root of the ratio of colonization and extinction rates. This power-law increase with C is superposed by slight irregularities at the persistence thresholds (see Fig. 5.2 d). Note, that this result, and the quadratic decay of patch occupancy with C in Eq. 5.4, is in contrast to a previous estimation of the food chain length $L \leq C/e + 1$ (Gravel et al., 2011a). These authors, however, did not consider bottom-up extinctions.

Mid-domain effect in a one-dimensional domain

Next, we investigate the influence of hard boundaries in a one-dimensional lattice. For this, we simulate the dynamics of a food chain (with an in principle arbitrary number of species) on a one-dimensional lattice with $N = 1000$ patches and hard boundaries. We

are interested in the spatial profile of occupation probabilities of all surviving species, and the resulting food chain length, resolved to individual patches. As before, we parametrize our model by the total colonization rate $C = n(r)c$, but for a lattice with hard boundaries we define $n(r)$ as the number of neighbours of a non-boundary patch. In the simulations, we pay specific attention to the total colonization rate $C = 20$, but repeated the simulations for a large range of C values. Our simulation runs, shown exemplary in Fig. 5.3, confirm that for sufficiently large colonization range ($r = 100$), we obtain an excellent agreement between the ODE approach and stochastic simulations also in the spatially explicit non-homogeneous system, similar to the case of a spatially homogeneous system (Fig. 5.2) where we used spatial averages.

In a homogeneous system we found that for a total colonization rate of $C = 20$ a number of $S = 5$ species are able to persist (Fig. 5.2 d). As shown in Fig. 5.3, this result holds true also in a one-dimensional lattice with hard boundaries (see also Appendix 5.A, Fig. 5.6, showing a characteristic spatial profile from the stochastic model). Additionally, we observe a clear MDE: All species show a clear plateau in the inner parts (mid-domain) of the lattice and decay in occupation probability towards the boundary. The transition from the plateau to the boundary occurs roughly at patch r , though the transition is less sharp for higher trophic levels. On the other hand, the MDE is more pronounced for species at higher trophic levels that have overall smaller occupation probabilities. Since according to Eq. 5.2 food chain length is the sum of the occupation probabilities of all species, the food chain length must inherit the MDE pattern from the single species. Fig. 5.3 (b) confirms that this

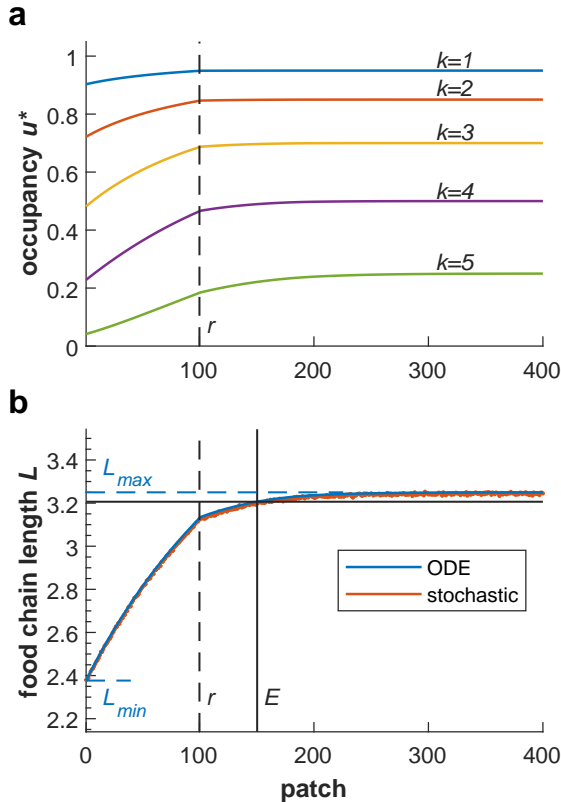


Figure 5.3: Mid-domain effect and spatial profile of food chain characteristics in a one-dimensional lattice with hard boundaries. **a)** Equilibrium occupancy u^* as a function of patch number for different trophic levels, from $k = 1$ (blue) to $k = 5$ (green), obtained from numeric simulation of the ODE model, Eq. 5.1. Since the solution is spatially symmetric, only the left part (patches 1 to 400) is shown. **b)** Corresponding food chain length L , obtained from the ODE model (blue line) and from temporally averaged stochastic simulations (red dots). The horizontal black solid line marks the 95% value between L_{\min} and L_{\max} (see Eq. 5.9) and the solid vertical line marks the corresponding edge length E . The dashed vertical line marks the colonization range r . Note that the figure shows time averaged quantities; a snapshot of a corresponding stochastic simulation is shown in Appendix 5.A, Fig. 5.6. Parameter values: number of patches $N = 1000$, colonization range $r = 100$, total colonization rate $C = 20$, extinction rate $e = 1$.

is indeed the case. Both ODE and stochastic simulations reveal a clear MDE for food chain length, meaning that food chain length also reaches a plateau value in the middle of the domain and decreases towards the boundary.

To characterize the MDE, we first measure the maximal average food chain length L_{\max} within the plateau in the interior of the lattice and the minimal average food chain length L_{\min} at the boundary of the lattice. Based on these values we define the relative strength of the MDE as the ratio

$$R_L = (L_{\max} - L_{\min}) / L_{\max}. \quad (5.8)$$

In general, this index measures the relative magnitude of the decay of the food chain length towards the boundaries. It is bounded by $0 \leq R_L \leq 1$ and larger values indicate a stronger spatial decay. For the example, shown in Fig. 5.3, we obtain the values $L_{\min} = 2.38$ and $L_{\max} = 3.25$, yielding a MDE strength of $R_L = 0.27$. Note that L_{\max} does not give the maximum number of species or trophic levels that can persist in the middle of the lattice (that would be $S = 5$ in this example), but instead gives the maximal value of the expected food chain length (see previous subsection).

While the index R_L measures the ‘vertical’ aspect of the MDE in Fig. 5.3, we next define a measure for the ‘horizontal’ aspect, that is, the characteristic spatial scale of the MDE. For this we define the edge length E as the distance to the boundary at which the food chain length reaches the level

$$\begin{aligned} L_E &= L_{\min} + 0.95(L_{\max} - L_{\min}) \\ &= 0.05L_{\min} + 0.95L_{\max}, \end{aligned} \quad (5.9)$$

that is, the level at which the food chain length has increased from its boundary value L_{\min} by

95% of its range between L_{\max} and L_{\min} . For the example shown in Fig. 5.3 we find $E \approx 150$ which is in the same order as the used value of the colonization range $r = 100$. Thus, the colonization range defines a characteristic spatial scale of the MDE and approximately separates the plateau from the boundary regime over which the food chain length declines.

Next, we explore the dependence of the MDE indices on the total colonization rate C . This is shown in Fig. 5.4 for maximal and minimal food chain length, L_{\max} and L_{\min} , the relative MDE strength R_L , and the normalized edge length E/r . As expected from Fig. 5.2, L_{\max} and L_{\min} increase with increasing C (Fig. 5.4 a). Since L_{\max} increases faster, the absolute strength of the MDE, $L_{\max} - L_{\min}$, is an increasing function of C as well. The relative strength, R_L , on the other hand, on average is a decaying function of C (Fig. 5.4 b). The MDE is thus stronger for longer food chains in absolute numbers, but weaker on a relative scale.

As shown in Fig. 5.4 (b) the relative edge length is largest at the persistence threshold of the first species at which the food chain starts to exist. For increasing C the edge length has a decreasing tendency, though this tendency is superposed by an oscillating pattern, where typically minima of E/r arise at the persistence thresholds of additional species. The magnitude of these irregularities decreases with increasing C since the effect of a newly persistent species is weaker the more species are already present in the community. The relative edge length roughly converges to $E/r \approx 1.5$ which is also the value that we found in Fig. 5.3. In Appendix 5.B, Fig. 5.7 we elaborate on the dependence of the edge length E on the coloniza-

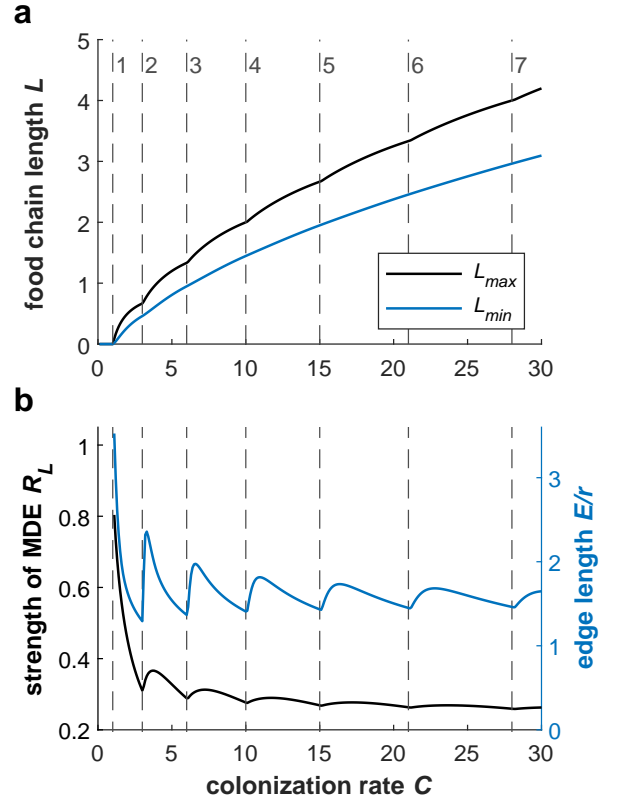


Figure 5.4: Several MDE quantifiers as functions of the total colonization rate C on a one-dimensional lattice ($N = 1000$ patches, hard boundaries, colonization range $r = 100$). Dashed vertical lines mark the persistence thresholds $C_t^{(k)}$ of species $1 \leq k \leq 7$, see Eq. 5.5. For $C < C_1^{(k)}$ no food chain exists. Most quantities show an irregular behaviour at the persistence thresholds. **a)** Plateau chain length L_{\max} (black) and boundary chain length L_{\min} (blue). **b)** Relative MDE strength R_L (black) and edge length normalized by colonization range E/r (blue).

tion range r . We find that for increasing r , food chain length L_{\max} and L_{\min} quickly converge to the values already observed in Fig. 5.3 ($L_{\max} \rightarrow 3.25$ and $L_{\min} \rightarrow 2.38$) (Appendix 5.B, Fig. 5.7 a). For sufficiently large r (≥ 30) the edge length becomes a linear function of the colonization range, $E \approx 7.2 + 1.5r$ (Appendix 5.B,

Fig. 5.7 b). From a theoretical point of view, these results imply that r (if not too small) primarily serves as a spatial scale while relevant results (L_{\max} , L_{\min} and E/r) are independent of r . This underlines the role of C being essentially the only free parameter in the system and justifies why we usually consider the ratio E/r .

Similar to the irregularities observed in Fig. 5.4, also in Fig. 5.7 in Appendix 5.B we can observe irregularities in the behaviour of L_{\max} , L_{\min} and E , in the regime of small r . These irregularities occur exactly at the ‘persistence thresholds’ of the fourth and fifth species. The term ‘persistence threshold’ is here not meant with respect to the total colonization rate C but with respect to the colonization range r . For $r < 11$ only four of the five species are able to persist. For $r < 3$ the fourth species goes regionally extinct as well. Even though the total colonization rate is constant, a large colonization range has a stabilizing effect on the food chain. This can be understood by acknowledging that for larger r the effective distance between patches becomes smaller and that there are more alternative paths from one patch to another. For small r the dynamics are less robust and local extinctions do more often lead to regional extinctions. Note, that we have already seen this effect in Fig. 5.2 (a, b), where for $r = 1$ the persistence of any species required a significantly larger colonization rate than for $r = 100$.

We can calculate L_{\max} and L_{\min} analytically, by directly solving the set of equations (5.1) with an approximate ansatz. To this end we use a

continuous limit of Eq. 5.1

$$\begin{aligned} \frac{du^{(k)}(x)}{dt} = & c \left(u^{(k-1)}(x) - u^{(k)}(x) \right) \\ & \cdot \int_{\max\{0, x-r'\}}^{\min\{1, x+r'\}} u^{(k)}(y) dy \\ & - keu^{(k)}(x). \end{aligned} \quad (5.10)$$

Here, the discrete patches are replaced by continuous space ($i \rightarrow x, j \rightarrow y$) and the sum over i 's neighbours is now an integral over x 's colonization range, which is $x \pm r'$ if we are not too close to the boundary. The total habitat is normalized to be of unity length. In order to use the same range-to-habitat-size ratio as before ($r = 100, N = 1000$) we set the normalized colonization range to $r' = 0.1$. To find the equilibrium occupation probabilities $u^{(k)*}(x)$ we set the left hand side of Eq. 5.10 to zero. The resulting set of equations for different trophic levels k has to be solved iteratively, since the equation for species k depends on the solution for species $k - 1$. Only the basal species depends on no other species. To solve the integral in Eq. 5.10 we assume for each single $u^{(k)}(x)$ a linear growth from the boundary value $u_{\min}^{(k)}$ to the plateau value $u_{\max}^{(k)}$ over an edge of length r' . In Fig. 5.3 (b) we have seen that this approximation is not entirely correct. But incorporating more details into the calculation (e.g. replacing the range r by our previous definition of the edge length E) does not improve the result. We therefore prefer to employ the simpler approach that only depends on qualitative observations instead of quantitative results. Within our approximation, it is straightforward to solve the integral in Eq. 5.10. By further using Eq. 5.2 we obtain for $C = 20$ the analytical food chain length results $L_{\min}^{\text{ana}} = 2.38$ and $L_{\max}^{\text{ana}} = 3.25$

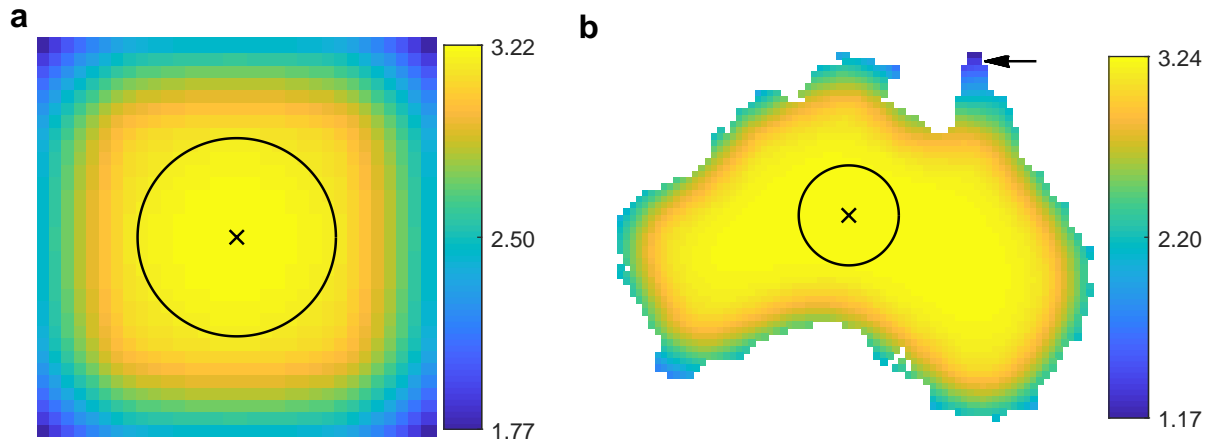


Figure 5.5: Mid-domain effect in a two-dimensional domain. The figure shows the patterns of food chain length on a two-dimensional square lattice (**a**, $N = 32 \times 32$ patches) and an analogous lattice placed on the mainland of Australia (**b**, $N = 2801$ patches). In both cases we used hard boundaries, colonization range $r = 8$ as depicted by the circles, and total colonization rate $C = 20$. On both networks food chain length shows a clear MDE, with the largest value attained at the center. The respective minima are attained at the corners (square lattice), and at the north-eastern land tongue marked by the arrow (Australia).

which coincide with the values extracted from Fig. 5.3 (b).

Mid-domain effect in a two-dimensional domain

Finally, we explore whether the results from the previous sections hold also in a two-dimensional domain. For this we repeated the ODE simulations for the case $C = 20$ on a two-dimensional square lattice ($N = 32 \times 32 = 1024$ patches) and on a two-dimensional lattice placed on the mainland of Australia ($N = 2801$ patches). For the colonization range, that is now a radius, we used $r = 8$. This amounts to $n(r) = 196$ neighbours (roughly $\pi r^2 \approx 201$) for any central patch that is not too close to any boundary. The connectivity of the networks is thus comparable to our choice in the one-dimensional case with $n(r) = 200$ for a colonization range of $r = 100$.

We considered again hard boundaries and were interested in the food chain length resolved to individual patches.

Our numerical simulation (Fig. 5.5) demonstrates that the MDE emerges also on spatial networks embedded in two-dimensional space. In fact, the effect in two dimensions is even more pronounced than in the one-dimensional case. For the relative strength of the MDE we find $R_L = 0.45$ for the square lattice and $R_L = 0.64$ for the lattice placed on the mainland of Australia (for the one-dimensional lattice it was $R_L = 0.27$). We used a total colonization rate of $C = 20$ in all cases so that the results can be properly compared, and differences are caused only by the different spatial structures.

Using the same total colonization rate implies that we should find the same maximal chain length in all cases. For the example shown in

Fig. 5.5 we find that this is true at least approximately ($L_{\max} = 3.22$ for the square lattice and $L_{\max} = 3.24$ for Australia compared to $L_{\max} = 3.25$ for the one-dimensional lattice). The reason for the small differences is related to the total extension of the domains, used in the simulation. In our finite two-dimensional networks a larger fraction of patches belongs to the boundary and a smaller fraction belongs to the mid-domain. As a result, the lattice size is too small to support a true mid-domain plateau. We repeated the simulations for larger networks with a larger mid-domain to boundary ratio (i.e., having more patches but the same value of r) and found that the maximal food chain length indeed increased to $L_{\max} = 3.25$ for both two-dimensional structures.

The differences in the relative strength R_L , observed in different network topologies, are caused by differences in the minimal chain length L_{\min} . For the square lattice we observe $L_{\min} = 1.77$ at the outmost corners, and for Australia we find $L_{\min} = 1.17$ at the north-eastern land tongue marked by the arrow in Fig. 5.5. Note, that in the one-dimensional case we had $L_{\min} = 2.38$.

5.4 Discussion

In this study we calculated the colonization-extinction dynamics of a food chain in spatial networks of different topologies. We found that the persistence and occupation probabilities of all species in the chain, as well as the fit between the stochastic and the ODE approach, strongly depend on the colonization range r . A larger colonization range makes spread and persistence easier for all species. This happens even when the per-neighbour colonization rate

is simultaneously decreased in such a way that the total colonization rate C remains constant. This can be understood by the following two arguments: (1) For all species a larger colonization range (i.e., shorter path lengths between patches) means that empty patches can typically be (re)colonized faster (see also Barter and Gross, 2017). This increases robustness against local extinctions. (2) For species at higher trophic levels we can further interpret the colonization range as the species' ability to traverse through unsuitable habitat patches, where the required prey species is absent. For small ranges the remaining suitable patches are more likely to be disconnected, which strongly diminishes the species' colonization ability.

The large deviation between the results of the stochastic and the ODE approach for $r = 1$ can be understood as follows: For small ranges the slow step-wise propagation of a species through the habitat network implies that occupied patches tend to form clusters, i.e., lie next to each other. This leads to strong correlations between the occupation status of adjacent patches (see also Newman, 2010). For larger values of the colonization range these correlations are much weaker, first since there exist much more alternative paths through the network, and second because the average distance between patches is much shorter. For this reason, the agreement between the ODE approach, that neglects these correlations, and the stochastic approach, that contains these correlations, improves with larger colonization ranges (Fig. 5.2 a, b). Note that it is possible to augment the ODE approach to partially include the correlations. This would require, however, additional and more complex equations, at the same time still being only an approximation (New-

man, 2010).

In the ODE approach used here, a lattice with periodic boundaries is formally equivalent to fully mixed space. To actually obtain fully mixed space from our one-dimensional lattice with periodic boundaries, we could use a colonization range $r \geq N/2$. In Eq. 5.3 the colonization range does, however, enter only implicitly via the number of neighbours per patch, $n(r)$, which is absorbed into the total colonization rate C . Accordingly, Eq. 5.4 shows that in equilibrium the fraction of occupied patches depends only on C , and not explicitly on the range r . The structure of the spatial network does also not enter the equation in any other way. This means that in our ODE approach we obtain the same results for $r = 1$, an actual lattice with only next-neighbour interactions, and for $r \geq N/2$, i.e., fully mixed space.

We found that the fraction of occupied patches decreases with trophic level, see Eq. 5.4 and Fig. 5.2 (a, b, c). This result is not surprising and has already been observed, e.g., by Pillai et al. (2011). It is simply a consequence of the fact that species at higher trophic levels can make fewer colonizations, as they are restricted to patches where their prey is present, and go extinct more frequently due to bottom-up extinctions. Both effects inhibit the spread of the species. The increase of the persistence threshold with trophic level, see Eq. 5.5 and Fig. 5.2 (d), is then simply a consequence of the decrease of the occupation probabilities. As another remarkable result we found that the average food chain length roughly increases with the square root of the ratio of colonization and extinction rates. This result deviates from previous estimation of the food chain length (Gravel

et al., 2011a) which, however, did not consider bottom-up extinctions.

The most notable finding of this study is the MDE for food chain length. The effect can be explained as a direct consequence of the underlying spatial structure. Habitat patches close to the boundary have a smaller number of neighbours and thus receive fewer incoming colonizations. Since outgoing colonizations do not take away anything from the source patch, and since extinctions are purely local events, having fewer neighbours has no other counteracting positive effects. A fewer number of neighbours thus leads to smaller species occupation probabilities and consequently to shorter food chains.

We want to stress that the MDE for food chain length emerges in the absence of any environmental gradients, except for the existence of the boundaries; it is solely caused by spatial constraints and can thus be considered a null expectation for spatial patterns of food chain length. Thereby, the MDE is not supposed to fully explain an actually observed pattern, such as food chain length or (traditionally) species richness. The MDE should rather be part of a multivariate explanation (Colwell and Lees, 2000; Jetz and Rahbek, 2002; Colwell et al., 2004). Other factors potentially contributing to observed spatial patterns are heterogeneities in temperature, productivity, habitat diversity, or even ‘historical gradients’ like time since the last glaciation, see for example Colwell et al. (2004) and Jetz and Rahbek (2002) and references therein. We also want to point out that, while there is no environmental gradient (other than the boundary) as input to our model, the model generates its own gradients for species at higher trophic levels (see Fig. 5.3 a). The mid-domain pattern of

the occupation probability of the basal species is solely caused by the spatial constraints. Due to the dependence of higher trophic levels on lower ones, the patch occupancy of a higher level is additionally influenced by the occupation pattern of the next lower one. In this way the MDE cascades up the food chain, being stronger for species at higher trophic levels and finally leading to a significant MDE for food chain length. The mechanistic explanation of the MDE for food chain length, as presented here, slightly deviates from the classic explanation of the MDE for species richness. The MDE is classically explained by randomly placing species ranges into a large habitat (Colwell and Hurtt, 1994; Colwell and Lees, 2000; Jetz and Rahbek, 2001). The mid-domain peak or plateau of species richness then emerges since the centers of these ranges must not lie too close to the boundary in order to not overlap with the inhabitable zone. This theory, even though being very compelling, is not sufficient to explain a MDE for food chain length. In this framework it is not sufficient that the richness at all trophic levels decline towards the boundary. A MDE for food chain length, i.e., a decline in the number of trophic levels towards the boundary, can only arise if the richness at higher trophic levels decline more rapidly than that at lower trophic levels. To obtain this, we would need to require that species ranges increase with the trophic level, which however seems not to be supported by empirical evidence. While a scaling with body mass, and thus with trophic level, has been well established for the home range of a species, i.e., the area or territory in which an individual animal lives and moves on a periodic basis (Jetz et al., 2004), there is no evidence that the same holds true for the species range, i.e., the full geo-

graphic area where all individuals of a particular species can be observed (Gaston, 1996).

In addition, there are several noteworthy differences between the MDE for food chain length and the classical MDE for species richness as described by Colwell and Hurtt (1994): (i) Classically, species ranges span only over a fraction of the totally available habitat. In our case, species span over the full habitat. In the absence of any additional factors that shape occupation patterns, this result is only natural. (ii) Classically, species ranges are cohesive (but for exceptions see for example Grytnes and Vetaas, 2002; Dunn et al., 2006). In our case, at a given point in time, species ranges are highly fragmented (see Appendix 5.A, Fig. 5.6). Only at the level of expected values, i.e. time averages, do species ranges appear to be continuous. In real data the fragmentation might be caused by undersampling but also by actual breaks in species ranges (Dunn et al., 2006). (iii) Classically, species richness declines to zero at the boundary (but for exceptions see for example Jetz and Rahbek, 2001; Grytnes and Vetaas, 2002). In our case food chain length declines to non-zero values at the boundary.

Even though the MDE for species richness has been subject to criticism (Bokma et al., 2000; Laurie and Silander, 2002; Colwell et al., 2004), it has become clear that boundary constraints affect spatial patterns of species richness. This should also be true for patterns of food chain length, i.e., we assume that the MDE for food chain length will also be observed when changing details of the model, or when using an entirely different one, as long as spatial constraints are included. Spatial constraints should thus always be considered as one possible explanatory

factor for spatial patterns of food chain length (or any other ecologically interesting quantity).

We observed that the MDE characterized by its relative strength R_L is stronger for two-dimensional habitats (e.g., $R_L^{(2d, \text{Australia})} = 0.64$ and $R_L^{(2d, \text{square})} = 0.45$) than for the one-dimensional lattice (e.g., $R_L^{(1d)} = 0.27$). This observation is in agreement with our general explanation of the MDE for food chain length in our model, i.e., that the MDE is caused by the fewer number of neighbours of boundary patches compared to central patches. The larger this difference becomes, the stronger the MDE should be. The ratios of the number of neighbours of the outmost boundary patches to central patches, n_{bound} , were $n_{\text{bound}}^{(1d)} = 0.5$, $n_{\text{bound}}^{(2d, \text{square})} = 0.29$ and $n_{\text{bound}}^{(2d, \text{Australia})} = 0.16$. As expected, the decreasing tendency of n_{bound} matches the increasing tendency of R_L .

In this study we were mainly concerned with a theoretic exploration of the MDE for food chain length and we leave it as a challenge for future work to test our theoretic predictions in field data. One simple reason for this focus of our study is that empiric data on spatial food web structure are hard to come by. While topological aspects for food webs at single patches have been characterized in depth (Thompson et al., 2012), data on spatial food web structure are scarce. Nevertheless there are empirical observations that suggest an MDE for food chain length. For example, it has been well established in fisheries that large top-predatory fish are dominantly observed in mid ocean, but are rarely observed in coastal areas (Worm et al., 2003). In another study, Komonen et al. (2000) observed that a food chain consisting of the bracket fungus *Fomitopsis rosea*,

the tineid moth *Agnathosia mendicella* and the parasitic tachinid fly *Elfia cingulata*, reduced to the first one or two trophic levels in isolated forest fragments. For more complex spatial structures it becomes more difficult to classify patches into boundary and central, or isolated and non-isolated patches. In fact, a continuous ‘degree of connectedness’, in network theory known as centrality measures (Newman, 2010), is needed to properly characterize patches. For our lattices we simply used the distance to the boundary as such a measure, but for more complex networks the choice of centrality measure is less straight forward. Properly quantifying and predicting spatial patterns of food chain length on arbitrary habitat networks could thus prove challenging.

In general, not only the spatial structure but also the food web structure will be more complex than studied here. In our spatial setting, the mechanism causing the MDE, i.e., the smaller number of neighbours in boundary patches, is rather generic and does not depend on the food web structure or the nature of the trophic interactions. More complex food webs and top-down effects could, however, have additional effects that might alter the mid-domain pattern. For example, the decrease of the occupation probability of one species towards the boundary could open a niche for other species better adapted to this range, but that are out-competed in the mid-domain. Such community effects might well lead to more complex spatial profiles, possibly yielding even an inverted mid-domain pattern. Additionally, an interesting avenue for further explorations would be to extend this analysis to the spatial patterns of other food web properties, such as connectance or food web branching (Martinez, 1991; Thomp-

son et al., 2012), in particular when investigating more complex food webs.

Acknowledgements This work was supported by the German Research Foundation (DFG) as part of the research unit 1748.

Author Contributions BB conceived the study, KvP implemented the model, both authors prepared the manuscript.

Conflict of interest The authors declare that they have no conflict of interests

5.A Appendix 1: Snapshot of a stochastic simulation in a one-dimensional habitat

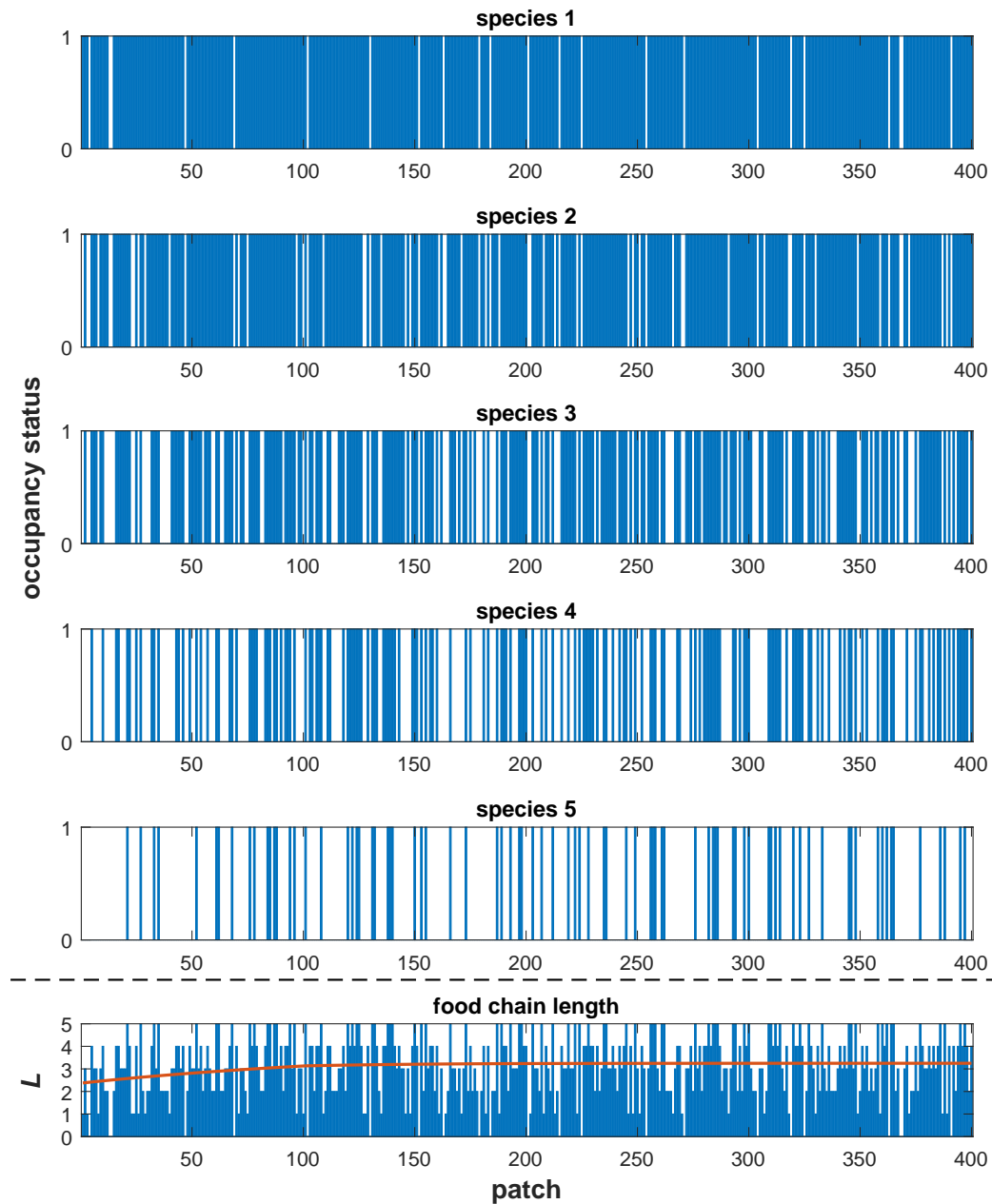


Figure 5.6: Snapshot of a stochastic simulation in a one-dimensional habitat with hard boundaries, depicting the characteristic rough spatial profile in a colonization-extinction model. The top five rows plot the occupancy status (1 if patch is occupied and 0 if patch is empty) of species 1 to 5 at one time instance as a function of the patch number, respectively. The bottom panel shows the corresponding food chain length. For comparison, the average food chain length is shown as red line. Due to random extinction and colonization events the instantaneous spatial profile stochastically deviates from the smooth averaged profile, yielding highly fragmented species ranges. Nevertheless, expected patch occupancies and food chain length decrease towards the boundary of the habitat, revealing a mid domain effect of food chain length. Parameters as in Fig. 5.3: number of patches $N = 1000$, colonization range $r = 100$, total colonization rate $C = 20$, extinction rate $e = 1$, only the left part (patches 1 to 400) is shown.

5.B Appendix 2: Food chain length and edge length vs colonization range

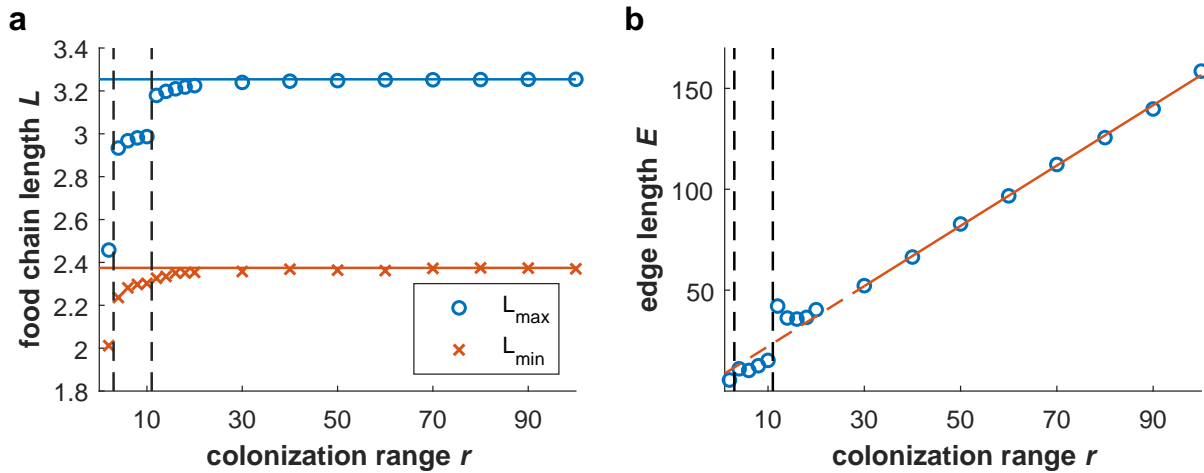


Figure 5.7: Dependence of MDE properties on the colonization range. **a)** Plateau food chain length L_{\max} (blue circles) and boundary food chain length L_{\min} (red crosses) as a function of the colonization range r . **b)** The same as (a) but for the edge length E . The spatial network is a one-dimensional lattice with $N = 1000$ patches and hard boundaries. Since we are also interested in small values of r , for which the ODE approach might yield erroneous results (see Fig. 5.2), we use the stochastic approach. For each value of r we run the stochastic simulations only once, but exemplary repetitions indicate that the results are robust. In all runs each patch was initialized with a probability of 0.5 to be occupied by the whole food chain. We fix the total colonization rate to $C = 2rc = 20$ and thus compensate an increase of r by a decrease of the per-neighbour colonization rate c . The extinction rate is as always set to $e = 1$. For $C = 20$ in principle $S = 5$ species should be able to persist. The dashed vertical lines indicate persistence thresholds (with respect to r) of the fourth and fifth species.

6 Food chain length and the SIS centrality

The SIS centrality: Predicting spatial patterns of food chain length on random graphs

Kai von Prillwitz¹

¹Institute for Chemistry and Biology of the Marine Environment,
University of Oldenburg, Germany

Keywords colonization-extinction dynamics, spatial networks, centrality measures, multilayer networks, food webs

Abstract In Chapter 5 we found a mid-domain effect for food chain length, stating that food chain length is largest in the center of a habitat and decreases towards the boundaries even in the absence of environmental gradients. Here we aim to generalize this effect from habitats with a regular lattice structure to habitats represented by random networks. For random networks the concept of center and boundary is replaced by the concept of *centrality*, and a generalization of the mid-domain effect means that food chain length should increase with centrality. To quantify the centrality of patches we use several known centrality measures and additionally introduce a new centrality measure based on susceptible-infected-susceptible dynamics from epidemics on networks. We call our new centrality measure the *SIS centrality*. Food chain length results are obtained by simulations of spatially explicit colonization-extinction dynamics of a simple food chain. We find for all considered centrality measures that food chain length tends to increase with centrality. In our study the SIS centrality shows the strongest correlations with food chain length and is thus particularly well suited for the generalization of the mid-domain effect to random networks. Our results demonstrate how the spatial structure alone can influence the spatial pattern of food chain length in a patchy habitat. The (SIS) centrality of a patch can thus be considered as an additional determinant of food chain length, similar to factors such as primary productivity or ecosystem size.

6.1 Introduction

The mid-domain effect for food chain length, formulated in Chapter 5, states that even in the absence of other environmental gradients food chains should be shorter towards the boundaries of a habitat and longer towards the center. Food chain length results were based on a colonization-extinction model of species forming a food chain (see also Pillai et al., 2010, 2011, and Section 3.3). Habitats were represented by regular networks (or graphs; here used interchangeably), more precisely by one- and two-dimensional lattices with long-distance interactions and hard boundaries. In reality this will often be an unsuitable assumption. Instead, habitats can often be considered as being non-regularly fragmented into patches, like forests that suffer from deforestation and are interrupted by roads or other human-caused as well as natural borders (Skole and Tucker, 1993; Vitousek et al., 1997; Fahrig, 2003; Broadbent et al., 2008; Liao et al., 2017b). More examples of non-regular, patchy habitats are formations of islands in an ocean or lakes on a continent. A class of networks suited to model such habitats are random geometric graphs, where patches are embedded in two-dimensional space and are connected if they lie within a given maximal distance to each other (Gilbert, 1961; Dall and Christensen, 2002; Penrose, 2003). Other typical classes of random networks without this explicit spatial embedding are Erdős-Rényi random graphs (Erdős and Rényi, 1959, 1960, 1961) and scale free graphs (Albert and Barabási, 2002; Barabási, 2016). Generalizing the mid-domain effect for food chain length to such networks broadens its applicability to a larger class of habitats and to more realistic ones.

Translating the mid-domain effect to random networks is not straightforward as it is difficult to define boundary and center (mid-domain) of such networks. Fortunately, however, so-called centrality measures are a well known concept in network theory (Borgatti, 2005; Newman, 2010). A centrality measure tries to quantify and order the ‘connectedness’ or ‘importance’ of nodes in a network. The arguably simplest centrality measure is the degree, which is simply the number of neighbours of a node. Some more sophisticated and well known centrality measures are the eigenvector centrality (Bonacich, 1972a,b, 1987), Katz centrality (Katz, 1953), Google’s PageRank (Brin and Page, 1998), Closeness (Bavelas, 1950), and Betweenness (Freeman, 1977, 1979). If the mid-domain effect translates to random networks, we should find that food chain length increases with increasing patch centrality. Since it is unlikely that all centrality measures yield the same result, choosing the right measure is an important task.

Some centrality measures have been specifically designed with the intention to predict the outcome of dynamical processes on networks, like the spread of an epidemic. Epidemic models are related to the food web model that we use here in the sense that the colonization-extinction dynamics of each species in the food chain (in particular the basal species) are equivalent to the dynamics of a so-called *susceptible-infected-susceptible* (SIS) model from epidemics (see Section 3.5). Two measures that have been used in the context of epidemics on networks are the *Expected Force* (Lawyer, 2015) and the *k-shell* index (Seidman, 1983; Bollobás, 1984; Kitsak et al., 2010; Garas et al., 2012). These measures have been used to relate global quanti-

ties, like the size of an epidemic outbreak, to the centrality of the seed node of the infection (Kitsak et al., 2010; Lawyer, 2015). Concerning our goal to generalize the mid-domain effect for food chain length to random networks there are two main differences compared to the above application: (1) we are not interested in global quantities (like the size of an outbreak) but in results resolved to individual patches, and (2) we are not interested in results of the spread of a single infection but in results for many species forming a food web. Some work in this direction has been done by Barter and Gross (2017) who investigated how species occupancies (of several species in a food web) depend on the degree of patches and how this depends on the network type. The difference of our study is that, for the purpose of generalizing the mid-domain effect for food chain length to random networks, we are interested not in the occupancies of individual species but directly in the resulting food chain length (which in turn implies the presence of species at specific trophic levels). We furthermore relate the food chain length not only to the degree of patches but to multiple centrality measures. Our overall objective can thus be stated as follows: We want to predict the food chain length on all individual patches of a random network by the centrality of the patches. It is not clear how well currently known centrality measures perform at this task. Thus, we (1) introduce and characterize a new centrality measure specifically designed for this task and (2) exemplary and systematically compare the performance of our new measure at predicting food chain length with other known measures.

6.2 Methods

Food web model

To simulate food web dynamics and calculate food chain length we use a spatially explicit version of the colonization-extinction model by Pili-lai et al. (2010, 2011) (see also Section 3.3). As in Chapter 5 we consider a simple food chain of stacked specialists and neglect top-down effects. The spatial network, however, can now be of any form and is not restricted to regular lattices. On a given patch a species can either be present or absent. Population dynamics are neglected, assuming that they occur on a much faster time scale than the colonization-extinction dynamics. The food chain structure is enforced by the con-

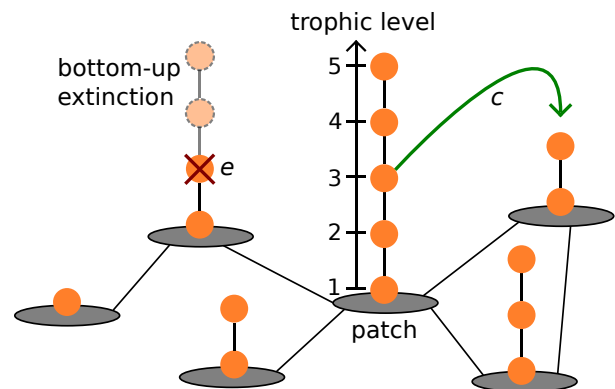


Figure 6.1: Schematic representation of the colonization-extinction model of a food chain on a random network as described in the main text. Species are represented by the orange circles and are stacked vertically on top of each other according to their trophic levels. The spatial network is represented by the grey patches and the edges between them. An extinction process (crossed out species, associated rate e) with induced bottom-up extinctions, and a colonization process between neighbouring patches (green arrow, associated rate c) are indicated. The colonization requires the presence of the colonizer's prey on the target patch.

dition that species k ($k = 1, \dots, S$) can only be present on patches on which its prey species $k-1$ is present. This means (1) that a species can only colonize a neighbouring patch if its prey is present on that patch and (2) that the extinction of a species causes all species at higher trophic levels on the same patch to go extinct as well (bottom-up extinction). Extinctions occur randomly with rate e , and with any possible colonization we associate the rate c (per-neighbour colonization rate). These rates as well as the spatial network are assumed to be identical for all species. The only difference between the species is thus their position within the food chain. Note that the basal species has access to the full network and can suffer no bottom-up extinction. Fig. 6.1 shows a schematic representation of the described model.

Simulating model dynamics and calculating food chain length

The model dynamics can in principle be described by a set of $S \cdot N$ (S : number of species, N : number of patches) differential equations for the occupation probabilities (or occupancies) $u_i^{(k)}$ of each species k on each patch i ,

$$\frac{du_i^{(k)}}{dt} = c \left(u_i^{(k-1)} - u_i^{(k)} \right) \sum_{j=1}^N A_{ij} u_j^{(k)} - k e u_i^{(k)}, \quad (6.1)$$

($u_i^{(0)} = 1$) which can be solved numerically (see Subsection 3.4.2). While these equations incorporate the explicit spatial network structure via the adjacency matrix A , spatial correlations between adjacent patches are neglected (see Subsection 3.4.1). This means that Eq. 6.1 is only an approximation to the true model dynamics,

and whereas for strongly connected networks the spatial correlations are negligible, they can make a significant difference for weakly connected networks (see Chapter 5, Fig. 5.2). Since we here consider networks with different connectivities and want the food chain length results to be as precise as possible, we refrain from the approximate differential equation approach. Instead, we use long-term stochastic simulations that automatically incorporate all spatial correlations.

To run the stochastic simulations we use the Gillespie algorithm (Gillespie, 1977) which simulates the model dynamics step by step, one colonization or extinction event after another (see Subsection 3.4.3). At each step we know exactly which species is present on which patches and we also know how much time passes until the next event is executed. This allows us to calculate the fraction of time any patch i is occupied by any species k , which is the equivalent of the above mentioned occupation probability $u_i^{(k)}$. The food chain length can then be calculated via the formula $L_i = \sum_{k=1}^S u_i^{(k)}$ (see Chapter 5, Eq. 5.2).

For given network size N and species number S we run the Gillespie algorithm for $110\,000 \cdot S \cdot N$ steps and calculate the $u_i^{(k)}$ over the last $100\,000 \cdot S \cdot N$ steps. This large averaging time is needed since patch-wise quantities converge only slowly. To choose an appropriate value for S we have to predict already before the simulations how many species will survive. We do this by first solving the corresponding differential equations (Eq. 6.1) with some large species number S' and then choose S as the number of species that have regional occupancy (spatially averaged occupation probability) larger than $1/N$. This thresh-

old value corresponds to one occupied patch in the stochastic version of the model. A species that is on average present on less than a single patch should go extinct due to stochastic fluctuations. Furthermore, for a chain of stacked specialists occupation probabilities are typically smaller in the stochastic approach than in the differential equation approach (see Chapter 5, Fig. 5.2). Thus, the value of S obtained in the above way should be an upper bound for the number of persisting species in the stochastic model. If spatial correlations are not too large (i.e. if Eq. 6.1 is a good approximation for the system dynamics) the upper bound should be tight. Note that we could artificially restrict the food chain length by running the simulations with a smaller number of species, which might affect the results presented in this chapter. We do, however, think that it is a reasonable assumption that the system is populated by all species that can possibly persist, or in other words, that all ecological niches allowed by the model are indeed occupied.

Without loss of generality we set the extinction rate to $e = 1$ for all simulations. For better comparability of results among different graphs we also fix the total colonization rate $C = \langle m \rangle \cdot c$ (typically to $C = 20$) where $\langle m \rangle$ is the mean degree of the spatial network.

Spatial networks

To cover some of the most important classes of random graphs we consider Erdős-Rényi (ER) random graphs (Erdős and Rényi, 1959, 1960, 1961), random geometric graphs (RGGs) with periodic boundary conditions (Gilbert, 1961; Dall and Christensen, 2002; Penrose, 2003), and scale free (SF) graphs generated

by the BA-algorithm (Albert and Barabási, 2002; Barabási, 2016). ER graphs are ordinary random graphs where edges between patches are placed completely at random. This gives rise to the *small-world property*, meaning that paths between patches tend to be short. RGGs have their patches randomly placed in two-dimensional space and only patches within a certain Euclidean distance to each other are connected. This explicit *spatial embedding* leads to long path lengths and strong degree correlations of neighbouring nodes. ER graphs and RGGs have, nevertheless, the same (Poisson) degree distribution. SF graphs are (ultra) small-world graphs characterized by a power law degree distribution, leading to the emergence of some highly connected patches (hubs). For more details see Section 2 and Newman (2010). All random graphs we consider here have $N = 1000$ patches since for larger graphs the stochastic food web model simulations would become extremely time consuming. We do, however, vary the network *connectivity* measured by the mean degree, $\langle m \rangle = 10, 15, \dots, 50$. For smaller connectivities RGGs and ER graphs often fall apart into different components, which we want to avoid.

Centrality measures

Since we want to investigate the relation between the topological positions of patches in the network and food chain length, we have to somehow quantify the positions of patches. Note that in contrast to the geographical position of a patch in a network, the topological position of a patch describes its connectivity to other patches (in general including non-adjacent patches) via edges of the network. Quantifying the topologi-

cal positions of patches can be accomplished by centrality measures. We consider the following known centrality measures:

The degree of a patch is the number of its direct neighbours.

The eigenvector centrality (Bonacich, 1972a,b, 1987) is the eigenvector corresponding to the largest eigenvalue of the adjacency matrix A , $x_i \sim \sum_j A_{ij}x_j$. The eigenvector centrality of a patch depends not only on the number of its neighbours but also on their centralities. We calculate the eigenvector centrality, for all patches in parallel, by using the above equation as an iteration rule starting with some initial guess. After each iteration the x_i are normalized since they would otherwise diverge to infinity. This method is also known as the *power method* and the x_i do indeed converge to the eigenvector belonging to the largest eigenvalue of the adjacency matrix (Golub and Van Loan, 1996).

The Katz centrality (Katz, 1953; see also Newman, 2010) is a generalization of the eigenvector centrality satisfying the equation, $x_i = \alpha \sum_j A_{ij}x_j + \beta$. By $\beta > 0$ a small amount of ‘free’ centrality is added to each patch. Without loss of generality one can set $\beta = 1$. The relative strength between the two terms has to satisfy $\alpha < 1/\kappa_{\max}$ where κ_{\max} is the largest eigenvalue of the adjacency matrix. We use $\alpha = 0.6/\kappa_{\max}$ which yielded comparatively good results at predicting food chain length on some exemplary graphs. We calculate Katz centrality in the same iterative way as the eigenvector centrality (but without the normalization since the x_i here converge naturally).

PageRank (Brin and Page, 1998; see also Newman, 2010) is another generalization of the eigenvector centrality satisfying the equation, $x_i = \alpha \sum_j \frac{A_{ij}x_j}{m_j} + \beta$, where m_j is the degree of patch j . Compared to Katz centrality, patches profit less from the centrality of neighbours with large degree. The offset can again be set to $\beta = 1$. The parameter α has to satisfy $\alpha < 1$ (for undirected networks) and we choose $\alpha = 0.9$, again found by initial tests at predicting food chain length on some exemplary graphs. We calculate PageRank in the same iterative way as the eigenvector centrality (but without the normalization since the x_i here converge naturally).

The Expected Force (Lawyer, 2015) estimates the potential spreading power that a node should have in an epidemic model. To this end, it is assumed that initially only the patch of interest, i , is infected and that two transmissions of the infection occur. The three then infected and connected patches are called a *cluster*. By that procedure many clusters $j = 1, \dots, J$ around patch i can be generated (some of them multiple times). Next, the *cluster degree*, d_j , of each cluster j is calculated as the number of links from patches within cluster j to patches outside of cluster j . The cluster degrees are then normalized to form a probability distribution, $\bar{d}_j = \frac{d_j}{\sum_k d_k}$. The Expected Force of patch i is finally calculated as the entropy of the distribution of the normalized cluster degrees, $\text{ExF}_i = -\sum_j \bar{d}_j \log \bar{d}_j$.

The k-shell index (Seidman, 1983; Bollobás, 1984; Kitsak et al., 2010; Garas et al., 2012) divides the network into different layers, from the outmost periphery to the most central

core. In detail, all nodes with degree $m = 1$ belong to the periphery shell, are assigned the value $k_s = 1$, and are then removed from the network. This is repeated for the remaining network until only patches with remaining degree $m \geq 2$ are left. Next, patches with remaining degree $m = 2$ are assigned the value $k_s = 2$ and the iterative removal-procedure starts again until only patches with remaining degree $m \geq 3$ are left and so on.

6.3 The SIS centrality

Here we introduce and examine a new centrality measure that we use in the next section to predict food chain length. In the introduction we mentioned the equivalence between colonization-extinction dynamics and susceptible-infected-susceptible (SIS) dynamics where, for example, the spread of an infection through a human population is modelled (see also Section 3.5). While the outcomes of SIS dynamics have been subject to being predicted by centrality measures themselves (Kitsak et al., 2010; Lawyer, 2015), we here want to use the solution of the standard SIS equation (on networks) as a centrality measure. This measure might in general be used to predict the outcomes of even more complex dynamical processes on networks. The standard SIS equation on networks reads,

$$\frac{dx_i}{dt} = \lambda(1 - x_i) \sum_j A_{ij}x_j - \mu x_i, \quad (6.2)$$

(Newman, 2010) where λ is the infection rate (the analog of the colonization rate c), μ the recovery rate (the analog of the extinction rate e),

and x_i the probability that node i is currently infected (the analog of the occupation probability $u_i^{(1)}$ of the basal species; compare to Eq. 6.1 with $k = 1$). By setting the left hand side of Eq. 6.2 to zero and rearranging appropriately we obtain,

$$x_i = \frac{[Ax]_i}{g + [Ax]_i}, \quad (6.3)$$

where we further used the shorter notation $[Ax]_i = \sum_j A_{ij}x_j$ and defined $g = \mu/\lambda$. We define the *SIS centrality* as the solution of Eq. 6.3, and g is a free parameter of the SIS centrality. To calculate the SIS centrality we use Eq. 6.3 as an iteration rule starting with some initial guess. As Katz centrality and PageRank the SIS centrality is a modification of the eigenvector centrality obtained by adding the $[Ax]_i$ in the denominator. In fact, for large g Eq. 6.3 can be approximated by the eigenvector (centrality) equation $x_i \approx \frac{[Ax]_i}{g}$. Note that when this equation is used as an iteration rule the x_i may converge to zero, but this does not affect the relation between them and can be prevented by a renormalization after each iteration. Furthermore, the SIS centrality reduces to the eigenvector centrality already before taking the limit $g \rightarrow \infty$. Since the x_i are the solution of an SIS epidemic process, and since (on most networks) the SIS model has an *epidemic threshold* (Pastor-Satorras and Vespignani, 2001a,b, 2002; Newman, 2010), all x_i converge to zero as soon as g is above this threshold. In this case the approximation $x_i \approx \frac{[Ax]_i}{g}$ of Eq. 6.3 becomes exact meaning that SIS centrality and eigenvector centrality coincide. In terms of $g^{-1} = \frac{\lambda}{\mu}$ the epidemic threshold is $g_{\text{crit}}^{-1} = \frac{1}{\kappa_{\text{max}}}$, where κ_{max} is the largest eigenvalue of the network's adjacency matrix (Newman, 2010; Goltsev et al., 2012), and the infection dies out for $g^{-1} < \frac{1}{\kappa_{\text{max}}}$.

Thus, for the parameter g the infection dies out as soon as $g > \kappa_{\max}$. Confirming this line of arguments, we find for an exemplary random geometric graph that for $g > \kappa_{\max}$ (but not for $g < \kappa_{\max}$) SIS centrality and eigenvector centrality are indeed perfectly correlated (see Fig. 6.2). Similar results can be observed for other graphs (not shown).

In the opposite case, for $g \rightarrow 0$ the SIS centrality converges to $x_i \approx 1$. As long as we still have $g > 0$ the x_i do, however, not converge exactly to 1 and the precise value of x_i will still depend on the patch i . The SIS centrality might therefore still be a useful centrality measure for small g .

For the purpose of predicting food chain length we are interested in neither of the extreme cases but aim for an intermediate g . To find a promising value we use the following heuristic approach: (1) We note that the x_i are bounded between 0 and 1. This can be seen from Eq. 6.3 and also makes sense since in Eq. 6.2 we interpreted the x_i as probabilities. (2) We want the x_i to cover a large range of values between 0 and 1 to give the SIS centrality a good ‘resolution’. (3) We argue that (2) is satisfied when the x_i are centered around 0.5, that is, $\langle x_i \rangle = 0.5$. (4) We assume that we can apply the expectation to all terms on the right hand side of Eq. 6.3 separately. This means that we apply the expectation individually to numerator and denominator as well as to adjacency matrix elements and x values. Mathematically, the latter leads to $\langle [Ax]_i \rangle = \langle \sum_j A_{ij} x_j \rangle \approx \sum_j \langle A_{ij} \rangle \langle x_j \rangle = N \cdot \frac{\langle m \rangle}{N} \cdot \frac{1}{2} = \frac{\langle m \rangle}{2}$, where we used that \sum_j includes all N patches, that each pair of patches is connected with probability $\langle A_{ij} \rangle = \frac{\langle m \rangle}{N}$, where

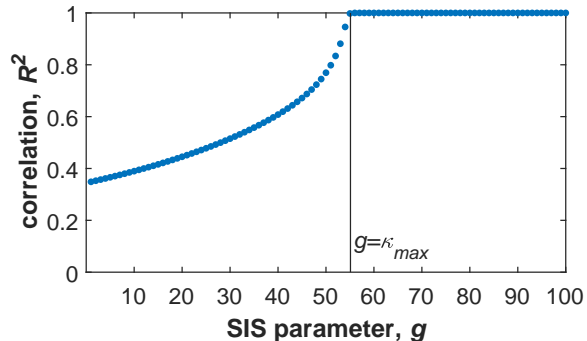


Figure 6.2: Correlation between eigenvector centrality and SIS centrality for varying SIS parameter g measured by the R^2 value of a linear fit between them. The underlying network is a random geometric graph with $N = 1000$ patches and mean degree $\langle m \rangle = 50$. After a sharp transition at $g = \kappa_{\max}$ (the largest eigenvalue of the network’s adjacency matrix) the two centrality measures perfectly coincide.

$\langle m \rangle$ is the mean degree of the network, and that according to (3) we have $\langle x_j \rangle = 0.5$. By applying this expectation to both instances of $[Ax]_i$ on the right hand side of Eq. 6.3, and also demanding $\langle x_i \rangle = 0.5$ on the left hand side, we obtain $\frac{1}{2} = \frac{\frac{\langle m \rangle}{2}}{g + \frac{\langle m \rangle}{2}}$ from which we finally find

$$g = \frac{\langle m \rangle}{2}. \quad (6.4)$$

For the graph underlying Fig. 6.2 the value $g = \frac{\langle m \rangle}{2} = 25$ lies roughly in the middle between the extreme cases $g = 0$ and $g = \kappa_{\max} \approx 55$. In the following section, and in general when not specifying the parameter, we implicitly use $g = \frac{\langle m \rangle}{2}$.

6.4 Predicting food chain length

In this section we investigate how well centrality measures fit simulated food chain length results and thus how well they are suited for the generalization of the mid-domain effect for food chain

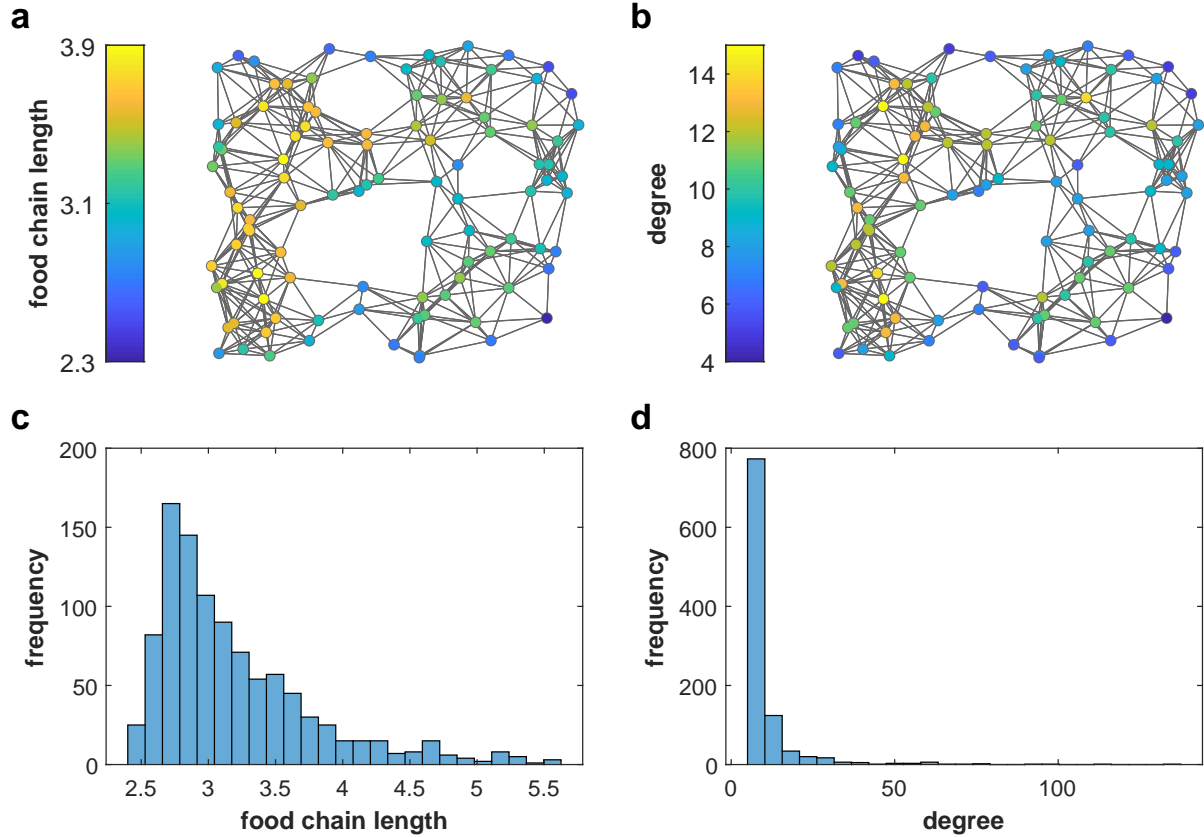


Figure 6.3: **a, b**) Patterns of food chain length **(a)** and degree **(b)** on a small random geometric graph (with hard boundaries). **c, d**) Distributions of food chain length **(c)** and degree **(d)** on a scale free graph with $N = 1000$ patches.

length to random networks. For a first impression we start by comparing the patterns of food chain length and the degree on a small random geometric graph (Fig. 6.3 a, b). The patterns are qualitatively similar but food chain length is large not only on high-degree patches but also on surrounding patches with smaller degree. In other words, to some extent the food chain dynamics even out degree differences. The second observation is that food chain length spans over a much smaller range, also on a relative scale, of values ($2.3 < L < 3.9$) compared to the degree

($4 < \text{degree} < 15$). Both observations are even more pronounced on the scale free graph underlying Fig. 6.3 (c, d). The distribution of food chain length values is much less widely-spread and more even than the scale free degree distribution. Here, food chain length ranges only between $2.4 < L < 5.6$ compared to the long tailed degree distribution with $5 < \text{degree} < 137$. We conclude from this first impression that the degree will not be the most accurate predictor of food chain length.

Relation between centrality measures and food chain length on two exemplary graphs

In order to quantitatively assess the agreement between food chain length and degree (or any other centrality measure) we calculate the R^2 value of a linear fit between them. We use a linear fit, first since R^2 then amounts to the square of the usual Pearson correlation coefficient between the two quantities, and second since we want to avoid the search for the optimal functional form or variable transformation for each individual centrality measure. In the worst case we might have to repeat this optimization for each spatial network, or at least for each network type. By always using linear fits we thus intentionally favor centrality measures with the most simple relation to food chain length. The goodness-of-fit statistic R^2 is bounded between 0 and 1, where 1 indicates perfect correlation and 0 corresponds to no correlation at all. For an exemplary random geometric graph with $N = 1000$ patches and mean degree $\langle m \rangle = 25$ we find $R_{\text{deg}}^2 \approx 0.93$ for the linear fit between food chain length and degree (upper left panel of Fig. 6.4 a). Given the simplicity of the degree this fit is remarkably good, but we observe both a small systematic deviation of the data points from the line (systematic error) as well as moderate scattering of the data points (statistical error). Beyond that, the observation that food chain length tends to increase with the degree is exactly what we expect and require for the generalization of the mid-domain effect for food chain length to random networks.

For the same graph we also investigate the relation between food chain length and the other centrality measures introduced in the *Methods*

(eigenvector centrality, Katz centrality, PageRank, Expected Force, and k-shell index) and the SIS centrality from the previous section (next six panels of Fig. 6.4 a). As for the degree, we find for all centrality measures that food chain length tends to increase with centrality. The centrality measure with the best fit to food chain length is the SIS centrality, resulting in an almost perfect line ($R_{\text{SIS}}^2 \approx 1.00$). At least for the random geometric graph considered here, the SIS centrality is thus perfectly suited for the generalization of the mid-domain effect for food chain length to random networks. The SIS centrality is closely followed by the Expected Force ($R_{\text{ExF}}^2 \approx 0.99$) and the third best measure is already the degree ($R_{\text{deg}}^2 \approx 0.93$). The eigenvector centrality is the worst measure ($R_{\text{eigen}}^2 \approx 0.19$) mostly since a large fraction of patches has eigenvector centrality close to zero. The difference between statistical and systematic error can best be seen when comparing the fits for Katz centrality and PageRank. Katz centrality ($R_{\text{Katz}}^2 \approx 0.88$) and food chain length form a concave function with minimal scattering, corresponding to a systematic error. For PageRank ($R_{\text{PRank}}^2 \approx 0.75$), on the other hand, there is no significant deviation from a line but strong scattering, corresponding to a statistical error. This implies that the performance of Katz centrality could be increased by fitting a non-linear function, while the performance of PageRank cannot be increased. For the k-shell index ($R_{\text{k-shell}}^2 \approx 0.75$) the error is mainly due to scattering as well. It is also noteworthy that on all the 1000 patches the k-shell index takes only 13 different values, compared to 36 different degree values and almost a continuum of values for all other centrality measures as well as the food chain length.

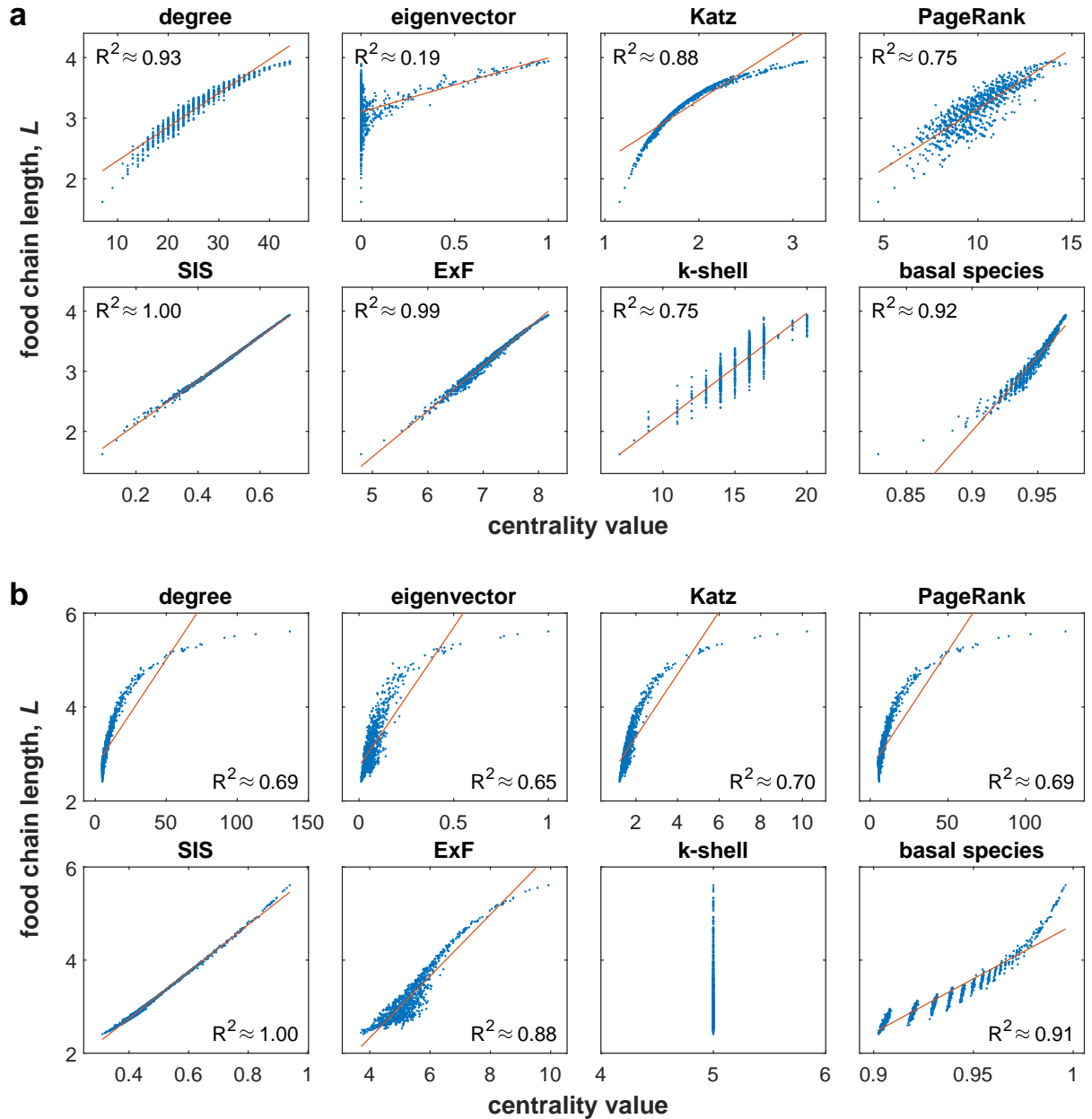


Figure 6.4: Simulated food chain length (for total colonization rate $C = 20$) vs centrality measures **(a)** on a random geometric graph with $N = 1000$ patches and mean degree $\langle m \rangle = 25$, and **(b)** on a scale free graph with $N = 1000$ patches and mean degree $\langle m \rangle = 10$. The R^2 values belong to the corresponding linear fits and characterize the goodness of fit between food chain length and the centrality measures. Centrality measures from top left to bottom right are: degree, eigenvector centrality, Katz centrality, PageRank, SIS centrality, Expected Force, k-shell index, and occupancy of the basal species.

To test the importance of the choice $g = \frac{\langle m \rangle}{2}$ for the SIS parameter we finally consider the fit between the occupancy $u_i^{(1)}$ of the basal species and the food chain length. The basal species follows the same dynamics that underlie the SIS centrality but uses the actual colonization-extinction parameters (here $e = 1$ and $c = \frac{C}{\langle m \rangle} = \frac{20}{25} = 0.8$) of the food chain dynamics. The occupancy of the basal species thus corresponds to the SIS centrality with $g = \frac{e}{c} = 1.25$, which is significantly smaller than $\frac{\langle m \rangle}{2} = 12.5$. We find that the occupancy of the basal species fits food chain length roughly as well as the degree ($R_{\text{basal}}^2 \approx 0.92$, lower right panel of Fig. 6.4 a) which implies that it is in particular inferior to the SIS centrality with $g = \frac{\langle m \rangle}{2}$. Since the eigenvector centrality, which is only weakly correlated to food chain length, corresponds to the SIS centrality with $g \gg \frac{\langle m \rangle}{2}$, we conclude that our choice of the intermediate value $g = \frac{\langle m \rangle}{2}$ plays an important role for the remarkable performance of the SIS centrality.

We repeat the whole analysis for an exemplary scale free graph with $N = 1000$ patches and mean degree $\langle m \rangle = 10$ (Fig. 6.4 b). The SIS centrality ($R_{\text{SIS}}^2 \approx 1.00$) is in this case by far the best predictor of food chain length, also clearly outperforming the Expected Force ($R_{\text{ExF}}^2 \approx 0.88$). Degree, eigenvector centrality, Katz centrality, and PageRank show qualitatively similar behaviour and lead to $R^2 \approx 0.65 - 0.70$. The occupancy of the basal species ($R_{\text{basal}}^2 \approx 0.91$) is again significantly inferior to the SIS centrality as well. The k-shell index leads to $R_{\text{k-shell}}^2 = 0$ which is discussed in the next subsection. Overall, by visual evaluation of Fig. 6.4 we find that already $R^2 \lesssim 0.95$ indicates a suboptimal fit between food chain length and centrality measure.

Note that for all results in this and the following subsections food chain simulations were performed with total colonization rate $C = 20$, but for $C = 10$ and $C = 30$ results are qualitatively similar (results not shown).

Large-scale results for different graph types and connectivities

Systematic results (Fig. 6.5) for random geometric graphs (RGGs), Erdős-Rényi (ER) random graphs, and scale free (SF) graphs with varying mean degree confirm the above exemplary results. The SIS centrality is the best predictor of food chain length for all graphs and mean degrees, typically followed by the Expected Force. The classical centrality measures are clearly outperformed by these two measures. If we define $R^2 = 0.95$ as the threshold above which we consider the performance of a measure as satisfying, the SIS centrality is the only measure that leads to satisfying results in all considered cases. A full analysis of which centrality measures perform satisfyingly on which graphs and for which mean degrees is shown in Table 6.1. Based on this analysis we can sort the centrality measures according to their performances. Starting with the best measure we find: 1. SIS centrality, 2. Expected Force, 3. occupancy of the basal species, 4. degree, 5. Katz centrality, 6. PageRank, 7. eigenvector centrality, and 8. k-shell index.

For fixed graph type the performance of all centrality measures, except for the k-shell index, increases with increasing mean degree. On ER and in particular on SF graphs this connectivity dependence is much weaker for the SIS centrality than for the Expected Force, degree, Katz centrality, PageRank, and eigenvector central-

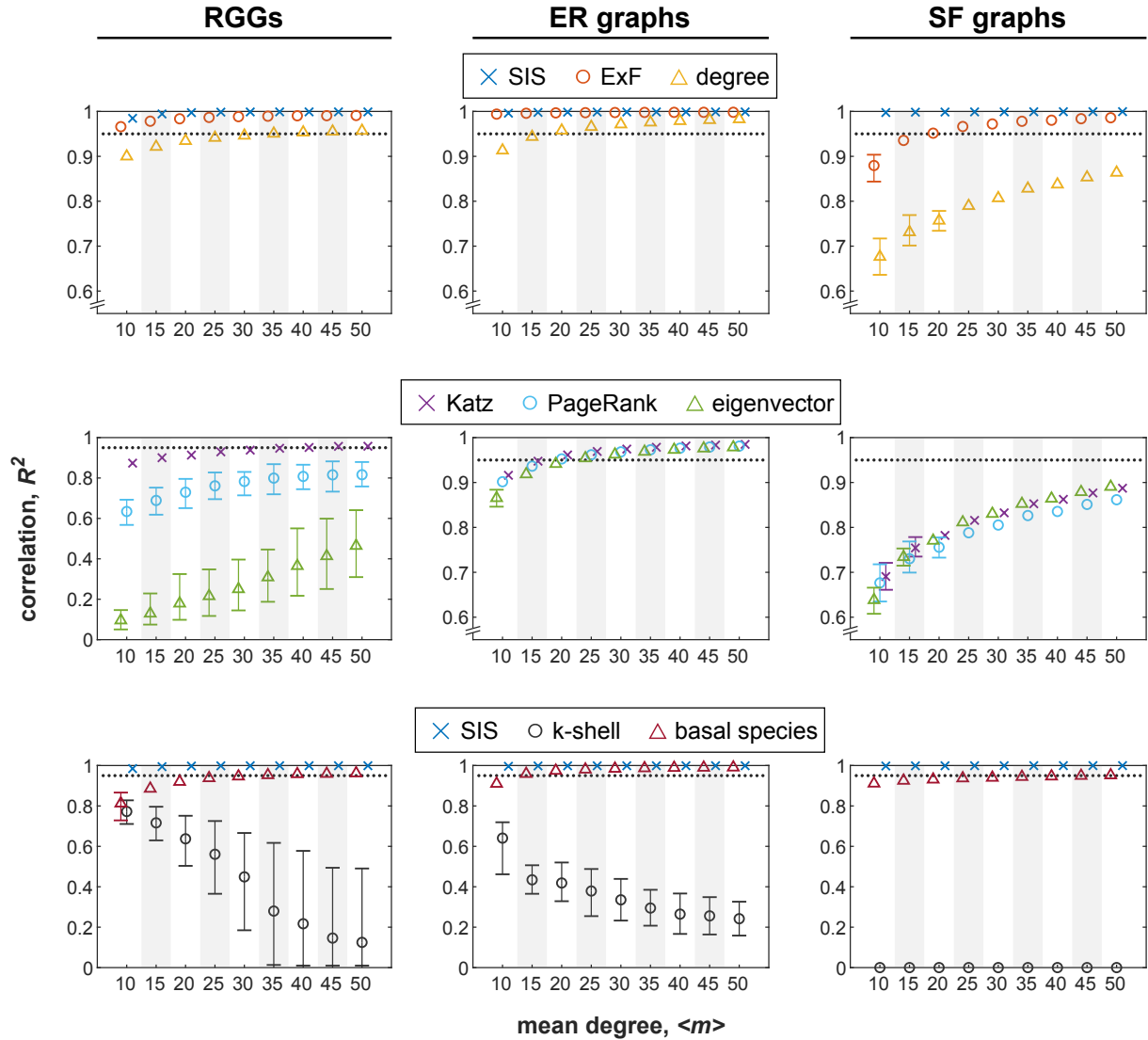


Figure 6.5: Correlation between centrality measures and simulated food chain length (for total colonization rate $C = 20$) on random geometric graphs (RGGs, left column), Erdős-Rényi random graphs (ER graphs, middle column), and scale free graphs (SF graphs, right column) with $N = 1000$ patches and varying mean degree $\langle m \rangle = 10, 15, \dots, 50$. The correlation is measured as the R^2 value of a linear fit between food chain length and centrality measure. Plot markers show mean R^2 values over 100 realizations of the same network type and mean degree. Error bars indicate the 5th and 95th percentiles of the corresponding full distributions of R^2 values. When no error bars are shown the distribution is so narrow that the error bars would collide with the plot marker. **Top row:** SIS centrality, Expected Force, and degree; **middle row:** Katz centrality (roughly the same mean R^2 values as the degree for all graphs), PageRank, and eigenvector centrality; **bottom row:** SIS centrality (as benchmark), k-shell index, and occupancy of the basal species.

	SIS	ExF	degree	eigenvec.	Katz	PageRank	k-shell	basal species
RGG	always	always	$\langle m \rangle \geq 35$	never	$\langle m \rangle \geq 40$	never	never	$\langle m \rangle \geq 35$
ER graph	always	always	$\langle m \rangle \geq 20$	$\langle m \rangle \geq 25$	$\langle m \rangle \geq 20$	$\langle m \rangle \geq 20$	never	$\langle m \rangle \geq 15$
SF graph	always	$\langle m \rangle \geq 20$	never	never	never	never	never	$\langle m \rangle = 50$

Table 6.1: Summary under which conditions (mean degree $\langle m \rangle = 10, 15, \dots, 50$) which centrality measure yields satisfying results on which graph type (RGG: random geometric graph; ER graph: Erdős-Rényi random graph; SF graph: scale free graph). For a single graph the goodness of fit between centrality measure and food chain length is quantified by the R^2 value of a linear fit between them. For a specified graph type and mean degree we define the performance of a centrality measure as satisfying if the mean R^2 value is larger than 0.95, where the mean is taken over all 100 realizations of that graph type and mean degree.

ity (see first two rows of Fig. 6.5). The advantage of the SIS centrality is thus typically larger on sparser graphs. We moreover find that all centrality measures, except for the SIS centrality and the k-shell index, perform best on ER graphs. The SIS centrality performs best on SF graphs. The advantage of the SIS centrality over the other centrality measures is smallest on ER graphs and typically much more significant on RGGs and SF graphs. Against the Expected Force, degree, and Katz centrality the advantage of the SIS centrality is largest on SF graphs while against the eigenvector centrality, PageRank, and occupancy of the basal species the advantage of the SIS centrality is largest on RGGs.

The eigenvector centrality has by far its worst performance on RGGs ($R_{\text{eigen}}^2 < 0.5$). A general problem of the eigenvector centrality is that it is often strongly localized on a few patches (Martin et al., 2014; Pastor-Satorras and Castellano, 2016). The food chain length, on the other hand, is more evenly distributed (see also Fig. 6.3). This discrepancy is particularly pronounced on the spatially embedded RGGs, leading to the observed weak fits between eigenvector centrality and food chain length. On

the non-spatially embedded ER and SF graphs eigenvector centrality, its variants Katz centrality and PageRank, as well as the degree all lead to similar fit performances.

The k-shell index shows a distinctly different behaviour than all other centrality measures. On RGGs and ER graphs the performance of the k-shell index decreases with increasing mean degree, which is in contrast to all other centrality measures. At least on RGGs this seems to be caused by a more pronounced k-shell structure (i.e. more different k-shell values) of graphs with smaller mean degree. On SF graphs the performance of the k-shell index is strictly zero ($R_{\text{k-shell}}^2 = 0$), independently of the mean degree. This happens because SF graphs generated by the BA-model (Albert and Barabási, 2002; Barabási, 2016) have no k-shell structure at all (i.e. all patches have the same k-shell value). The BA-model neglects many mechanisms that might play a role for the formation of real-world SF graphs (Dorogovtsev and Mendes, 2000; Albert and Barabási, 2000; Barabási, 2016) so that the weak performance of the k-shell index is most likely caused by our choice of a too theoretical graph model. By taking all considered graph types into account we

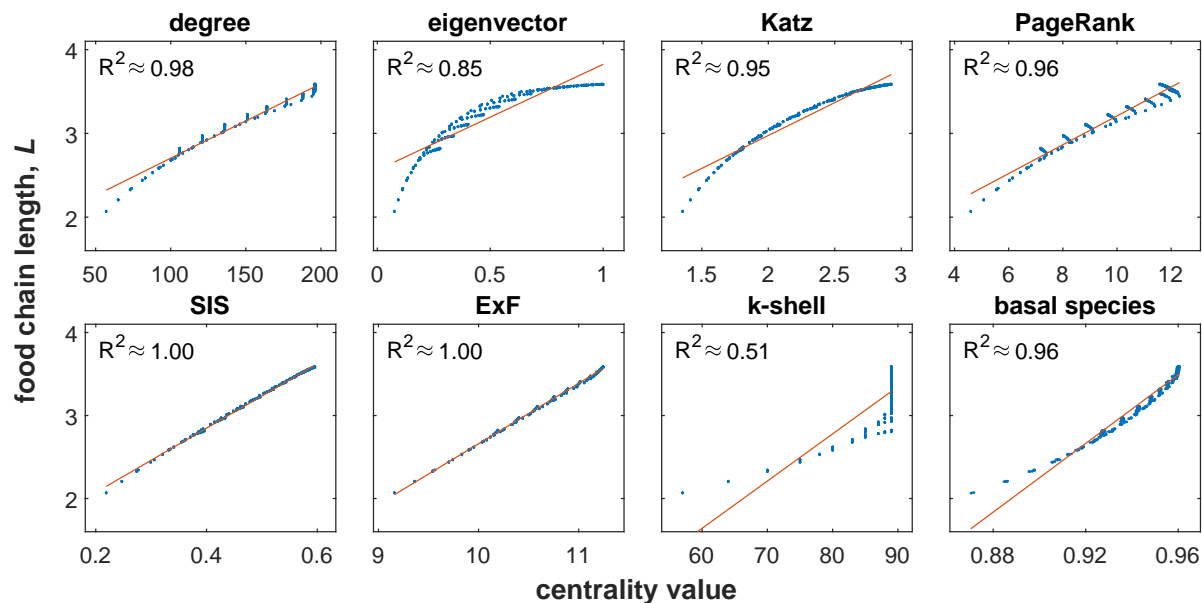


Figure 6.6: Same as Fig. 6.4 but here the underlying spatial network is a two-dimensional square lattice with hard boundaries, $N = 32 \times 32$ patches, and circular colonization range $r = 8$. The resulting mean degree of the network is $\langle m \rangle \approx 157$. For exactly this graph we demonstrated the mid-domain effect for food chain length in two dimensions in Chapter 5 (Fig. 5.5 a).

nevertheless conclude that the k-shell index is not suited to predict food chain length resolved to individual patches.

On a two-dimensional lattice

Our motivation for this research chapter was to generalize the mid-domain effect for food chain length from lattices to random graphs. In this context, we expect from a good centrality measure that it also properly fits food chain length on lattices. Here, we thus investigate how well the centrality measures from the previous subsections perform at fitting food chain length on the square lattice for which we observed the mid-domain effect in Chapter 5 (Fig. 5.5 a) (Fig. 6.6). Both, the SIS centrality ($R_{\text{SIS}}^2 \approx 1.00$) and the Expected Force ($R_{\text{ExF}}^2 \approx 1.00$)

perform almost perfectly on this lattice. Most other measures perform better than on the previously considered random graphs. The degree, Katz centrality, PageRank, and occupancy of the basal species are all satisfying according to our $R^2 > 0.95$ criterion. Only the eigenvector centrality ($R_{\text{eigen}}^2 \approx 0.85$) and in particular the k-shell index ($R_{\text{k-shell}}^2 \approx 0.51$) are not satisfying. Note that the good performance of most centrality measures might partially be due to the large mean degree of the considered lattice, $\langle m \rangle \approx 157$, which is the result of allowing long-range colonizations. In Chapter 5 this strong connectivity had the purpose of reducing spatial correlations and thus allowing us to use the differential equation approach instead of the stochastic approach used here. The random graphs from the previous subsections, on the other hand, had

mean degrees $\langle m \rangle = 10, 15, \dots, 50$, and we found that most centrality measures fitted food chain length better when $\langle m \rangle$ was larger.

6.5 Discussion

We have introduced a new centrality measure based on the solution of an epidemic susceptible-infected-susceptible (SIS) model on networks, and consequently called this measure the SIS centrality. We investigated how well the SIS centrality and several other centrality measures fit simulated food chain length results (based on colonization-extinction dynamics) and found that the SIS centrality shows the largest (linear) correlation with food chain length on all considered habitat networks. A strong correlation between a centrality measure and food chain length constitutes the desired generalization of the mid-domain effect for food chain length to random networks, and in our study the SIS centrality is the most suitable centrality measure for this task. Since the SIS dynamics underlying the SIS centrality are equivalent to the colonization-extinction dynamics of the basal species of the food chain, it might not be surprising that the SIS centrality fits food chain length so well. The occupancy of the basal species, however, shows significantly weaker correlations with food chain length, comparable to the correlations between the degree and food chain length. The key to the remarkable performance of the SIS centrality thus additionally lies in the choice of its free parameter g . This parameter should not be based on the parameters of the colonization-extinction dynamics but rather on the spatial network. Our heuristically motivated, ‘optimal’ choice is $g = \frac{\langle m \rangle}{2}$, where $\langle m \rangle$ is the mean degree of the network. In

this case the SIS centrality is centered around 0.5, and since the SIS centrality is naturally bounded between 0 and 1, 0.5 is exactly the midpoint of its range. This centeredness and boundedness have two consequences that might be helpful for predicting food chain length. First, the centeredness does arguably lead to an optimal ‘resolution’ of the SIS centrality, which helps discriminating different patches. Second, the centeredness and boundedness together imply that even the most central patch of a network can have SIS centrality maximally twice as large as the average patch. Large degree differences, like on scale free graphs where hubs can have extraordinarily large degrees, are thus evened out much stronger by the SIS centrality than by many other centrality measures. Since we observed a similar ‘flattening’ for the food chain length (Fig. 6.3), this seems to be an important characteristic for a centrality measure to properly predict food chain length. Since degree differences, and thus also the flattening, are particularly strong on scale free graphs, this also explains why the advantage of the SIS centrality (for fitting food chain length) over the other considered centrality measures is larger on scale free graphs than on Erdős-Rényi random graphs.

Note that the centeredness and boundedness of the SIS centrality, or more generally the graph-dependent choice $g = \frac{\langle m \rangle}{2}$, have the additional consequence that the SIS centrality should not be used to directly compare patches between different graphs (in particular graphs with different mean degrees $\langle m \rangle$). The SIS centrality of a patch is rather meant to describe the relative importance of that patch within the particular network.

Similar to the observation that the advantage of the SIS centrality (for fitting food chain length) over the other considered centrality measures is larger on scale free graphs than on Erdős-Rényi (ER) random graphs, we found that this advantage of the SIS centrality is typically also larger on random geometric graphs (RGGs) than on ER graphs. Since in the context of ecology and epidemics spatially embedded networks, like RGGs, are of high interest (Riley et al., 2015; Estrada et al., 2016), this result increases the usefulness of the SIS centrality. More generally, we found for most centrality measures that the fit between centrality measure and food chain length is better on ER graphs than on RGGs. Going in a similar direction, Barter and Gross (2017) showed that species occupancies on patches with fixed degree vary much stronger on RGGs than on ER graphs. This implies that a fit between degree and species occupancies would most likely have been better on ER graphs than on RGGs. Since in the model we used here food chain length is the sum of the occupancies of all species, our above stated result can be considered a confirmation and generalization of this result by Barter and Gross (2017).

The SIS centrality is a non-linear generalization of the eigenvector centrality and can be calculated with similar computational effort essentially by using the power method (Golub and Van Loan, 1996). In fact, since the SIS centrality does not have to be normalized after each iteration of the power method, its calculation is even faster than the calculation of the eigenvector centrality (see Appendix 6.A). This is in stark contrast to the Expected Force, the second best centrality measure at predicting food chain length in our study, that required the most com-

putation time of all considered centrality measures (see Table 6.2 in Appendix 6.A). Lawyer (2015) point out that one advantage of the Expected Force is that it can be calculated with incomplete knowledge of the spatial network. This is possible since the Expected Force is calculated for each patch separately and only requires knowledge of the neighbourhood of the patch of interest up to network distance three. If, however, one wants to calculate the Expected Force for all patches of a network, it is exactly this patch-wise calculation that slows it down so significantly compared to the eigenvector centrality and its modifications. The Expected Force can also be generalized to take a larger environment of the patch of interest into account (Lawyer, 2015). This might on one hand increase the performance of the Expected Force further, but would, on the other hand, slow down its calculation even more.

We stated several times that we would *predict* food chain length by centrality measures but actually we only considered the case that we already know the food chain length on all patches and simply calculated the correlations between food chain length and centrality measures (and fitted linear functions between the quantities). *Predicting* food chain length makes sense in the scenario where we have full knowledge of the spatial network, so that we can calculate the (SIS) centrality of all patches, but that in contrast to our study here, we know the food chain length only on a small number of patches. In this case we can fit a (linear) function to the available food chain length vs (SIS) centrality data, and then *predict* the food chain length on the remaining patches by evaluating the fitted function at the corresponding centrality values. We assume that centrality

measures that yielded larger correlations with food chain length in our study will also be better suited to predict food chain length in the here explained sense. Note that in our study the parameters of the function fitted between food chain length and a specific centrality measure depend on the graph type and the mean degree of the spatial network (see Appendix 6.B) as well as on the colonization-extinction parameters (which affect food chain length results). This also means that in the scenario where we want to predict food chain length from incomplete data, there will not be some universal function that we might know beforehand. Knowledge of the food chain length values on at least a few patches is thus indeed necessary to predict the food chain length on the remaining patches.

In reality food chain length may depend on many factors like primary productivity (Kaunzinger and Morin, 1998), ecosystem size (Post et al., 2000), metacommunity dynamics (not investigating spatially explicit patterns of food chain length) (Holt, 2002; Calcagno et al., 2011), or the foraging behaviour of predators (Kondoh and Ninomiya, 2009). It is likely that several explanatory factors are at work simultaneously (Post, 2002). Our results suggest that in a patchy environment the (topological) position of a patch within the landscape should influence its food chain length as well. The idea that quantities like food chain length, species richness or population densities depend in some way on some notion of centrality or isolation of a patch is supported by many studies including field or experimental data (Komonen et al., 2000; Carrara et al., 2012; Gilaranz et al., 2015; Buse et al., 2016; Altermatt and Fronhofer, 2018). The simple colonization-

extinction model considered here could be generalized in various ways to implement some of the above mentioned explanatory factors of food chain length. Effects of productivity or system size (here patch size) could be accounted for by allowing patch- or species-dependent extinction rates. Predator-induced effects could be implemented by introducing top-down effects or by allowing different patch connectivities or colonization rates for species at different trophic levels.

Conclusion

The strong linear correlations found between simulated food chain length and several centrality measures amount to the sought generalization of the mid-domain effect for food chain length to random spatial networks. The introduced SIS centrality with our specific choice of its free parameter is particularly well suited to predict food chain length. In a multivariate context the (SIS) centrality of a patch in a fragmented landscape may be an important determinant of food chain length.

Acknowledgements This work was supported by the German Research Foundation (DFG) as part of the research unit 1748.

6.A Appendix 1: Computational effort for calculating centrality measures

Here we compare the computational effort for calculating several centrality measures (SIS centrality, eigenvector centrality, Katz centrality, PageRank and Expected Force) and for running the stochastic food web simulations. We measured the calculation and simulation times for 100 random geometric graphs with $N = 1000$ patches and mean degree $\langle m \rangle = 25$. The precise computation times depend on the used hardware, software, and optimization of the used algorithms. We wrote all algorithms ourselves in MATLAB R2018b and even though we put some effort into their optimization, the here presented comparison between the computation times should not be seen too rigorous but rather as a general tendency.

In the *Methods* section we explained that we calculate the eigenvector centrality, Katz centrality, PageRank and SIS centrality with an iterative method using the defining equation as an iteration rule. We assumed convergence of this method if from one iteration to the next, the centrality values x_i changed less than a pre-defined precision, $|x_i - x_i^{(\text{old})}| < 10^{-4}$, on all patches i . Some details about speeding up the Gillespie algorithm for the stochastic simulations of the food web model can be found in Subsection 3.4.3.

We find that the SIS centrality needs the shortest computation time of all considered quantities (on the used local machine roughly 0.033s for all 100 considered graphs together). The computation times for the other quantities, normalized by the computation time for the SIS centrality, are shown in Table 6.2. Maybe

surprisingly, calculating eigenvector centrality, Katz centrality, or PageRank is slower than calculating the SIS centrality. The main reason for this is that the iterative algorithms corresponding to the four measures need different numbers of iterations until convergence. The eigenvector centrality is slowed down additionally, since it needs to be normalized after each iteration (to avoid divergence to infinity). Katz centrality needs fewer iterations until convergence than the eigenvector centrality but since we have to know the largest eigenvalue of the adjacency matrix before calculating the Katz centrality, the time that is required to calculate the eigenvector centrality (and thus the required eigenvalue) has to be added to the calculation time of the Katz centrality. PageRank has the slowest convergence and the longest calculation time among the considered eigenvector based centrality measures. Among all considered centrality measures the Expected Force has the largest computation time. One reason for this might be that the Expected Force has to be calculated for each patch separately. The stochastic food web simulations need far more time than the calculation of any centrality measure.

quantity	computation effort
SIS centrality	1
eigenvector	10
Katz centrality	5(+10)
PageRank	20
Expected Force	450
stoch. food web model	$2 \cdot 10^7$

Table 6.2: Relative computation times for several centrality measures and the stochastic simulations of the food web model, normalized by the computation time for the SIS centrality. Computation times were determined for 100 random geometric graphs with $N = 1000$ patches and mean degree $\langle m \rangle = 25$.

6.B Appendix 2: Dependence of fit parameters on graph type and connectivity

Here we investigate how the parameters of the linear fit between SIS centrality and food chain length depend on the graph type and the mean degree (Fig. 6.7). We find that, both, slope and offset depend quite significantly on the graph type. For fixed graph type both parameters also depend weakly on the mean degree. Similar results can be obtained for other centrality measures (not shown).

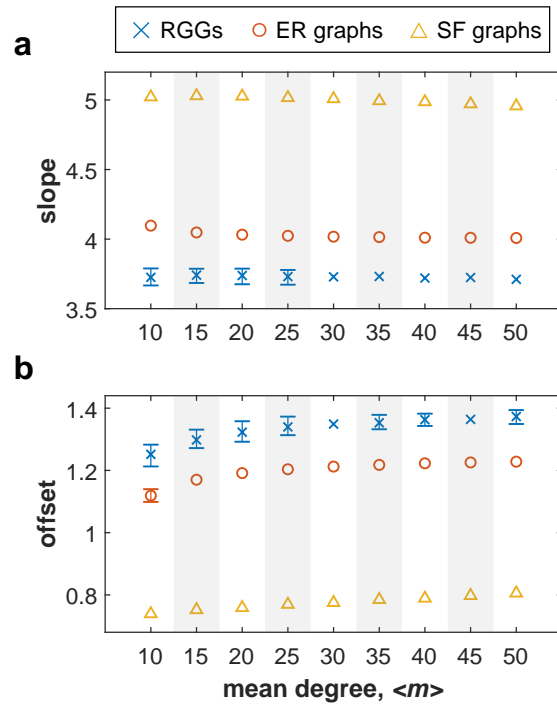


Figure 6.7: Fit parameters (**a**: slope; **b**: offset) of linear fits between SIS centrality and simulated food chain length (for total colonization rate $C = 20$) on random geometric graphs (RGGs), Erdős-Rényi (ER) random graphs, and scale free (SF) graphs with $N = 1000$ patches and varying mean degree $\langle m \rangle = 10, 15, \dots, 50$. Plot markers show mean values over 100 realizations of the same network type and mean degree. Error bars indicate the 5th and 95th percentiles of the corresponding full distributions. When no error bars are shown the distribution is so narrow that the error bars would collide with the plot marker. Qualitatively similar results are observed for other colonization rates.

7 Spatial niche partitioning in food webs

Spatial niche partitioning in trophic and competitive communities mediated by geometric edge effects

Kai von Prillwitz¹

¹Institute for Chemistry and Biology of the Marine Environment,
University of Oldenburg, Germany

Keywords colonization-extinction dynamics, meta-food-webs, spatially explicit, competition-colonization trade-off, omnivory

Abstract In Chapter 5 we found a mid-domain effect for food chain length stating that food chain length is maximal in the center of a habitat and decreases towards the boundaries even in the absence of other environmental gradients. The mid-domain effect is instead caused by the geometric constraints posed by the boundaries of the habitat. The results from Chapter 5 were based on a spatially explicit version of the meta-food-web model by Pillai et al. (2010), and the regional food web was represented by a simple food chain. Here we generalize this study by adding omnivores to the food web. We investigate how the presence of omnivores changes the mid-domain pattern of food chain length, and characterize the emerging spatial occupancy patterns of the individual species. We find that for certain parametrizations of the model food chain length achieves its maximum at an intermediate distance to the boundary. This effect is, however, rather weak, implying that the spatial pattern of food chain length is still dominated by the mid-domain effect. Individual species show diverse spatial occupancy patterns where overall more omnivorous species are driven successively towards the boundary. We observe this spatial niche partitioning on one- and two-dimensional habitats and investigate the dependence of the spatial patterns on the habitat size. In addition to the meta-food-web we consider a purely competitive metacommunity (without trophic interactions) and find almost the same spatial niche partitioning between the competing species. Our study shows how the interplay of geometric edge effects and species interactions can shape complex spatial patterns. The geometry of a habitat, specifically the spatial position of a patch within a habitat, should thus be considered as one explanatory factor for food chain length, species occupancies, and similar quantities.

7.1 Introduction

An intensely studied topic in spatial ecology are so-called edge effects (Laurance, 2000; Ries et al., 2004; Débarre and Lenormand, 2011), describing the change of species abundances or species compositions near habitat edges (Murcia, 1995; Olson and Andow, 2008; Peyras et al., 2013) and how far these changes extend towards the center of the habitat (Laurance, 2000; Ewers and Didham, 2006, 2008). One frequently studied type of habitats are for example single forest patches which is motivated by an increasing forest fragmentation and thus an increasing impact of potential edge effects (Murcia, 1995; Esseen and Renhorn, 1998; Laurance, 2000; de Paula Ferreira et al., 2015). Many studies of edge effects are concerned only with populations of individual species or small competitive communities, while trophic interactions, e.g. in the form of predation pressure, are sometimes used to explain observed edge effects (Ries and Sisk, 2004; Olson and Andow, 2008; Débarre and Lenormand, 2011; Vasseur and Leberg, 2015). Other recent studies explicitly investigate edge effects on trophic communities (Wimp et al., 2011; de Paula Ferreira et al., 2015; Peralta et al., 2017; Wimp et al., 2019). One interesting and frequently observed result is that generalist predators and omnivores, in contrast to specialists, have an increased abundance near habitat edges.

Empirical studies often try to explain observed edge effects with changing environmental conditions (for example light, wind, or resource availability) at the habitat boundary (Murcia, 1995; Esseen and Renhorn, 1998; Ries and Sisk, 2004). Prevedello et al. (2013), however, investigated the pure effect of the geometric con-

straints posed by the boundary of the habitat. The authors found that in the absence of other environmental factors the abundance of any species should decrease towards the habitat boundary and labelled this result the *geometric edge effect*. The geometric edge effect is in strong analogy to the so-called *mid-domain effect* which states that in a bounded habitat species richness should peak in the center of the habitat and decrease towards the boundary, again in the absence of other environmental gradients Colwell and Hurtt (1994); Jetz and Rahbek (2001); Connolly (2005). Despite its name, the mid-domain effect is also caused by the habitat boundary. The main difference between the geometric edge effect and the mid-domain effect lies in their spatial scales. While the mid-domain effect is supposed to act on large, geographical scales, the geometric edge effect should act in smaller habitats like single forest fragments.

In Chapter 5, based on a colonization-extinction model, we found that the mid-domain effect also holds true for food chain length as well as for the occupancy of each individual species in a food chain. That is, all of these quantities decrease monotonically from the center of a habitat towards the boundaries, and this decrease is caused by the boundaries themselves. One shortcoming of this study was, however, that no food webs other than simple chains have been considered. Real food webs are often much more complex (Polis, 1991; Martinez, 1991, 1992; Goldwasser and Roughgarden, 1993), where one ubiquitous feature is the presence of omnivores, i.e., predators that feed on more than one trophic level (Sprules and Bowerman, 1988; Thompson et al., 2007, 2009; Sánchez-Hernández et al., 2015). Using a

spatially explicit version of the meta-food-web framework by Pillai et al. (2010), Barter and Gross (2017) exemplarily showed that an omnivore and a specialist predator, that competes with the omnivore for one of its prey species, show to some extent complementary spatial patterns, i.e., they tend to occupy different regions of the habitat. Since Barter and Gross (2017) modelled the habitat as a random network of patches, a relation of the results to edge effects is difficult.

Here, we go in a similar direction as Barter and Gross (2017) and extend our study from Chapter 5 by adding omnivores to the food chain. In contrast to Barter and Gross (2017) we use simple, bounded, lattice-like spatial networks (lattices with long-range interactions) which allows us to observe and analyze edge effects. Our goals are (1) to find out if and how the extended trophic structure changes the mid-domain pattern of food chain length from Chapter 5 and (2) to characterize the spatial occupancy patterns of individual species, in particular comparing patterns of specialist predators and omnivores. In the general context of edge effects our study can be characterized as follows: We investigate edge effects (a) on large spatial scales (comparable to the scale of the mid-domain effect), (b) caused primarily by the geometric constraints, and (c) affecting whole food webs, precisely, food chains extended by omnivores. Points (b) and (c) are not independent since the edge effect on one species in the food web might affect other species as well. In that sense we here investigate the interplay between spatial dynamics, restricted by the habitat boundaries, and trophic interactions.

7.2 Methods

The model

As Chapters 5 and 6, this study is based on a spatially explicit version of the meta-food-web model by Pillai et al. (2010) (see also Section 3.3). The model describes colonization-extinction dynamics of trophically interacting species on a habitat represented by a network of N patches. Population dynamics are neglected (assuming that they occur on a much faster time scale than the colonization-extinction dynamics) which means that each species is either present or absent on a patch. Locally, the trophic interactions follow three main principles: (1) A predator can only persist on patches on which at least one of its prey species is present. (2) When on the same patch several predators want to feed on a common prey species, only one predator can persist (competitive exclusion principle). (3) Specialist predators are superior competitors compared generalists/omnivores. Point (2) implies that all local food webs are simple chains, and the full food web emerges only on the regional scale.

The habitat network can be described by an adjacency matrix A where $A_{ij} = 1$ ($A_{ij} = 0$) indicates that patches i and j are (not) connected. From any patch i on which species k is currently present it can colonize any other adjacent patch j where it is currently absent with colonization rate c . The colonization requires the presence of a suitable prey species and absence of any superior competitor for that prey on the target patch. The only exception is the basal species that needs no prey and has no competitors. After the colonization, species k is present on both the source and the target patch. If a superior

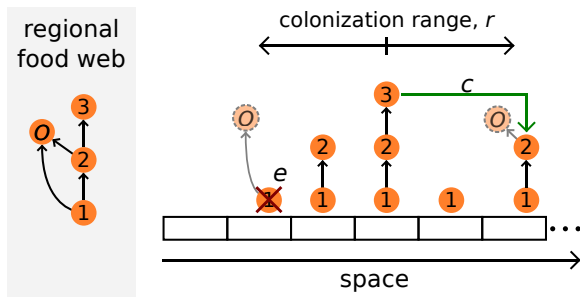


Figure 7.1: **Left:** Schematic representation of the omnivore web consisting of a basal species (1), an intermediate predator (2), a specialist top-predator (3), and an omnivore (O) that can feed on two species. Arrows indicate the feeding relations and point from prey to predator. **Right:** Schematic representation of the colonization-extinction model based on the omnivore web on a one-dimensional habitat. Locally, only one predator can persist on a common prey (competitive exclusion) so that all local food webs are chains (see Pillai et al., 2010). The full food web emerges only on the regional scale. Species can go randomly extinct (crossed out species, associated rate e), possibly inducing the bottom-up extinction of higher species. A colonization process (green arrow, associated rate c) requires the presence of a colonizer's prey and the absence of a possible superior competitor on the target patch. Since the specialists (species 2 and 3) are locally stronger competitors than the omnivore, the indicated colonization event of the top-predator leads to the local extinction of the omnivore on the target patch. With colonization range $r > 1$ colonizations between distant patches are possible.

competitor for some common prey colonizes a patch, the currently present inferior competitor will be displaced and go extinct, or, if possible, it starts to prey on the newly invaded species. Additionally, any species can go randomly extinct on any patch with extinction rate e . Upon losing its prey any predator will immediately go extinct as well. This bottom-up extinction can be prevented if the predator can switch feeding on another persisting prey. In contrast to the

general model by Pillai et al. (2010), we neglect top-down effects. A predator can thus not drive its prey to extinction.

As a specific example we consider a food web consisting of a small food chain of three species and an omnivore that can feed on the basal species and the intermediate predator (Fig. 7.1 left). The omnivore can persist solely on the basal species as long as the intermediate predator is not present. If the intermediate predator colonizes such a patch the omnivore is outcompeted at feeding on the basal species but it can switch feeding on the intermediate predator. If the intermediate predator goes extinct again the omnivore can switch back feeding on the basal species (assuming that the basal species did not go extinct as well since this would cause the bottom-up extinction of all other species). If the top-predator colonizes a patch where all other three species are present, the omnivore will also be outcompeted at feeding on the intermediate predator and will thus go extinct. Since we neglect top-down effects and since the omnivore is the inferior competitor for both of its prey species, the omnivore has no effect on any other species. The dynamics of the other three species are thus exactly the same as if we would consider only the food chain.

As habitat networks we here consider one- and two-dimensional lattices with hard boundaries and long-range interactions. By ‘hard boundaries’ we mean that we do *not* use periodic boundary conditions but that the lattices have actual endpoints. By ‘long-range interactions’ we mean that species can not only colonize spatially adjacent patches but all patches that lie within the colonization range r around the source patch. In the one-dimensional case a

patch that is not too close to one of the boundaries has thus r network neighbours in each direction, meaning that its *degree* is $2r$. In the two-dimensional case r is the radius of a circle that is truncated if it hits a boundary. The circular colonization range leads to degree $\approx \pi r^2$ for the most central patches of the lattice (we properly determine the degrees of all patches by counting neighbours).

We use the same model parameters, i.e., colonization range r , colonization rate c , as well as extinction rate e for all species. The species thus only differ via their positions in the food web. Without loss of generality we set the extinction rate to $e = 1$ which simply fixes the time scale. As in Chapter 5, we define the total colonization rate C as the product of the per-neighbour colonization rate c and the maximal degree of the habitat network (note that in Chapter 6 we used the mean degree instead of the maximal degree in this definition). The total colonization rate is thus $C = 2rc$ in the one-dimensional case and $C \approx \pi r^2 c$ in the two-dimensional case. In contrast to the per-neighbour colonization rate the total colonization rate comes closer to the colonization rate of spatially implicit models and is also better comparable with the extinction rate (in a fully connected habitat a single species could persist if $C > e$).

Model equations and food chain length

The stochastic dynamics of the Pillai model can be simulated using the Gillespie algorithm (Gillespie, 1977). The advantage of the stochastic approach is that it automatically incorporates all spatial correlations between occupancies of adjacent patches. For larger food webs and spatial networks the Gillespie algorithm be-

comes, however, extremely time consuming. In Chapter 5 (Fig. 5.2) we have seen that with a colonization range of $r = 100$ (on the one-dimensional lattice) spatial correlations become negligible and the dynamics can be properly described by differential equations. In Chapters 3 (Eq. 3.9), 5 (Eq. 5.1) and 6 (Eq. 6.1) we have already presented the equation for the occupation probability $u_i^{(k)}$ of a species in a simple food chain at trophic level k on patch i ,

$$\frac{du_i^{(k)}}{dt} = c \left(u_i^{(k-1)} - u_i^{(k)} \right) \sum_{j=1}^N A_{ij} u_j^{(k)} - k e u_i^{(k)}. \quad (7.1)$$

The first term on the right hand side of Eq. 7.1 is the colonization term, where $u_i^{(k-1)} - u_i^{(k)}$ takes account of the requirement that the predator species k can colonize a patch only if its prey species $k - 1$ is present, and $\sum_{j=1}^N A_{ij} u_j^{(k)}$ incorporates the explicit structure of the spatial network. Note that for $k = 1$ we set $u_i^{(0)} = 1$ implying that the basal species has access to all patches. The second term on the right hand side of Eq. 7.1 describes extinction processes. Bottom-up extinctions are included via the factor k which effectively increases the total extinction rates of species at higher trophic levels. Since we neglect top-down effects, Eq. 7.1 remains valid for species that are part of a standard food chain even after the introduction of additional omnivores. Eq. 7.1 is thus in particular valid for species 1, 2, and 3 from the regional food web shown in Fig. 7.1.

For species that feed on more than one prey, Pillai et al. (2010) argue that it is not possible (or a bad approximation) to write down a single differential equation for the occupation probability, or occupancy, of that species. Instead,

one has to write down one equation for the occupancy of each trophic link. For the omnivore from Fig. 7.1 we thus need one equation for the link $(1, O)$ and one equation for the link $(2, O)$. In Subsection 3.3.3 (see also supplemental material of Pillai et al., 2011) we have already presented the corresponding equations for the spatially implicit scenario (where all patches are connected to each other; also called mixed space scenario) and in Subsection 3.4.1 we have also explained how to obtain the spatially explicit versions of such equations. The final equations for the occupancies of the two omnivore links on an arbitrary patch network read,

$$\begin{aligned} \frac{du_i^{(1,O)}}{dt} = & c \left(u_i^{(1)} - u_i^{(2)} - u_i^{(1,O)} \right) \sum_{j=1}^N A_{ij} u_j^{(O)} \\ & + eu_i^{(2,O)} - 2eu_i^{(1,O)} \\ & - cu_i^{(1,O)} \sum_{j=1}^N A_{ij} u_j^{(2)}, \end{aligned} \quad (7.2)$$

$$\begin{aligned} \frac{du_i^{(2,O)}}{dt} = & c \left(u_i^{(2)} - u_i^{(3)} - u_i^{(2,O)} \right) \sum_{j=1}^N A_{ij} u_j^{(O)} \\ & + cu_i^{(1,O)} \sum_{j=1}^N A_{ij} u_j^{(2)} - 3eu_i^{(2,O)} \\ & - cu_i^{(2,O)} \sum_{j=1}^N A_{ij} u_j^{(3)}, \end{aligned} \quad (7.3)$$

where $u_i^{(O)} = u_i^{(1,O)} + u_i^{(2,O)}$ is the total occupancy of the omnivore on patch i . The equations contain all possible effects like bottom-up extinctions, competitive displacement, and prey-switching. A discussion of the spatially implicit version of Eq. 7.2 can be found in Subsection 3.3.3.

For more complex food webs it becomes cumbersome to write down all individual equations.

Pillai et al. (2010) provide general equations for the occupancies of all trophic links in arbitrary food webs (in the mixed space scenario). Using these general equations we were, however, not able to reobtain the specific equations for some simple example food webs. In Appendix A (at the end of the thesis) we thus derive the equations for general food webs from the basic principles of the model, and use these equations for all food webs that are more complex than the simple omnivore web from Fig. 7.1. We are only interested in the equilibrium solutions of the differential equations, and to obtain these solutions we use an iterative method described in Subsection 3.4.2.

In Chapter 5 (Eq. 5.2) we have shown for a simple food chain that the expected food chain length on patch i can be calculated as $L_i = \sum_{k=1}^S u_i^{(k)}$, where S is the number of species. This formula holds true also for arbitrary food webs in the Pillai framework. The reason is that locally all food webs are still chains implying that the presence of any species will increase the local food chain length by one. Since $u_i^{(k)}$ is the probability to find species k on patch i , $u_i^{(k)}$ is also the contribution of species k to the expected food chain length L_i .

7.3 Results

Occupancies for the omnivore web

We start by considering the omnivore web introduced in Fig. 7.1 and first qualitatively address the question if and under which conditions the omnivore can persist and coexist with the top-predator. To this end we consider the regional, i.e. spatially averaged, occupancies of all four species as function of the colonization rate

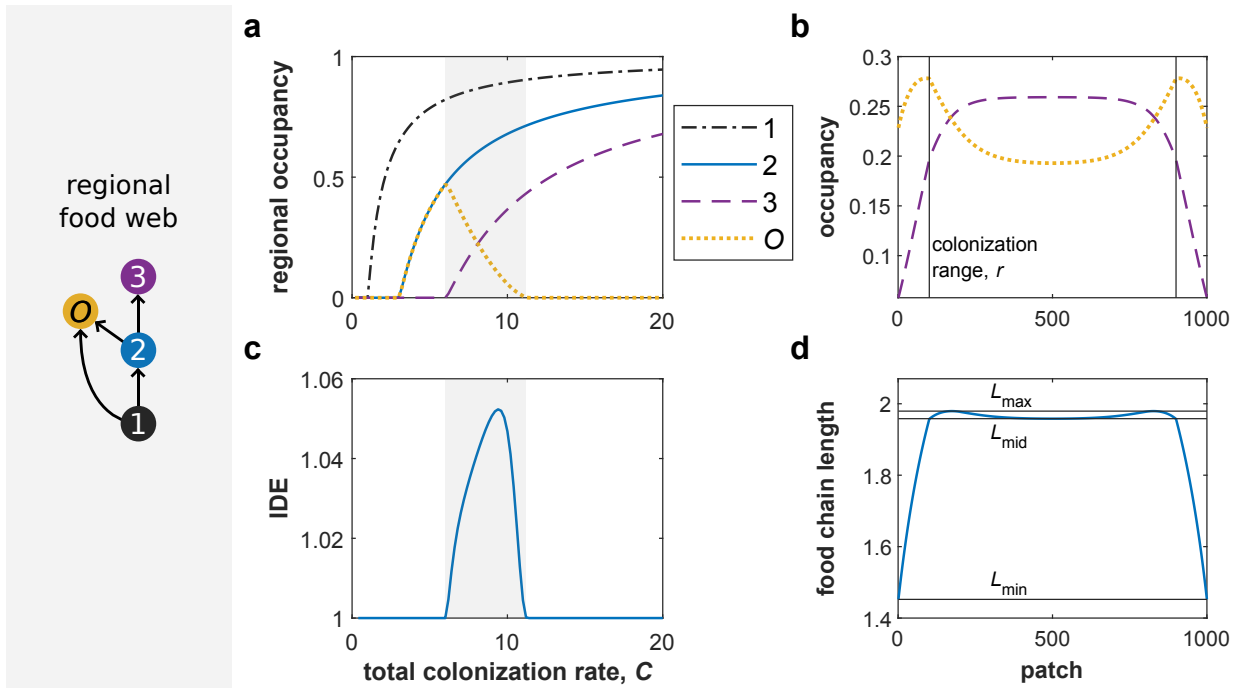


Figure 7.2: Results for the simple omnivore web (shown on the left) on a one-dimensional lattice with $N = 1000$ patches, colonization range $r = 100$, and hard boundaries. The legend is valid for panels (a) and (b). **a**) Regional occupancies of all four species as functions of the total colonization rate, C . The shaded area indicates the regime in which top-predator (3) and omnivore (O) coexist. **b**) Spatial occupancy patterns of the top-predator and the omnivore for $C = 8.1$. The vertical lines indicate the patches with distance to the boundary equal to the colonization range, r . Species 1 and 2 show qualitatively similar patterns as the top-predator but at higher occupancy values. **c**) Strength of the intermediate distance effect (IDE; see main text and panel d) as function of the total colonization rate, C . The shaded area is as in panel (a). **d**) Spatial pattern of food chain length (for $C = 8.1$) showing large values in the center (L_{mid}), a strong decrease towards the boundary (L_{min} ; mid-domain effect), but also a weak local maximum at an intermediate distance to the boundary (L_{max}). We calculate the strength of this intermediate distance effect as $IDE = (L_{max} - L_{min}) / (L_{mid} - L_{min})$.

(Fig. 7.2 a). The underlying habitat is a one-dimensional lattice with $N = 1000$ patches, colonization range $r = 100$, and hard boundaries. Each specialist species has a persistence threshold below which it cannot persist and above which the occupancy increases monotonically. The persistence threshold is larger for species at higher trophic levels and we roughly find $C_{\text{thresh}}^{(1)} \approx 1$, $C_{\text{thresh}}^{(2)} \approx 3$, and $C_{\text{thresh}}^{(3)} \approx 6$ for

trophic levels 1, 2, and 3, respectively. Note that we have seen this result already in Chapter 5 (Fig. 5.2). The omnivore has the same persistence threshold as the intermediate predator. This makes sense since the omnivore has the same minimal requirement to persist on a patch as the intermediate predator, namely the presence of the basal species. Since the omnivore can switch its feeding between the basal

species and the intermediate predator, the omnivore can effectively coexist (even locally) with the intermediate predator. Without the top-predator, the omnivore thus has the same regional occupancy as the intermediate predator. The regional occupancy of the omnivore starts to decrease as soon as the top-predator is able to persist, since the omnivore can then be competitively displaced by the top-predator. Above some additional threshold value, $C_{\text{extinct}}^{(O)} \approx 11$, the omnivore cannot persist anymore. Below that threshold and above the persistence threshold of the top-predator, the omnivore and the top-predator can coexist regionally (see also Pillai et al., 2011; Böhme and Gross, 2012; Barter and Gross, 2017).

Next we are interested in the spatial occupancy patterns of the four species in the coexistence regime of the omnivore and the top-predator. We already know from Chapter 5 (Fig. 5.3 a) that the spatial occupancy patterns of the specialist species show a mid-domain effect pattern, i.e., a plateau in the habitat center and a monotonic decrease towards the boundary. For the omnivore, however, we find a qualitatively different pattern (Fig. 7.2 b). The spatial occupancy of the omnivore has a valley in the habitat center, a maximum at an intermediate distance to the boundary (roughly coinciding with the colonization range), and then also a slight decrease towards the boundary. The valley in the center can be explained by the competitive pressure caused by the top-predator which is strongest in the center. The trophic interaction thus drives the omnivore towards the boundary. The following decrease even closer to the boundary occurs since the geometric constraints posed by the boundary negatively affect all species, including the omnivore. The full pattern of the

omnivore can thus be explained by a combination of trophic interactions and geometric edge effects. Note that Barter and Gross (2017) also observed to some extent complementary spatial patterns of the specialist top-predator and the omnivore on random spatial networks. On random networks, patterns are, however, more difficult to describe and cannot be easily related to edge effects.

The intermediate distance effect

Here we investigate how the mid-domain effect pattern of food chain length (see Chapter 5, Fig. 5.3 b) is affected by the omnivore. Since food chain length in the model by Pillai et al. (2010) is the sum of the occupancies of all species, food chain length might inherit the occupancy pattern of the omnivore from Fig. 7.1 (b). For a qualitative change of the food chain length pattern the increase of the omnivore's occupancy at the intermediate distance to the boundary has to be large enough to compensate the simultaneous decrease of the occupancies of all other species. We find that food chain length is indeed largest at an intermediate distance to the boundary (Fig. 7.2 d) and call this observation the *intermediate distance effect*. Compared to the decrease of food chain length towards the boundary, i.e., the mid-domain effect, the difference between the mid-domain value and the maximal value is, however, very small.

We quantify the magnitude of the intermediate distance effect by $\text{IDE} = (L_{\text{max}} - L_{\text{min}}) / (L_{\text{mid}} - L_{\text{min}})$, which is the relative increase of the food chain length from the mid-domain to the maximum, on the scale of the observed range of food chain length values (subtraction of the boundary value L_{min}). $\text{IDE} = 1$ means that there

is no intermediate distance effect while values $\text{IDE} > 1$ indicate that there is an effect. With the model parametrization used for Fig. 7.1 (d) we get $\text{IDE} = 1.042$. Without subtracting the offset L_{\min} in the calculation of IDE the value would be even smaller. Even when optimizing over the colonization rate, the intermediate distance effect remains small ($\text{IDE}_{\max} = 1.052$, see Fig. 7.2 c). We also find that the intermediate distance effect occurs exactly for those values of the colonization rate for which the omnivore and the top-predator coexist (compare Fig. 7.2 a and c). This makes sense since we explained the intermediate distance effect of food chain length by the spatial pattern of the omnivore which emerges due to the competition between the omnivore and the top-predator.

Next, we test if the intermediate distance effect gets stronger for larger, more complex food webs. To this end we consider a generalized omnivore web (shown in Fig. 7.3 on the left) consisting of a longer food chain with a specialist top-predator and three omnivores that can feed on two, three, and four trophic levels, respectively. In this order, we also call the omnivores the level-1, level-2, and level-3 omnivore. Concerning the competitive-exclusion principle for a common prey, the local competition strength decreases with the increasing level of omnivory. For this food web, the maximal magnitude of the intermediate distance effect is $\text{IDE}_{\max} = 1.060$, again found by optimization over the colonization rate (Fig. 7.3 b). The effect is thus only slightly stronger than for the simple omnivore web and in general still rather weak. We further find that IDE_{\max} is obtained when only the specialist top-predator and the level-3 omnivore coexist and compete (compare Fig. 7.3 a and b). Also a second, al-

ready much smaller peak ($\text{IDE} = 1.023$) is obtained when only two of the omnivores coexist (without the specialist top-predator). When all four top species coexist the effect is even smaller ($\text{IDE} < 1.014$). For some colonization rates the intermediate distance effect does not occur at all, despite the coexistence of at least two of the top species. In our study, the interaction (competition for prey) of more than two species can thus not increase the intermediate distance effect of food chain length.

Overall, we conclude that the addition of omnivorous species to a food chain can alter the mid-domain effect pattern of food chain length but that this alteration is rather weak and that the mid-domain effect is still the dominant pattern.

Space partitioning of four species

One-dimensional lattice with $N = 1000$ patches

Here we investigate the spatial occupancy patterns of the specialist top-predator and the three omnivores from the generalized omnivore web introduced in Fig. 7.3. We find that all species show qualitatively different patterns, where more omnivorous species have their maxima gradually closer to the boundary (Fig. 7.3 c, d). In detail, the top-predator and the level-1 omnivore show qualitatively the same patterns as the top-predator and the omnivore from the simple omnivore web from Fig. 7.2. The level-2 omnivore shows a new and more complex pattern: Its occupancy has a local maximum in the mid-domain since the joint competitive pressure by the specialist top-predator and the level-1 omnivore is weaker in the mid-domain than at

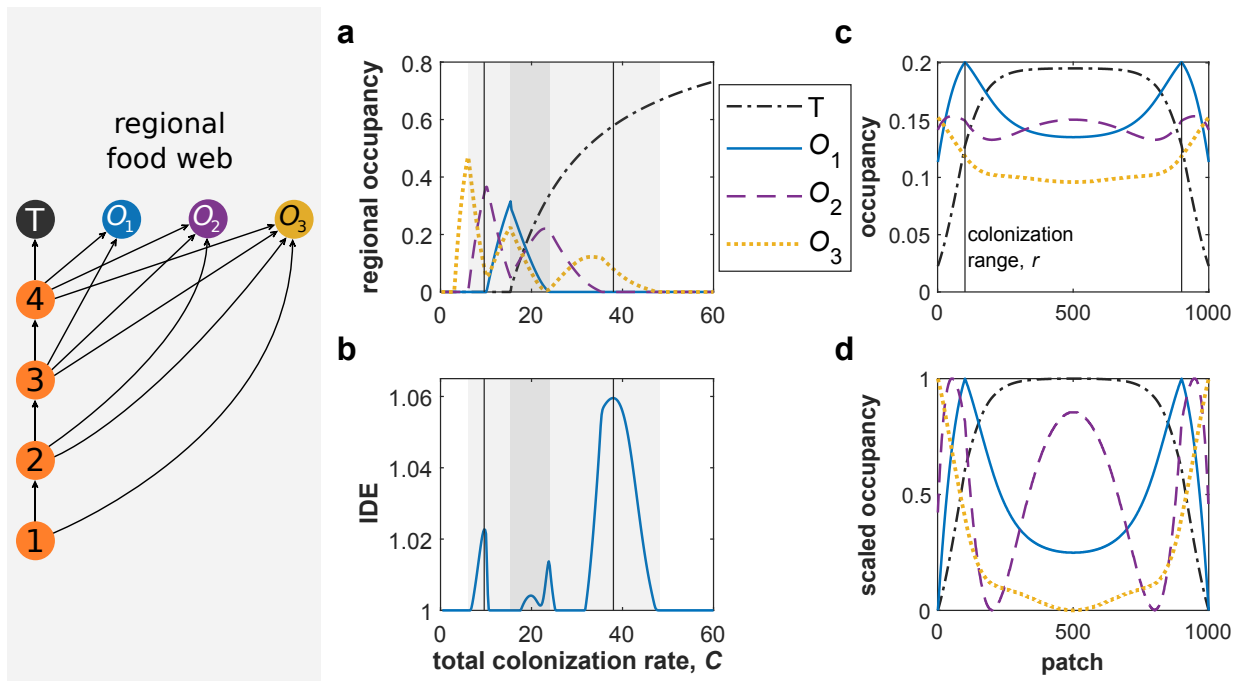


Figure 7.3: Generalization of the results from Fig. 2 (same underlying habitat) to the generalized omnivore web shown on the left. The web consists of a chain (species 1 to 4 and T as the top-predator) and three omnivores that can feed on an increasing number of species in the lower food chain. **a)** Regional occupancies of the top-predator and the omnivores as function of the total colonization rate, C . The light (dark) shaded area indicates the regime in which at least two (all four) of these species coexist. The vertical lines mark prominent points from panel (b). **b)** Strength of the intermediate distance effect (IDE; see Fig. 2 and main text) as function of the total colonization rate, C . The shaded areas are as in (a). The two vertical lines mark the two larger maxima of IDE. **c)** Spatial occupancy patterns of the top-predator and the omnivores for $C = 18.64$. The vertical lines indicate the patches with distance to the boundary equal to the colonization range, r . **d)** Same as (c) but for better qualitative comparability of the different patterns the occupancy of each species has been scaled individually to lie exactly between 0 and 1.

some intermediate distance to the boundary. At this intermediate distance the level-2 omnivore has its global minimum. Going from that minimum even closer towards the boundary, the competitive pressure on the level-2 omnivore decreases again, resulting in the global maximum of the level-2 omnivore. This maximum lies closer to the boundary than the maximum of the occupancy of the level-1 omnivore. Directly at the boundary, the negative effect of the ge-

ometric constraints leads to a final decrease of the occupancy of the level-2 omnivore. Among all observed patterns, this pattern of the level-2 omnivore is, on one hand, the most complex one but, on the other hand, the least significant one in the sense that the occupancy of the level-2 omnivore spans over the smallest range of occupancy values (Table 7.2). The occupancy of the level-3 omnivore shows an inverted mid-domain pattern, with the maximal occupancy exactly at

the boundary and a monotonic decrease towards the center of the habitat. This pattern is caused by a plateau of the combined competitive pressure on the level-3 omnivore in the mid-domain that extends rather close towards the boundary. Even closer to the boundary the positive effect of the decreasing competitive pressure on the level-3 omnivore overcompensates the negative effect of the geometric constraints, resulting in the observed maximum directly at the boundary.

We also observe that each species has at least a small range of patches on which it is dominant (Fig. 7.3 c). While this observation is rather specific for the chosen colonization rate, the qualitative patterns of all four species (Fig. 7.3 d) are quite universal, as long as all four species coexist at non-negligible occupancies.

Effects of lattice size

Here we investigate how the spatial occupancy patterns of the specialist top-predator and the omnivores from Fig. 7.3 (c, d) depend on the habitat size. One might suspect that on larger habitats the patterns become even more complex, showing more oscillations. While we find that this is not the case, the full emergence of the patterns requires a certain habitat size (Fig. 7.4). Once the patterns have emerged, increasing the habitat size further leads only to small, minor changes of the patterns. In detail, the main difference between habitat sizes $N = 2000$ and the original $N = 1000$ is that for $N = 2000$ the maxima/minima in the mid-domain are proper plateaus (Fig. 7.4 a). The additional habitat patches thus primarily lead to a larger spatial extent of the mid-domain area. The behaviour at the boundary does

not change significantly and the boundary only seems to be narrower since the rest of the habitat is larger. One additional minor change is that for $N = 2000$ the level-2 omnivore has its global maximum now in the mid-domain while the maximum at the intermediate distance to the boundary has become a local one. For $N = 500$, on the other hand, we find a qualitatively different pattern for the level-2 omnivore, without the (local) maximum in the mid-domain. Instead, the global minimum, that for larger habitats can be found at an intermediate distance to the boundary, now extends towards the mid-domain. Overall, the pattern is less complex with fewer local extrema. We conclude that for $N = 500$ the habitat is simply not large enough to allow the emergence of the full, complex pattern of the level-2 omnivore. In general, it seems that for the full emergence of the patterns the habitat has to be large enough to allow the establishment of a proper mid-domain.

Considering for each individual species the occupancy values in the mid-domain, at the boundary, and at the local extrema (if they exist), the value that changes most significantly for varying habitat size is the mid-domain value (Fig. 7.4 b). For large enough N all values, including the mid-domain values, converge. This supports our assumption that for the emergence of the final patterns the habitat has to be large enough to establish a proper mid-domain. To formally characterize the convergence we say

species	T	O_1	O_2	O_3
converged for $N =$	800	1100	1400	1600

Table 7.1: Habitat sizes required for the convergence of the mid-domain values of the occupancies of the specialist top-predator and the omnivores from Fig. 7.4.

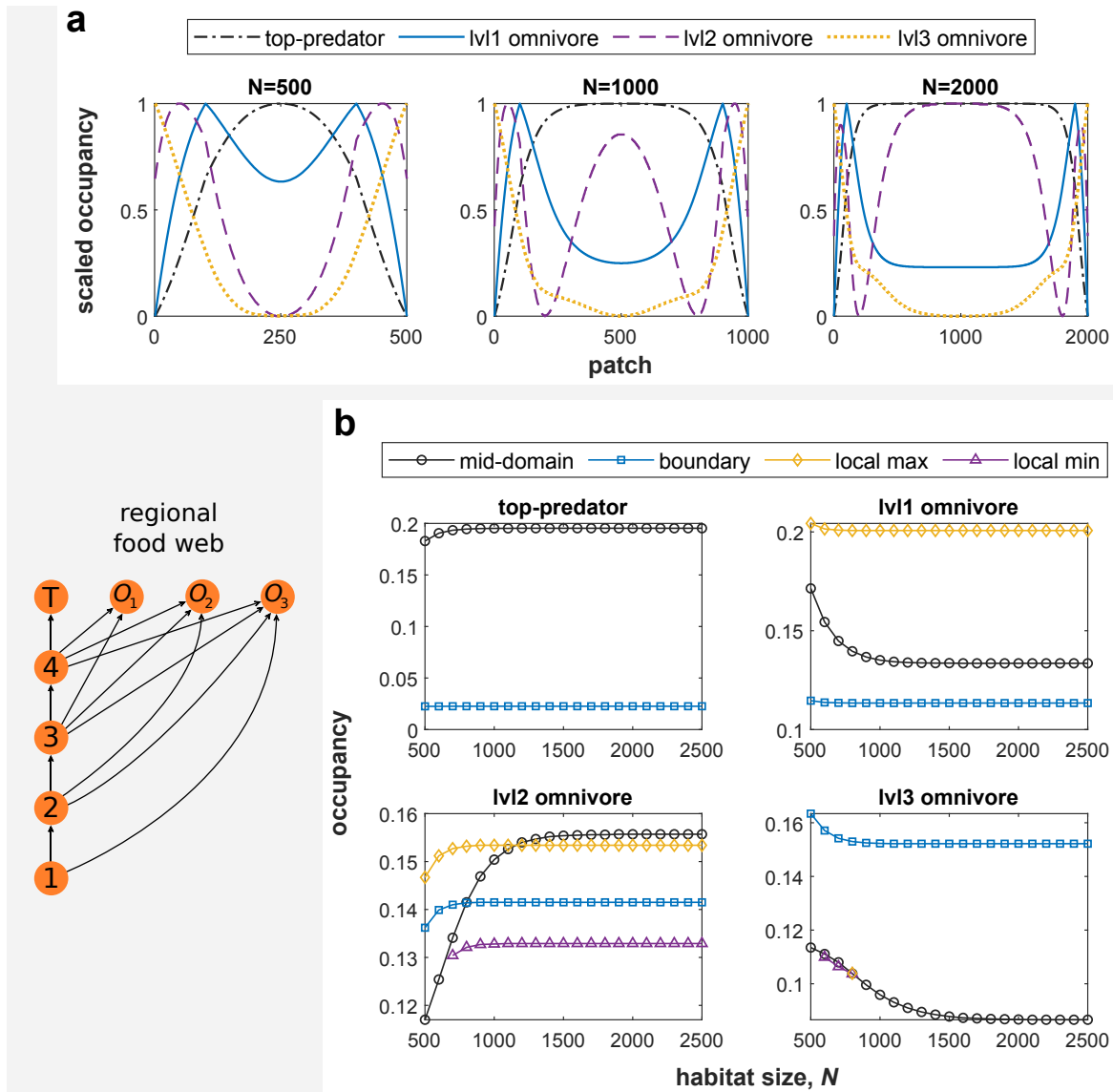


Figure 7.4: Dependence of the spatial occupancy patterns (see Fig. 3 c, d) of the top-predator and the omnivores from the generalized omnivore web (shown on the bottom-left) on the habitat size. The colonization range, $r = 100$, and the colonization rate, $C = 18.64$, are kept constant. **a**) Scaled occupancy patterns for the exemplary habitat sizes $N = 500$, $N = 1000$ (same as Fig. 3 d), and $N = 2000$. When increasing N further the only change to the patterns is that the spatial extent of the mid-domain increases. **b**) Dependence of some prominent occupancy values (mid-domain, boundary, and local extrema if they exist) of the four top species on the habitat size.

that an occupancy value has converged when the corresponding values for three consecutive habitat sizes (in steps of $\Delta N = 100$) have absolute difference smaller than 0.001 to the final value obtained for $N = 10\,000$. Using this criterion we find that more omnivorous species need larger habitats for the convergence of their mid-domain occupancies (Table 7.1).

Aside from this convergence behaviour the species with the strongest qualitative changes of its occupancies is the level-2 omnivore. The mid-domain value of the level-2 omnivore starts as the global minimum for small N and increases until it is the global maximum for large N . This confirms our observations for the exemplary habitat sizes from Fig. 7.4 (a). Another observation in Fig. 7.4 (b) is the emergence of local extrema for the level-3 omnivore for some particular habitat sizes. The values of these extrema are, however, very close to the mid-domain value. They do not significantly change the inverted mid-domain pattern of the level-3 omnivore. Finally, we found only weak, insignificant dependencies of the positions of the local extrema (if they exist) of the occupancies of all species on the habitat size (results not shown).

Another parameter that affects the spatial occupancy patterns of the species is the colonization range r . For all example habitat sizes from Fig. 7.3 (a) we find that the maximal occupancy of the level-1 omnivore lies exactly at the patches with distance to the boundary equal to the colonization range. We confirmed this observation for colonization ranges other than the usual $r = 100$ (results not shown). Moreover, when varying r and N simultaneously by the same factor the occupancy patterns do not change (r and N should not become too small

and space has to be measured in units of the colonization range; results not shown). We thus conclude that only the ratio r/N is important and that increasing (decreasing) r has the same effect as decreasing (increasing) N . In other words, the colonization range r , if not too small, can simply be regarded as a spatial scale. Note that when varying r the per-neighbour colonization rate c has to be adjusted such that the total colonization rate $C = 2rc$ is kept constant.

Two-dimensional lattice

We conclude our study of the generalized omnivore web by investigating how the spatial occupancy patterns generalize to a two-dimensional habitat (a square lattice). We find that, as expected, the top-predator dominates the mid-domain while the omnivores are successively driven towards the boundaries, in particular towards the corners (Fig. 7.5). The level-2 omnivore also shows its complex pattern known from the one-dimensional case with a local maximum in the mid-domain. A difference between the one- and the two-dimensional case is that in the two-dimensional case the occupancy values of each species span over a larger range than in the one-dimensional case (see Table 7.2). Note that the system has been parametrized slightly differently in the two cases (for visual reasons)

species	T	O_1	O_2	O_3
1d	0.17	0.09	0.02	0.06
2d	0.25	0.16	0.06	0.07

Table 7.2: Occupancy ranges $u_{\max} - u_{\min}$ of the top-predator and the omnivores in the one-dimensional case (Fig. 7.3 c) and the two-dimensional case (Fig. 7.5). The ranges of all species are larger in the two-dimensional case.

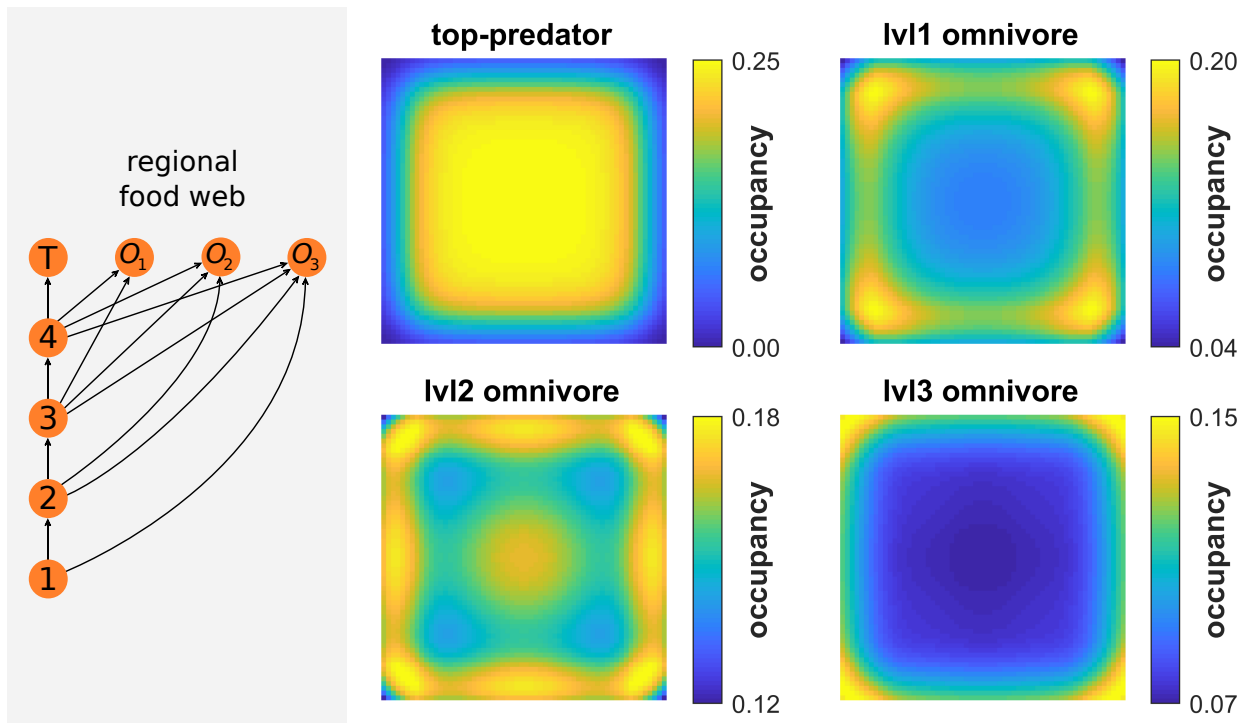


Figure 7.5: Spatial occupancy patterns of the top-predator and the omnivores from the generalized omnivore web (shown on the left) on a two-dimensional lattice (with $N = 60 \times 60$ patches, radial colonization range $r = 8$, and hard boundaries) for total colonization rate $C = 20$. The patterns are straightforward generalizations of the one-dimensional patterns from Fig. 7.3 (c, d).

but we made the same qualitative observation with other parametrizations. The intermediate distance effect of food chain length, measured by $\text{IDE} = (L_{\max} - L_{\min}) / (L_{\text{mid}} - L_{\min})$, is, however, not stronger in the two-dimensional case. When optimizing over the colonization rate we here find $\text{IDE}_{\max}^{(2d)} = 1.055$ (results not shown) compared to $\text{IDE}_{\max}^{(1d)} = 1.060$ in the one-dimensional case.

Spatial occupancy patterns in a purely competitive community

The spatial occupancy patterns of the omnivorous species found above occur as a result

of an interplay of geometric edge effects and competitive pressure caused by superior predators. The competition between the specialist top-predator and the omnivores was mediated by trophic interactions (competition for common prey). Here we test if we can find similar spatial occupancy patterns for species that form a purely competitive community. Tilman (1994) showed that colonization-extinction dynamics of a purely competitive metacommunity can lead to the coexistence of an in principle arbitrary number of species. The coexistence requires a competition-colonization trade-off between the species, meaning that superior competitors have to be weaker colonizers (smaller

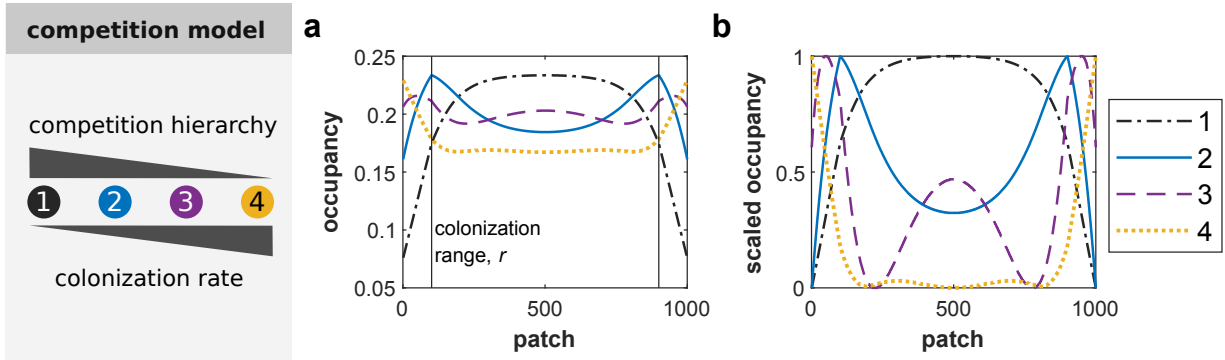


Figure 7.6: Left: Schematic representation of a purely competitive species community. The species have a clear competition hierarchy and less competitive species have larger colonization rates (competition-colonization trade-off). Right: Spatial occupancy patterns of the four competitors on a one-dimensional lattice with $N = 1000$ patches, colonization range $r = 100$, and hard boundaries (**a**: raw patterns, **b**: occupancy of each species scaled to lie exactly between 0 and 1). In (a), the vertical lines indicate the patches with distance to the boundary equal to the colonization range, r . The patterns are almost identical to the patterns of the top-predator and the omnivores from the food web model (see Fig. 7.3 c, d).

colonization rate). Weaker competitors cannot colonize patches that are occupied by a superior competitor, and weaker competitors are displaced on a patch if a superior competitor invades. The Tilman model uses mixed space which means that no spatial patterns can be observed in this version of the model. Here we put the Tilman model on spatially explicit habitat networks. The differential equation for the occupancy $u_i^{(k)}$ of species k on patch i reads,

$$\begin{aligned} \frac{du_i^{(k)}}{dt} = & c_k \left(1 - \sum_{l=1}^k u_i^{(l)} \right) \sum_{j=1}^N A_{ij} u_j^{(k)} - e u_i^{(k)} \\ & - u_i^{(k)} \sum_{l=1}^{k-1} c_l \sum_{j=1}^N A_{ij} u_j^{(l)}, \end{aligned} \quad (7.4)$$

where species with smaller index k are superior local competitors. The first term on the right hand side of Eq. 7.4 is the usual colonization term of species k , including colonization restrictions posed by superior competitors. The second term on the right hand side of Eq. 7.4

is the usual stochastic extinction term. The third term describes the competitive displacement of species k due to colonization of a superior competitor. The colonization rate c_k is species-dependent and increases with k , providing the competition-colonization trade-off required for species coexistence. The extinction rate ($e = 1$) and the spatial network, i.e. the adjacency matrix A and thus the colonization range, are still the same for all species. As before we also define the total colonization rates $C_k = 2rc_k$ on one-dimensional lattices. See Hastings (1980), Tilman (1994), and Section 3.2 for the model equations in the mixed space scenario. To obtain the equilibrium occupancies we solve Eq. 7.4 with the iterative method described in Subsection 3.4.2.

Considering a community of four competing species on a one-dimensional habitat with the same default parameters as before, we find that the four species show almost the same spatial

occupancy patterns as the top-predator and the omnivores from the generalized omnivore food web (compare Fig. 7.6 and Fig. 7.3 c, d). In particular, the strongest competitor dominates in the mid-domain while weaker competitors are driven successively towards the boundary. A minor difference are the small local maxima of species 4 close to the mid-domain. For the level-3 omnivore, the analogous species from the generalized omnivore web, we found these local extrema only for some particular, smaller habitat sizes. For Fig. 7.6 we used colonization rates $C_1 = 1.24$, $C_2 = 2.12$, $C_3 = 4.32$, and $C_4 = 11.80$ which have been chosen to yield a good visual impression. Qualitatively, the occupancy patterns are robust against parameter changes as long as the overall occupancy of no species becomes too small (results not shown). In a spatially explicit habitat the competition-colonization trade-off that allows the regional coexistence of species, despite the locally applied competitive exclusion principle, thus also shapes the spatial patterns of the species.

7.4 Discussion

We have shown that species in a food web can have qualitatively different spatial occupancy patterns depending on their role in the food web. Specialist species in a food chain show mid-domain patterns with maximal occupancy in the center of the habitat and monotonically decreasing occupancy towards the boundaries. Omnivorous species, on the other hand, show maximal occupancies at some intermediate distance to the boundary or possibly even directly at the boundary. The observation that omnivores and generalists can respond positively to habitat edges, resulting in larger richness or

increased abundances of such species near the boundaries, has also been reported in empirical studies (Wimp et al., 2011; de Paula Ferreira et al., 2015; Peralta et al., 2017; Wimp et al., 2019). In many such studies edge effects are explained by changing environmental conditions (for example abiotic factors or resource availability) at the boundary compared to the interior of the habitat. In contrast, in our model-based study the observed spatial patterns emerge in the absence of any environmental gradients. Instead, they are caused by the geometric constraints posed by the boundaries of the habitat and the interactions between the species. In that sense our results are a generalization of the geometric edge effect (Prevedello et al., 2013) and the mid-domain effect (Colwell and Hurtt, 1994; Jetz and Rahbek, 2001; Connolly, 2005; Chapter 5 – when considering patterns of individual species) to trophically interacting species beyond food chains.

We have further shown that the same spatial occupancy patterns that we found for the specialist top-predator and the omnivores (Fig. 7.3) can also be observed for species in a purely competitive community (with a strict competition hierarchy and locally applied competitive exclusion principle). The strongest competitor dominates the mid-domain while weaker competitors are driven successively towards the boundary. These patterns require a competition-colonization trade-off (Tilman, 1994; Amarasekare, 2003; Cadotte et al., 2006; Calcagno et al., 2006) between the competing species, which is implemented by giving inferior local competitors larger colonization rates. The boundary poses bad geometric conditions for all species, but weak colonizers are more strongly affected by these bad conditions and thus pre-

dominantly occupy patches in the center of the habitat. Stronger colonizers are more successful at colonizing the geometrically bad boundary patches but are more frequently outcompeted in the mid-domain by superior local competitors. Stronger colonizers (weaker competitors) can thus have an increased occupancy near the boundary and a decreased occupancy in the center of the habitat. The interaction of more than two species can lead to rather complex patterns of the occupancies of some species, but overall the described mechanism explains how weaker competitors (stronger colonizers) are driven successively towards the boundary.

The observed spatial patterns and the described mechanisms can also be considered as a form of spatial niche partitioning. Many empirical and model studies demonstrate how species can partition space between them, or occupy different spatial niches, to minimize local competition and allow regional coexistence (McKinney and Jaklin, 2000; Gilbert et al., 2008; Lyson and Longrich, 2011; Boeye et al., 2014). Again, in such studies different spatial niches are often characterized by different biotic or abiotic factors. Similarly, in metacommunity models, species sorting describes how heterogeneous environmental conditions can shape metacommunity patterns such that each species predominantly occupies patches with its preferred environment (Leibold et al., 2004). Our study shows that species sorting and spatial niche partitioning can be initiated simply by the existence of habitat boundaries and be shaped further by species interactions. The boundary constraints naturally lead to the emergence of a ‘preferred’ spatial niche in the center of the habitat (in principle preferred by any species in the model) that will be occupied by a dominant species.

This dominant species then leaves open areas closer to the boundary as spatial niches for other species. These niches effectively become the preferred habitat for the other species as they are less likely to encounter superior competitors closer to the boundary.

Since the spatial patterns in the food web model and the competition model are so similar (Fig. 7.3 and 7.6), it seems likely that in the food web model there is a mechanism similar to the competition-colonization trade-off. However, since in the food web model we used the same colonization rate for all species, the trade-off has to enter the model in some other way. One main assumption of the food web model by Pillai et al. (2010) is that more omnivorous species are weaker local competitors. In other words, the model straightforwardly includes a trade-off between competition strength and diet breadth. One can then realize that a larger diet breadth effectively leads to a colonization advantage. The specialist top-predator in Fig. 7.2, for example, can only colonize patches on which the intermediate predator is present. By contrast, the omnivore from the same web can additionally colonize patches on which only the basal species is present. In other words, as long as the specialist top-predator is not present on too many patches (making these patches uncolonizable for the omnivore), the omnivore has access to a larger part of the network than the top-predator. In this way, the trade-off between competition strength and diet breadth effectively becomes a competition-colonization trade-off. The observed spatial patterns, where more omnivorous species are driven successively towards the boundary, then emerge in a similar way as described above for the patterns in the competitive community. Overall, the

main difference between the food web model and the pure competition model is that in the food web model the ‘colonization part’ of the competition-colonization trade-off is mediated by trophic interactions while in the pure competition model it is implemented via a hierarchy of colonization rates. Note that Pillai et al. (2011) used a similar line of arguments to explain the coexistence of an omnivore and a specialist predator in the absence of a classical competition-colonization trade-off, but did not consider the emergence of spatial patterns.

One additional goal of this study was to investigate how the mid-domain effect for food chain length (Chapter 5) changes when considering food webs with omnivores instead of simple food chains. We found that the presence of an omnivore can indeed alter the mid-domain pattern of food chain length such that food chain length is maximal at an intermediate distance to the boundary. Consequently, we called this observation the intermediate distance effect. This effect is, however, rather weak and does not get significantly stronger when adding more than one omnivore to the food web. In fact, even for the generalized omnivore web (Fig. 7.3) the intermediate distance effect is strongest when only two of the four competing species persist (the specialist top-predator and one omnivore). We therefore suspect that the intermediate distance effect will also not get significantly stronger when considering even more complex food webs. Similarly, the intermediate distance effect does not get stronger when going from a one-dimensional to a two-dimensional habitat, even though the spatial occupancy patterns of the individual species are more pronounced in the two-dimensional case. We conclude that (within the Pillai model) the mid-domain effect

for food chain length is rather stable with respect to the food web structure, both on one-dimensional and two-dimensional habitats.

Finally, we want to point out that an observation similar to the intermediate distance effect has been made in a model of the standard mid-domain effect for species richness. First, note that in standard mid-domain effect models individual species do not extend over the full habitat but have finite ‘range sizes’. Colwell et al. (2009) showed that when all species have small range sizes, compared to the habitat size, then species richness peaks at an intermediate distance to the boundary. In the two-dimensional case the emerging ‘doughnut-like’ pattern looks similar to the spatial occupancy pattern of the level-1 omnivore from our study (Fig. 7.5; with an appropriate parametrization food chain length shows a similar pattern). In our study this pattern emerges due to an interplay of geometric edge effects and trophic interactions while in the study by Colwell et al. (2009) the pattern is essentially caused by ‘reflecting boundaries’. Even though the underlying mechanisms are different, and even though we consider food chain length while Colwell et al. (2009) consider species richness, we think that the emergence of these similar patterns is an interesting observation.

Conclusion

Overall, we have shown how the interplay of geometric edge effects and species interactions can shape complex spatial patterns of species occupancies (and food chain length). The observed patterns constitute a form of spatial niche partitioning that emerges in the absence of heterogeneous environmental factors. Future studies in

the field of spatial ecology concerned with edge effects, or spatial patterns of species occupancies, richness, abundances, and so on in general, should not only consider spatially varying environmental conditions as explanatory factors for these patterns, but should also take into account

effects caused by the geometric constraints of the habitat.

Acknowledgements This work was supported by the German Research Foundation (DFG) as part of the research unit 1748.

Part III
Final discussion

8 Joint discussion of research chapters

8.1 Summary and common message of research chapters

In the three research chapters (Chapters 5, 6, and 7) we combined the meta-food-web model by Pillai et al. (2010) with spatially explicit habitats and obtained the following main results:

1. We found a mid-domain effect for food chain length stating that food chain length is largest in the center of a habitat and decreases towards the boundaries even in the absence of other environmental gradients. The underlying food web was a simple food chain and habitats had lattice-like structure.
2. Based on the concept of centrality measures we generalized the mid-domain effect for food chain length to habitats that are represented by random networks of patches. Food chain length generally tends to be larger on more central patches and smaller on less central patches. We introduced a new centrality measure, the SIS centrality, based on susceptible-infected-susceptible dynamics from epidemics on networks, that is particularly well suited to obtain this result.
3. Based on the setup from the first research chapter we added omnivores to the food chain and found that the mid-domain effect for food chain length is rather stable to this modification. We observed only a small deviation from the mid-domain pattern, namely that food chain length can be slightly larger at an intermediate distance to the boundary compared to the mid-domain. For the spatial patterns of the individual species we found that a specialist top-predator dominates the mid-domain while more omnivorous species are driven successively towards the boundary. This observation amounts to a spatial niche partitioning between the species.

All these results have in common that they emerge in the absence of spatially heterogeneous environmental conditions. The results are instead caused by geometric constraints posed by the habitat structure (for example by the habitat boundaries in case of the first and third research chapter) and the interactions between the species. Our results, and the underlying mechanisms,

thus go in the same direction as (a) the mid-domain effect for species richness (Colwell and Hurtt, 1994; Jetz and Rahbek, 2001; Connolly, 2005), stating that species richness is maximal in the center of a habitat and decreases towards the boundaries even in the absence of environmental gradients, (b) the geometric edge effect (Prevedello et al., 2013) which is analogous to the mid-domain effect but formulated for species abundances and supposed to act on smaller spatial scales, and (c) results by Barter and Gross (2017) who showed for random habitat networks that an omnivore and a competing specialist predator have to some extent complementary spatial patterns even when patches do not differ in their environmental conditions.

Many other studies concerned with spatial variations of species abundances, richness, and similar quantities, consider other spatially changing environmental conditions as the drivers of these variations. Edge effect studies, for example, often focus on edge effects mediated by changes in light incidence, wind intensity, or resource availability close to the boundary of the habitat (Murcia, 1995; Esseen and Renhorn, 1998; Ries and Sisk, 2004; de Paula Ferreira et al., 2015). Other factors considered as determinants of food chain length are primary productivity (Kaunzinger and Morin, 1998), ecosystem size (Post et al., 2000), metacommunity dynamics (not investigating spatially explicit patterns of food chain length) (Holt, 2002; Calcagno et al., 2011), or the foraging behaviour of predators (Kondoh and Ninomiya, 2009). Similarly, patterns of species richness are, in addition to the mid-domain effect, explained by heterogeneities in temperature, productivity, and other factors (Jetz and Rahbek, 2002; Colwell et al., 2004). In reality no single explanatory factor will fully account for any spatial pattern of species abundance, richness, or a similar quantity. Our studies emphasize that geometric constraints posed by the habitat, or more precisely the positions of patches within a habitat, should be considered as an additional explanatory factor for such spatial patterns in future studies.

8.2 Simplifying model assumptions

The meta-food-web model by Pillai et al. (2010), underlying all three research chapters, makes several simplifying assumptions. For example, by strictly applying the competitive exclusion principle among predators for common prey, the most complex local food webs are chains. Also, as usual for a colonization-extinction model, population dynamics are neglected, implying that they occur on a much faster time scale than the colonization-extinction

dynamics. In our studies we additionally used the same colonization rate, extinction rate, and spatial network (or colonization range) for all species and neglected top-down effects. The model is kept as simple as possible since for a more complex model the interpretation of the results would also get more complicated. In the third research chapter (Chapter 7), for example, we observed the regional coexistence of several omnivorous species and a specialist top-predator, as well as a spatial niche partitioning between these species. Without the locally applied competitive exclusion principle, the coexistence of the species could simply be possible due to local coexistence mechanisms. Likewise, by allowing larger colonization rates for more omnivorous species (which are weaker local competitors), the regional coexistence as well as the spatial niche partitioning could also be established by a traditional competition-colonization trade-off (see the analogous result for a purely competitive metacommunity in Chapter 7). Due to the model simplifications neither of these two mechanisms could be at work in our study. We could therefore conclude that the coexistence of the omnivores and the specialist predator, as well as their spatial niche partitioning, was enabled by a trade-off between competition strength and diet breadth. Had we relaxed the assumption of competitive exclusion or species-independent colonization rates, we would not have been able to identify this coexistence (and pattern-forming) mechanism. Note that Pillai et al. (2011) provided similar arguments for the coexistence of an omnivore and a specialist predator, but did not investigate spatial patterns.

9 Future work

9.1 The fourth research chapter

The basic idea of this thesis was to model the dynamics of food webs on spatially explicit habitat networks and to characterize spatial patterns of food chain length and species occupancies. In the first research chapter (Chapter 5) we considered simple food chains and simple lattice-like networks. In the second research chapter (Chapter 6) we kept the simple food chains but considered more complex (random) spatial networks. In the third research chapter (Chapter 7), we considered more complex food webs but kept the simple lattice-like habitat networks. A missing piece and setup for a possible fourth research chapter is to consider both, complex food webs and complex spatial networks. Barter and Gross (2017) went in this direction by modelling the dynamics of a simple omnivore web on random networks. The main observation was that a specialist top-predator and the omnivore show to some extent complementary spatial patterns. This goes in the same direction as the spatial niche partitioning that we observed in the third research chapter on lattice-like networks, but on random networks the patterns are more difficult to characterize. On bounded, lattice-like networks it is natural to use the distance to the boundary to quantify the position of a patch and thus to characterize spatial patterns. On random networks the role of the distance to the boundary has to be replaced by centrality measures. In the second research chapter we succeeded at describing patterns of food chain length by centrality measures, in particular when using our newly introduced SIS centrality, if the underlying food web is a simple food chain. In some later tests we found, however, that none of the centrality measures considered in the second research chapter is suited to predict the spatial pattern of the omnivore from the simple omnivore web on random habitat networks (also when allowing non-linear functional relations; results not shown). It is thus an open challenge to find a centrality measure that is suited for this purpose. Ideally, the same centrality measure should also be able to describe the spatial patterns of additional omnivores (see third research chapter), species in other complex food webs, and food chain length. With such a centrality measure the (weak) intermediate distance effect that we found in the third research chapter (see Figs. 7.2 and 7.3), stating that on top of the mid-domain pattern food chain length can be largest at an intermediate distance to the boundary, could be generalized to an intermediate centrality

effect, stating that food chain length is largest on patches with intermediate centrality.

A second open challenge is to find other applications for the SIS centrality from the second research chapter beyond the scope of this thesis. Since the SIS centrality is based on susceptible-infected-susceptible dynamics from epidemics on networks, it should be used to predict outcomes of even more complex dynamical processes on networks or real-world observations where the underlying process is not precisely known.

9.2 Focusing on purely competitive communities

In the third research chapter (Chapter 7) we found the same spatial niche partitioning, that we observed for the specialist top-predator and a set of omnivores from the generalized omnivore food web (Fig. 7.3), also for species forming a purely competitive community (Fig. 7.6). To this end we used a spatially explicit version of the metacommunity model by Tilman (1994), who showed that in principle an arbitrary number of species can regionally coexist if weaker local competitors are stronger colonizers (competition-colonization trade-off). Our results show how this coexistence mechanism can additionally shape the spatial patterns of the coexisting species in a bounded habitat. While in this thesis we focused on the meta-food-web results, the spatial niche partitioning in the purely competitive metacommunity might actually be the more interesting result for ecologists. After all, the metacommunity model by Tilman (1994) has a longer standing in ecology than the meta-food-web model by Pillai et al. (2010). Furthermore, the generalized omnivore food web with its three increasingly omnivorous species is quite artificial and purposely designed to mimic the competition in a purely competitive community, but where the competition is mediated by trophic interactions. A possible future study could thus focus on the boundary-induced spatial niche partitioning in purely competitive metacommunities.

From another perspective, the strong similarity between the results in the metacommunity framework and the meta-food-web framework demonstrates that the details of how the competition is modelled plays no significant role. To some extent it might therefore be possible to draw conclusions for one framework from results obtained in the other one. This link could be used in future studies (drawing conclusions for a subset of species in a meta-food-web by investigating an appropriate metacommunity of purely competitive species) and might be worth to be investigated further.

Appendix

A Equations for general meta-food-webs

A.1 Introduction

Here we present the general differential equation for the fraction of patches $p^{(i,j)}$ occupied by the feeding link (i, j) from any prey i to any predator j in an arbitrary food web in the model by Pillai et al. (2010). An introduction to the model, including its general rules and differential equations for specific, simple food webs is given in Section 3.3. Pillai et al. (2010) split the general equation for $p^{(i,j)}$ into eight contributions,

$$\frac{dp^{(i,j)}}{dt} = A - B - C + D + E - F - G - H, \quad (\text{A.1})$$

each of which describes a distinct type of colonization, extinction, displacement, or food web rearrangement event. Pillai et al. (2010) further provided and explained analytical expressions for all eight terms. From these expressions, we were, however, not able to derive the omnivore equations (Eqs. 3.5 and 3.6), as well as similar equations given in Pillai et al. (2010). We therefore re-derived the general equation for $p^{(i,j)}$, that is, all terms from A to H , from the basic principles of the model. In the following, we present and explain the expressions that we found, highlight relevant differences to the Pillai version, and exemplarily show how our equation can be used to successfully derive the omnivore equations. For simplicity, we directly adapt the general equation to the special case of neglecting all top-down effects and assuming the same colonization and extinction rates for all species (or feeding links). Our expressions are therefore simpler than they would be in the most general case, since in colonization terms we do not have to sum over the different preys of the colonizing species (which can in the general case affect the colonization rate), and since in extinction terms we do not have to sum over the different predators of the species that goes extinct (which is in the general case required to include top-down effects). All terms can be augmented to the spatially explicit case as described in Section 3.4.1.

Note that while the basal species 1 has no modelled resource, we formally have to define a resource ‘species 0’ since some of the expressions require us to sum over the resources of species 1. ‘Species 0’ can also be regarded as ‘available habitat’ (not empty patches but the mere presence of patches). ‘Species 0’ cannot go extinct, be displaced, or colonize. In contrast to the actual species, its colonization and extinction rates are thus zero.

A.2 Terminology

Here we provide an overview of all quantities used in the differential equation. A similar overview is provided by Pillai et al. (2010).

- c' is the species-independent colonization rate.
- e is the species-independent intrinsic extinction rate.
- $p^{(i,j)}$ is the fraction of patches occupied by the link from prey i to predator j .
- $p^{(j)} = \sum_i p^{(i,j)}$ is the fraction of patches occupied by species j .
- $\rho^{(i,j)} = p^{(i,j)}/p^{(j)}$ is the fraction of j -occupied patches (in the following simply j -patches) on which species j feeds on species i . If $p^{(j)} = 0$ then $\rho^{(i,j)} = 0$.
- $R(j)$ is the set of all preys (resources) of species j .
- $C(i)$ is the set of all predators (consumers) of species i .
- χ is the directed adjacency matrix of the food web, that is, $\chi(i, j) = 1$ if j can prey on i , and 0 otherwise. We also use $\bar{\chi}(i, j) = 1 - \chi(i, j)$. Note that χ does not appear in the expressions by Pillai et al. (2010).
- $\kappa_i(j, k)$ is a competition function of predators j and k for prey i . We use $\kappa_i(j, k) = 1$ if j can displace k on i -patches and 0 otherwise. We assume that this is possible if j can actually feed on i and if $j < k$. Species labels have to be chosen such that this competition hierarchy is equivalent to the assumption that a specialist predator is locally superior to a generalist predator. Since a species cannot displace itself, we have $\kappa_i(j, j) = 0$.
- $\Phi_{j,k}^i$ is the probability that (on a given patch) an extinction of j leads to an extinction of k , given that i is present. This can only happen if $k \geq j$, thus $\Phi_{j,k}^i = 0$ if $j > k$. For $k = j$ we have $\Phi_{j,j}^i = 1$. Species k can avoid the bottom-up extinction if any species between j and k (including k itself) can switch prey onto i . There are two relevant cases concerning the relation between i and j . Either j preyed on i before going extinct, or i is a superior competitor to j (for some common prey) who just invaded and displaced j . The analytical expression for $\Phi_{j,k}^i$ is given below, after the expressions for terms A to H .

A.3 The equation

Term A

Term A describes the increase of $p^{(i,j)}$ due to colonization of j on an i -patch,

$$A = c'p^{(j)} \left(p^{(i)} - \sum_{k \in C(i)} p^{(i,k)} [1 - \kappa_i(j, k)] \right). \quad (\text{A.2})$$

- Colonizers of species j can be sent from any patch on which species j is present, $c'p^{(j)}$.
- Colonization of j on an i -patch requires presence of species i , $p^{(i)}$.
- The presence of a competitor k that cannot be displaced by j (including j itself) prevents colonization of species j , $-\sum_{k \in C(i)} p^{(i,k)} [1 - \kappa_i(j, k)]$.

Term B

Term B describes the decrease of $p^{(i,j)}$ due to extinction of species j on an (i, j) -patch,

$$B = ep^{(i,j)}. \quad (\text{A.3})$$

Term C

Term C describes the decrease of $p^{(i,j)}$ due to displacement of species j by a superior competitor for species i ,

$$C = p^{(i,j)} \sum_{k \in C(i)} \kappa_i(k, j) c'p^{(k)}. \quad (\text{A.4})$$

- Only possible on patches on which j currently feeds on i , $p^{(i,j)}$.
- Species j can be displaced by other consumers k of species i that are stronger competitors, $\sum_{k \in C(i)} \kappa_i(k, j) \dots$.
- Colonizers of species k can be sent from any patch on which species k is present, $c'p^{(k)}$.

Term D

Term D describes the increase of $p^{(i,j)}$ due to prey-switching of j onto i from an alternate resource after extinction of i 's current predator l , and (bottom-up) extinction of j 's current prey k ,

$$D = \sum_{\substack{k \in R(j) \\ k > i}} p^{(k,j)} \sum_{l \in C(i)} \rho^{(i,l)} e \Phi_{l,k}^i. \quad (\text{A.5})$$

- Species j can only switch prey onto i on patches on which j is currently present and feeds on one of its other resources, $\sum_{\substack{k \in R(j) \\ k > i}} p^{(k,j)} \dots$. Due to the local food chain structure and competition hierarchy by species label, the current prey k of j needs to satisfy $k > i$.
- The current consumer l of i has to go extinct (by its own intrinsic extinction), $\sum_{l \in C(i)} \rho^{(i,l)} e \dots$. $\rho^{(i,l)}$ makes sure that only patches on which species l actually feeds on i are considered. This also ensures the required presence of species i itself.
- The extinction of i 's consumer l has to lead to the extinction of j 's resource k , $\Phi_{l,k}^i$.

Important difference to Pillai version:

Term D in Pillai et al. (2010) contains an additional sum over all predators m of species l . This is necessary since in the most general case species l can also suffer a top-down extinction. Pillai et al. (2010) then used $\Phi_{m,k}^i$ instead of $\Phi_{l,k}^i$ for the bottom-up extinction probability of species k . Since the first species going extinct and causing any bottom-up extinction is l , $\Phi_{l,k}^i$ has to be used.

Term E

Term E describes the increase of $p^{(i,j)}$ due to prey-switching of j onto i , from an alternate resource, after invasion of i ,

$$E = c' p^{(i)} \sum_{\substack{k \in R(j) \\ k \neq i}} p^{(k,j)} \left[\kappa_k(i, j) + \sum_{\substack{q \in R(i) \\ q \neq k}} \sum_{\substack{r \in C(q) \\ r \neq i, j}} \rho^{(q,r)} \kappa_q(i, r) \bar{\chi}(i, r) \Phi_{r,k}^i \right]. \quad (\text{A.6})$$

- Colonizers can be sent from any patch on which species i is present, $c'p^{(i)}$.
- Species j has to be currently present and feed on one of its other resources, $\sum_{\substack{k \in R(j) \\ k \neq i}} p^{(k,j)} \dots$.
- The first term in the brackets, $\kappa_k(i, j)$, captures the case that the invading species i outcompetes species j for prey k . Species j then switches prey onto i . There is *no* extinction involved! We do not have to check that j can actually feed on i since this is automatically implied by the fact that we consider an equation for the link (i, j) .
- In the second term in the brackets, invader i outcompetes another species r for a common resource q . This is only possible on r -patches on which r actually feeds on q , $\rho^{(q,r)}$, and if i is the stronger competitor, $\kappa_q(i, r)$. Species r must also not be able to switch prey onto i , $\bar{\chi}(i, r)$, since this would prevent r 's extinction. The extinction of r must then lead to the bottom-up extinction of j 's prey k , $\Phi_{r,k}^i$. Extinction of r and k is necessary to allow species j to switch prey onto i . The exclusions in the sums are optional since they would have no contribution ($\Phi_{r,k}^i = 0$). The case $q = k$, $r = j$ is taken care of by the first term in the brackets.

Important differences to Pillai version:

- Pillai et al. (2010) missed the contribution of the first term in the brackets, $\kappa_k(i, j)$.
- Pillai et al. (2010) did not include the probability that r , if present on a patch, actually feeds on q , $\rho^{(q,r)}$.
- Pillai et al. (2010) did not check whether r actually goes extinct after being outcompeted by i , $\bar{\chi}(i, r)$. Species r could switch prey onto i and thus not go extinct. This possibility is not captured by $\Phi_{r,k}^i$, since $\Phi_{r,k}^i$ assumes that r already did go extinct.

Term F

Term F describes the decrease of $p^{(i,j)}$ due to extinction of species i (either its own intrinsic extinction or bottom-up extinction caused by intrinsic

extinction of a species s below it),

$$F = p^{(i,j)} \sum_{s \leq i} e \sum_{r \in R(s)} \rho^{(r,s)} \Phi_{s,i}^r. \quad (\text{A.7})$$

- Only contributes on patches on which j currently feeds on i , $p^{(i,j)}$.
- Species i or a species further down has to suffer intrinsic extinction, $\sum_{s \leq i} e \cdots$.
- The extinction of species s has to lead to the extinction of species i , $\Phi_{s,i}^r$. This depends on the current resource r of s , $\sum_{r \in R(s)} \cdots$, since some species could switch prey onto r and thus prevent the bottom-up extinction of i . With $\rho^{(r,s)}$ we take into account the probability that s actually feeds on r .

Important differences to Pillai version:

- Pillai et al. (2010) used the restriction $s < i$ instead of $s \leq i$. In this case i can only go extinct by bottom-up extinctions but not by its own intrinsic extinction.
- Term F in Pillai et al. (2010) contains an additional sum over all predators t of species s . This is necessary since in the most general case species s can also suffer a top-down extinction. Pillai et al. (2010) then used $\Phi_{t,i}^r$ instead of $\Phi_{s,i}^r$ for the bottom-up extinction probability of species i . Since the first species going extinct and causing any bottom-up extinction is s , $\Phi_{s,i}^r$ has to be used.
- In Pillai et al. (2010), r is still used outside the brackets in which \sum_r exists, even though r is then not defined anymore.

Term G

Term G describes the decrease of $p^{(i,j)}$ due to competitive displacement of species i , or of a species below i with following bottom-up extinction of i ,

$$G = p^{(i,j)} \sum_{t \leq i} \sum_{s \in R(t)} \rho^{(s,t)} \sum_{m \in C(s)} \kappa_s(m, t) \bar{\chi}(m, t) \Phi_{t,i}^m c' p^{(m)}. \quad (\text{A.8})$$

- $p^{(i,j)}$: only contributes on patches on which j currently feeds on i .

- $\sum_{t \leq i}$: t is the competitively displaced species.
- $\sum_{s \in R(t)}$: sum over all resource s that t can feed on. The resource s can influence the ability of an invader to displace t .
- $\rho^{(s,t)}$: probability that t currently feeds on s .
- $\sum_{m \in C(s)}$: m is the invasive species that tries to displace t .
- $\kappa_s(m, t)$: check if m is a stronger competitor for s than t .
- $\bar{\chi}(m, t)$: make sure that t cannot switch prey onto m which would prevent t 's extinction.
- $\Phi_{t,i}^m$: probability that the extinction of t also leads to extinction of i . Species m , after displacing t , is a potential target for prey-switching of any species between t and i .
- $c'p^{(m)}$: colonizers of species m can be sent from any patch on which species m is present.

Important differences to Pillai version:

Pillai et al. (2010) did not check whether t actually goes extinct after being displaced by m , $\bar{\chi}(m, t)$. Species t could switch prey onto m and thus not go extinct. This possibility is not captured by $\Phi_{t,i}^m$, since $\Phi_{t,i}^m$ assumes that t already did go extinct.

Term H

We can drop term H from Pillai et al. (2010) since it only includes top-down effects.

A.4 Bottom-up extinction probability $\Phi_{j,k}^i$

As introduced above, $\Phi_{j,k}^i$ is the probability that (on a given patch) an extinction of j leads to an extinction of k , given that i is present. To calculate this probability we have to know all directed feeding paths from j to k . Following Pillai et al. (2010) we denote such a path by $T_{j,k}$ and the set of all these paths by $S_{j,k}$. Each path is realized with probability $\prod_{(l,n) \in E_{T_{j,k}}} \rho^{(l,n)}$,

where $E_{T_{j,k}}$ is the set of links (l, n) contained in the path $T_{j,k}$. Due to the local food chain structure the realizations of the paths are mutually exclusive, so that the probabilities for different paths can be summed up. The probability that (on a given patch) any of the feeding paths from j to k is realized is thus,

$$f(S_{j,k}) = \sum_{T_{j,k} \in S_{j,k}} \left(\prod_{(l,n) \in E_{T_{j,k}}} \rho^{(l,n)} \right). \quad (\text{A.9})$$

Species k will, however, only suffer bottom-up extinction for paths on which no species between j and k (including k itself) can switch prey onto i . Note that species i is either the former prey of species j , or a superior competitor who displaced j . After j 's extinction, species i is the only intermediate species that has no predator, and is thus the only possible target for prey-switching. To calculate $\Phi_{j,k}^i$ we have to subtract from $f(S_{j,k})$ the probabilities of the paths on which the rescuing prey-switching is possible,

$$\Phi_{j,k}^i = f(S_{j,k}) - f \left(\bigcup_{\substack{m \in C(i) \\ m \neq j}} (S_{j,m} \cup S_{m,k}) \right). \quad (\text{A.10})$$

In the second term on the right hand side of Eq. A.10, m is a predator of i that can switch prey onto i . We have to exclude $m = j$ since j just went extinct and can thus not switch prey onto i anymore. $S_{j,m} \cup S_{m,k}$ is the set of paths obtained by concatenating all pairs of paths in $S_{j,m}$ and $S_{m,k}$. \bigcup_m is the typical set union. After this union, the set contains all paths from j to k on which some species is able to switch prey onto i . The same path might appear for different m but is only included once in the unified set.

Pillai et al. (2010) provided the same expressions (Eqs. A.9 and A.10) and in the appendix demonstrated the calculation of $\Phi_{j,k}^i$ by example. While in the main text they did not exclude the case $m = j$, they did do so in the calculation in the appendix.

A.5 Example: deriving the omnivore equations

We use the above expressions A to H to derive Eqs. 3.5 and 3.6 for the feeding links $(1, O)$ and $(2, O)$ related to the omnivore from the food web shown in Figs. 3.2 and 3.3. Note that when using the hierarchical labelling of species the omnivore O would get label 4 in this food web. Also note that

the specialist species 1, 2, and 3 in the food web have only a single feeding link, $(k-1, k)$. Thus, $p^{(k-1, k)} = p^{(k)}$ which we use in the following to shorten the notation.

For link (1, O):

- Term A: $c'p^{(O)}(p^{(1)} - p^{(2)} - p^{(1, O)})$ (colonization of the omnivore)
- Term B: $(-)ep^{(1, O)}$ (extinction of the omnivore)
- Term C: $(-)p^{(1, O)}c'p^{(2)}$ (decrease due to colonization of species 2 on $(1, O)$ -patches; the omnivore gets outcompeted by 2 for preying on 1)
- Term D: $ep^{(2, O)}$ (increase due to extinction of species 2 on $(2, O)$ -patches)
- Term E: 0 (prey-switching of the omnivore onto 1 from an alternate resource after invasion of 1 is not possible. Had 1 not been present from the beginning, the omnivore could not have persisted either.)
- Term F: $(-)ep^{(1, O)}$ (extinction of species 1)
- Term G: 0 (species 1 cannot be competitively displaced)

Putting all terms (with the correct signs) together, we arrive exactly at Eq. 3.5. We were not able to obtain the contributions of terms D and F by using the corresponding expressions from Pillai et al. (2010).

For link (2, O):

- Term A: $c'p^{(O)}(p^{(2)} - p^{(3)} - p^{(2, O)})$ (colonization of the omnivore)
- Term B: $(-)ep^{(2, O)}$ (extinction of the omnivore)
- Term C: $(-)p^{(2, O)}c'p^{(3)}$ (decrease due to colonization of species 3 on $(2, O)$ -patches; the omnivore gets outcompeted by 3 for preying on 2)
- Term D: 0 (there is no species between 2 and the omnivore that could go extinct and lead to prey-switching of the omnivore onto 2)
- Term E: $c'p^{(2)}p^{(1, O)}$ (colonization of species 2 on $(1, O)$ -patches)

- Term F: $(-)\ 2ep^{(2,O)}$ (intrinsic extinction of species 2 and bottom-up extinction caused by extinction of species 1)
- Term G: 0 (species 1 and 2 cannot be competitively displaced)

Putting all terms (with the correct signs) together, we arrive exactly at Eq. 3.6. We were not able to obtain the contributions of terms E and F by using the corresponding expressions from Pillai et al. (2010). In our case the contribution to term E comes from the first term in the bracket of Eq. A.6.

References

- Ahn, Y.-Y. and Jeong, H. (2006). Epidemic dynamics of two species of interacting particles on scale-free networks. *Phys. Rev. E*, 74:066113.
- Albert, R. and Barabási, A.-L. (2000). Topology of evolving networks: Local events and universality. *Phys. Rev. Lett.*, 85:5234–5237.
- Albert, R. and Barabási, A.-L. (2002). Statistical mechanics of complex networks. *Rev. Mod. Phys.*, 74:47–97.
- Altermatt, F. and Fronhofer, E. A. (2018). Dispersal in dendritic networks: Ecological consequences on the spatial distribution of population densities. *Freshwater Biol.*, 63:22–32.
- Amarasekare, P. (2003). Competitive coexistence in spatially structured environments: a synthesis. *Ecol. Lett.*, 6:1109–1122.
- Amarasekare, P. (2008). Spatial dynamics of foodwebs. *Annu. Rev. Ecol. Evol. Syst.*, 39:479–500.
- Antonioni, A. and Tomassini, M. (2012). Degree correlations in random geometric graphs. *Phys. Rev. E*, 86:037101.
- Azimi-Tafreshi, N. (2016). Cooperative epidemics on multiplex networks. *Phys. Rev. E*, 93:042303.
- Barabási, A.-L. (2016). *Network Science*. Cambridge University Press.
- Barter, E. and Gross, T. (2016). Meta-food-chains as a many-layer epidemic process on networks. *Phys. Rev. E*, 93:022303.
- Barter, E. and Gross, T. (2017). Spatial effects in meta-foodwebs. *Sci. Rep.*, 7:9980.
- Barthélemy, M. (2011). Spatial networks. *Phys. Rep.*, 499:1–101.
- Bascompte, J. and Solé, R. V. (1998). Effects of habitat destruction in a prey-predator metapopulation model. *J. Theor. Biol.*, 195:383–393.
- Bavelas, A. (1950). Communication patterns in task-oriented groups. *J. Acoust. Soc. Am.*, 22:725–730.
- Bell, G. (2001). Neutral macroecology. *Science*, 293:2413–2418.
- Boeye, J., Kubisch, A., and Bonte, D. (2014). Habitat structure mediates spatial segregation and therefore coexistence. *Landscape Ecol.*, 29:593–604.

- Böhme, G. A. and Gross, T. (2012). Persistence of complex food webs in metacommunities. *arXiv:1212.5025v1*.
- Bokma, F., Bokma, J., and Mönkkönen, M. (2000). The mid-domain effect and the longitudinal dimension of continents. *Trends Ecol. Evol.*, 15:288–289.
- Bokma, F., Bokma, J., and Mönkkönen, M. (2001). Random processes and geographic species richness patterns: why so few species in the north? *Ecography*, 24:43–49.
- Bollobás, B. (1984). Graph theory and combinatorics. In *Proceedings of the Cambridge Combinatorial Conference in Honour of Paul Erdős*. Academic Press.
- Bollobás, B. and Riordan, O. (2004). The diameter of a scale-free random graph. *Combinatorica*, 24:5–34.
- Bonacich, P. (1972a). Factoring and weighting approaches to status scores and clique identification. *J. Math. Sociol.*, 2:113–120.
- Bonacich, P. (1972b). Technique for analyzing overlapping memberships. *Sociol. Methodol.*, 4:176–185.
- Bonacich, P. (1987). Power and centrality: A family of measures. *Am. J. Sociol.*, 92:1170–1182.
- Borgatti, S. P. (2005). Centrality and network flow. *Soc. Networks*, 27:55–71.
- Brin, S. and Page, L. (1998). The anatomy of a large-scale hypertextual web search engine. *Comput. Netw.*, 30:107–117.
- Broadbent, E. N., Asner, G. P., Keller, M., Knapp, D. E., Oliveira, P. J. C., and Silva, J. N. (2008). Forest fragmentation and edge effects from deforestation and selective logging in the brazilian amazon. *Biol. Conserv.*, 141:1745–1757.
- Buse, J., Entling, M. H., Ranius, T., and Assmann, T. (2016). Response of saproxylic beetles to small-scale habitat connectivity depends on trophic levels. *Landscape Ecol.*, 31:939–949.
- Cadotte, M. W., Mai, D. V., Jantz, S., Collins, M. D., Keele, M., and Drake, J. A. (2006). On testing the competition-colonization trade-off in a multispecies assemblage. *Am. Nat.*, 168:704–709.
- Calcagno, V., Massol, F., Mouquet, N., Jarne, P., and David, P. (2011). Constraints on food chain length arising from regional metacommunity dynamics. *Proc. R. Soc. B*, 278:3042–3049.
- Calcagno, V., Mouquet, N., Jarne, P., and David, P. (2006). Coexistence in a metacommunity: the competition-colonization trade-off is not dead. *Ecol. Lett.*, 9:897–907.

- Carrara, F., Altermatt, F., Rodrigues-Iturbe, I., and Rinaldo, A. (2012). Dendritic connectivity controls biodiversity patterns in experimental metacommunities. *PNAS*, 109(15):5761–5766.
- Carrara, F., Rinaldo, A., Giometto, A., and Altermatt, F. (2013). Complex interaction of dendritic connectivity and hierarchical patch size on biodiversity in river-like landscapes. *Am. Nat.*, 183(1):13–25.
- Colwell, R. K., Gotelli, N. J., Rahbek, C., Entsminger, G. L., Farrell, C., and Graves, G. R. (2009). Peaks, plateaus, canyons, and craters: the complex geometry of simple mid-domain effect models. *Evol. Ecol. Res.*, 11:355–370.
- Colwell, R. K. and Hurtt, G. C. (1994). Nonbiological gradients in species richness and a spurious rapoport effect. *Am. Nat.*, 144:570–595.
- Colwell, R. K. and Lees, D. C. (2000). The mid-domain effect: geometric constraints on the geography of species richness. *Trends Ecol. Evol.*, 15:70–76.
- Colwell, R. K., Rahbek, C., and Gotelli, N. J. (2004). The mid-domain effect and species richness patterns: What have we learned so far? *Am. Nat.*, 163:E1–23.
- Connolly, S. R. (2005). Process-based models of species distributions and the mid-domain effect. *Am. Nat.*, 166:1–11.
- Dall, J. and Christensen, M. (2002). Random geometric graphs. *Phys. Rev. E*, 66:016121.
- De Domenico, M., Solé-Ribalta, A., Cozzo, E., Kivelä, M., Moreno, Y., Porter, M. A., Gómez, S., and Arenas, A. (2013). Mathematical formulation of multilayer networks. *Phys. Rev. X*, 3:041022.
- de Paula Ferreira, C., Casatti, L., Zeni, J. O., and Ceneviva-Bastos, M. (2015). Edge-mediated effects of forest fragments on the trophic structure of stream fish. *Hydrobiologia*, 762:15–28.
- de Roos, A. M., McCauley, E., and Wilson, W. G. (1998). Pattern formation and the spatial scale of interaction between predators and their prey. *Theor. Popul. Biol.*, 53:108–130.
- Débarre, F. and Lenormand, T. (2011). Distance-limited dispersal promotes coexistence at habitat boundaries: reconsidering the competitive exclusion principle. *Ecol. Lett.*, 14:260–266.
- Dorogovtsev, S. N. and Mendes, J. F. F. (2000). Evolution of networks with aging of sites. *Phys. Rev. E*, 62:1842–1845.
- Dunn, R. R., Colwell, R. K., and Nilsson, C. (2006). The river domain: why are there more species halfway up the river? *Ecography*, 29:251–259.

- Elton, C. (1927). *Animal Ecology*. New York: The Macmillan Company.
- Erdős, P. and Rényi, A. (1959). On random graphs. *Publicationes Mathematicae*, 6:290–297.
- Erdős, P. and Rényi, A. (1960). On the evolution of random graphs. *Publications of the Mathematical Institute of the Hungarian Academy of Sciences*, 5:17–61.
- Erdős, P. and Rényi, A. (1961). On the strength of connectedness of a random graph. *Acta Mathematica Scienta Hungary*, 12:261–267.
- Esseen, P.-A. and Renhorn, K.-E. (1998). Edge effects on an epiphytic lichen in fragmented forests. *Conserv. Biol.*, 12:1307–1317.
- Estrada, E., Meloni, S., Sheerin, M., and Moreno, Y. (2016). Epidemic spreading in random rectangular networks. *Phys. Rev. E*, 94:052316.
- Ewers, R. M. and Didham, R. K. (2006). Continuous response functions for quantifying the strength of edge effects. *J. Appl. Ecol.*, 43:527–536.
- Ewers, R. M. and Didham, R. K. (2008). Pervasive impact of large-scale edge effects on a beetle community. *PNAS*, 105:5426–5429.
- Fahrig, L. (2003). Effects of habitat fragmentation on biodiversity. *Annu. Rev. Ecol. Evol. Syst.*, 34:487–515.
- Freeman, L. C. (1977). A set of measures of centrality based on betweenness. *Sociometry*, 40:35–41.
- Freeman, L. C. (1979). Centrality in social networks: conceptual clarification. *Soc. Networks*, 1:215–239.
- Friedrich, T., Sauerwald, T., and Stauffer, A. (2013). Diameter and broadcast time of random geometric graphs in arbitrary dimensions. *Algorithmica*, 67:65–88.
- Garas, A., Schweitzer, F., and Havlin, S. (2012). A k-shell decomposition method for weighted networks. *New J. Phys.*, 14:083030.
- Gardner, M. R. and Ashby, W. R. (1970). Connectance of large dynamic (cybernetic) systems: Critical values for stability. *Nature*, 228:784.
- Gaston, K. J. (1996). Species-range-size distributions: patterns, mechanisms and implications. *Trends Ecol. Evol.*, 5:197–201.
- Gause, G. F. (1932). Experimental studies on the struggle for existence: 1. mixed population of two species of yeast. *J. Exp. Biol.*, 9:389–402.

- Gause, G. F. (1934). *The Struggle for Existence*. Baltimore: Williams & Wilkins Co.
- Gilarranz, L. J., Sabatino, M., Aizen, M. A., and Bascompte, J. (2015). Hot spots of mutualistic networks. *J. Anim. Ecol.*, 84:407–413.
- Gilbert, B., Srivastava, D. S., and Kirby, K. R. (2008). Niche partitioning at multiple scales facilitates coexistence among mosquito larvae. *Oikos*, 117:944–950.
- Gilbert, E. N. (1961). Random plane networks. *Journal of the Society for Industrial and Applied Mathematics*, 9:533–543.
- Gillespie, D. T. (1977). Exact stochastic simulation of coupled chemical reactions. *J. Phys. Chem.*, 81:2340–2361.
- Goldwasser, L. and Roughgarden, J. (1993). Construction and analysis of a large caribbean food web. *Ecology*, 74:1216–1233.
- Goltsev, A. V., Dorogovtsev, S. N., Oliveira, J. G., and Mendes, J. F. F. (2012). Localization and spreading of diseases in complex networks. *Phys. Rev. Lett.*, 109:128702.
- Golub, G. H. and Van Loan, C. F. (1996). *Matrix Computations*. The Johns Hopkins University Press.
- Gravel, D., Canard, E., Guichard, F., and Mouquet, N. (2011a). Persistence increases with diversity and connectance in trophic metacommunities. *PLoS ONE*, 6:e19374.
- Gravel, D., Massol, F., Canard, E., Mouillot, D., and Mouquet, N. (2011b). Trophic theory of island biogeography. *Ecol. Lett.*, 14:1010–1016.
- Grinnell, J. (1904). The origin and distribution of the chestnut-backed chickadee. *The Auk*, 21(3):364–382.
- Grinnell, J. (1917). The niche-relationships of the california thrasher. *The Auk*, 34:427–433.
- Grytnes, J. A. (2003). Ecological interpretations of the mid-domain effect. *Ecol. Lett.*, 6:883–888.
- Grytnes, J. A. and Vetaas, O. R. (2002). Species richness and altitude: a comparison between null models and interpolated plant species richness along the himalayan altitudinal gradient. *Am. Nat.*, 159:294–304.
- Hanski, I. and Gilpin, M. (1991). Metapopulation dynamics: brief history and conceptual domain. *Biol. J. Linn. Soc.*, 42:3–16.
- Hardin, G. (1960). The competitive exclusion principle. *Science*, 131(3409):1292–1297.

- Hassell, M. P., Comins, H. N., and May, R. M. (1991). Spatial structure and chaos in insect population dynamics. *Nature*, 353:255–258.
- Hastings, A. (1980). Disturbance, coexistence, history, and competition for space. *Theor. Popul. Biol.*, 18:363–373.
- Havens, K. (1992). Scale and structure in natural food webs. *Science*, 257:1107–1109.
- Hiebeler, D. (2000). Populations of fragmented landscapes with spatially structured heterogeneities: landscape generation and local dispersal. *Ecology*, 81:1629–1641.
- Holt, R. D. (1993). Ecology at the mesoscale: The influence of regional processes on local communities. In Ricklefs, R. E. and Schluter, D., editors, *Species Diversity in Ecological Communities*, pages 77–88. University of Chicago Press, Chicago.
- Holt, R. D. (1996). Food webs in space: An island biogeographic perspective. In Polis, G. and Winemiller, K., editors, *Food Webs: Contemporary Perspectives*, pages 313–323. Chapman and Hall.
- Holt, R. D. (2002). Food webs in space: On the interplay of dynamic instability and spatial processes. *Ecol. Res.*, 17:261–273.
- Hubbell, S. P. (2001). *The Unified Neutral Theory of Biodiversity and Biogeography*. Princeton University Press.
- Hutchinson, G. E. (1957). Concluding remarks. *Cold Spring Harbor Symposia on Quantitative Biology*, 22:415–427.
- Jetz, W., Carbone, C., Fulford, J., and Brown, J. H. (2004). The scaling of animal space use. *Science*, 5694:266–268.
- Jetz, W. and Rahbek, C. (2001). Geometric constraints explain much of the species richness pattern in african birds. *PNAS*, 98:5661–5666.
- Jetz, W. and Rahbek, C. (2002). Geographic range size and determinants of avian species richness. *Science*, 297:1548–1551.
- Katz, L. (1953). A new status index derived from sociometric analysis. *Psychometrika*, 18:39–43.
- Kaunzinger, C. M. K. and Morin, P. J. (1998). Productivity controls food-chain properties in microbial communities. *Nature*, 395:495–497.
- Kessler, M. (2001). Patterns of diversity and range size of selected plant groups along an elevational transect in the bolivian andes. *Biodivers. Conserv.*, 10:1897–1921.

- Kitsak, M., Gallos, L. K., Havlin, S., Liljeros, F., Muchnik, L., Stanley, H. E., and Makse, H. A. (2010). Identification of influential spreaders in complex networks. *Nat. Phys.*, 6:888–893.
- Komonen, A., Penttilä, R., Lindgren, M., and Hanski, I. (2000). Forest fragmentation truncates a food chain based on an old-growth forest bracket fungus. *Oikos*, 90:119–126.
- Kondoh, M. and Ninomiya, K. (2009). Food-chain length and adaptive foraging. *Proc. R. Soc. B*, 276:3113–3121.
- Laurance, W. F. (2000). Do edge effects occur over large spatial scales? *TREE*, 15:134–135.
- Laurie, H. and Silander, J. A. (2002). Geometric constraints and spatial pattern of species richness: critique of range-based null models. *Divers. Distrib.*, 8:351–364.
- Lawyer, G. (2015). Understanding the influence of all nodes in a network. *Sci. Rep.*, 5:8665.
- Lee, K.-M., Min, B., and Goh, K.-I. (2015). Towards real-world complexity: an introduction to multiplex networks. *Eur. Phys. J. B*, 88:48.
- Leibold, M. A. (1995). The niche concept revisited: Mechanistic models and community context. *Ecology*, 76:1371–1382.
- Leibold, M. A., Holyoak, M., Mouquet, N., Amarasekare, P., Chase, J. M., Hoopes, M. F., Holt, R. D., Shurin, J. B., Law, R., Tilman, D., Loreau, M., and Gonzalez, A. (2004). The metacommunity concept: a framework for multi-scale community ecology. *Ecol. Lett.*, 7:601–613.
- Levine, S. (1980). Several measures of trophic structure applicable to complex food webs. *J. Theor. Biol.*, 83:195–207.
- Levins, R. (1969). Some demographic and genetic consequences of environmental heterogeneity for biological control. *Bull. Entomol. Soc. Am.*, 15:237–240.
- Liao, J., Bearup, D., and Blasius, B. (2017a). Diverse responses of species to landscape fragmentation in a simple food chain. *J. Anim. Ecol.*, 86:1169–1178.
- Liao, J., Bearup, D., and Blasius, B. (2017b). Food web persistence in fragmented landscapes. *Proc. R. Soc. B*, 284:20170350.
- Liao, J., Bearup, D., Wang, Y., Nijs, I., Bonte, D., Li, Y., Brose, U., Wang, S., and Blasius, B. (2017c). Robustness of metacommunities with omnivory to habitat destruction: disentangling patch fragmentation from patch loss. *Ecology*, 98:1631–1639.
- Lomolino, M. V., Riddle, B. R., and J., W. R. (2017). *Biogeography*. Oxford University Press.

- Lotka, A. J. (1932). The growth of mixed populations: Two species competing for a common food supply. *J. Wash. Acad. Sci.*, 22:461–169.
- Lyson, T. R. and Longrich, N. R. (2011). Spatial niche partitioning in dinosaurs from the latest cretaceous (maastrichtian) of north america. *Proc. R. Soc. B*, 278:1158–1164.
- MacArthur, R. and Levins, R. (1967). The limiting similarity, convergence, and divergence of coexisting species. *Am. Nat.*, 101:377–385.
- MacArthur, R. and Wilson, E. O. (1967). *The Theory of Island Biogeography*. Princeton University Press.
- Martin, T., Zhang, X., and Newman, M. E. J. (2014). Localization and centrality in networks. *Phys. Rev. E*, 90:052808.
- Martinez, N. D. (1991). Artifacts or attributes? effects of resolution on the little rock lake food web. *Ecol. Monogr.*, 61:367–392.
- Martinez, N. D. (1992). Constant connectance in community food webs. *Am. Nat.*, 139:1208–1218.
- May, R. M. (1972). Will a large complex system be stable? *Nature*, 238:413–414.
- May, R. M. (1973). *Stability and Complexity in Model Ecosystems*. Princeton University Press.
- McCann, K. S., Rasmussen, J. B., and Umbanhowar, J. (2005). The dynamics of spatially coupled food webs. *Ecol. Lett.*, 8:513–523.
- McKinney, F. K. and Jaklin, A. (2000). Spatial niche partitioning in the cellaria meadow epibiont association, northern adriatic sea. *Cah. Biol. Mar.*, 41:1–17.
- Melián, C. J. and Bascompte, J. (2002). Food web structure and habitat loss. *Ecol. Lett.*, 8:37–46.
- Mougi, A. and Kondoh, M. (2015). Food-web complexity, meta-community complexity and community stability. *Sci. Rep.*, 6:24478.
- Murcia, C. (1995). Edge effects in fragmented forests: implications for conservation. *TREE*, 10:58–62.
- Newman, M. E. J. (2005). Threshold effects for two pathogens spreading on a network. *Phys. Rev. Lett.*, 95:108701.
- Newman, M. E. J. (2010). *Networks: An Introduction*. Oxford University Press.
- Newman, M. E. J. and Ferrario, C. R. (2013). Interacting epidemics and coinfection on contact networks. *PLoS ONE*, 8(8):e71321.

- Olson, D. and Andow, D. (2008). Patch edges and insect populations. *Oecologia*, 155:549–558.
- Pastor-Satorras, R. and Castellano, C. (2016). Distinct types of eigenvector localization in networks. *Sci. Rep.*, 6:18847.
- Pastor-Satorras, R. and Vespignani, A. (2001a). Epidemic dynamics and endemic states in complex networks. *Phys. Rev. E*, 63:066117.
- Pastor-Satorras, R. and Vespignani, A. (2001b). Epidemic spreading in scale-free networks. *Phys. Rev. Lett.*, 86:3200.
- Pastor-Satorras, R. and Vespignani, A. (2002). Epidemic dynamics in finite size scale-free networks. *Phys. Rev. E*, 65:035108.
- Penrose, M. D. (2003). *Random Geometric Graphs*. Oxford University Press.
- Peralta, G., Frost, C. M., Didham, R. K., Rand, T. A., and Tylianakis, J. M. (2017). Non-random food web assembly at habitat edges increases connectivity and functional redundancy. *Ecology*, 98:995–1005.
- Peyras, M., Vespa, N. I., Bellocq, M. I., and Zurita, G. A. (2013). Quantifying edge effects: the role of habitat contrast and species specialization. *J. Insect Conserv.*, 17:807–820.
- Pillai, P., Gonzalez, A., and Loreau, M. (2011). Metacommunity theory explains the emergence of food web complexity. *PNAS*, 108:19293–19298.
- Pillai, P., Loreau, M., and Gonzalez, A. (2010). A patch-dynamic framework for food web meta-communities. *Theor. Ecol.*, 3:223–237.
- Pilosof, S., Porter, M. A., Pascual, M., and Kéfi, S. (2017). The multilayer nature of ecological networks. *Nat. Ecol. Evol.*, 1:0101.
- Pineda, J. and Caswell, H. (1998). Bathymetric species diversity patterns and boundary constraints on vertical range distributions. *Deep-Sea Research II*, 45:83–101.
- Pocheville, A. (2015). The ecological niche: History and recent controversies. In Hems, T., Huneman, P., Lecointre, G., and Silberstein, M., editors, *Handbook of Evolutionary Thinking in the Sciences*, pages 547–586. Springer.
- Polis, G. A. (1991). Complex trophic interactions in deserts: An empirical critique of food-web theory. *Am. Nat.*, 138:123–155.
- Post, D. M. (2002). The long and short food-chain length. *Trends Ecol. Evol.*, 17:269–277.

- Post, D. M., Pace, M. L., and Hairston Jr, N. G. (2000). Ecosystem size determines food-chain length in lakes. *Nature*, 405:1047–1049.
- Prevedello, J. A., Figueiredo, M. S. L., Grelle, C. E. V., and Vieira, M. V. (2013). Rethinking edge effects: the unaccounted role of geometric constraints. *Ecography*, 36:287–299.
- Ries, L., Fletcher Jr., R. J., Battin, J., and Sisk, T. D. (2004). Ecological responses to habitat edges: Mechanisms, models, and variability explained. *Annu. Rev. Ecol. Evol. Syst.*, 35:491–522.
- Ries, L. and Sisk, T. D. (2004). A predictive model of edge effects. *Ecology*, 85:2917–2926.
- Riley, S., Eames, K., Isham, V., Mollison, D., and Trapman, P. (2015). Five challenges for spatial epidemic models. *Epidemics*, 10:68–71.
- Sánchez-Hernández, J., Cobo, F., and Amundsen, P.-A. (2015). Food web topology in high mountain lakes. *PLoS ONE*, 10:e0143016.
- Saunders, D. A., Hobbs, R. J., and Margules, C. R. (1991). Biological consequences of ecosystem fragmentation: A review. *Conserv. Biol.*, 5:18–32.
- Seidman, S. B. (1983). Network structure and minimum degree. *Soc. Netw.*, 5:269–287.
- Skole, D. and Tucker, C. (1993). Tropical deforestation and habitat fragmentation in the amazon: Satellite data from 1978 to 1988. *Science*, 260:1905–1910.
- Sprules, W. G. and Bowerman, J. E. (1988). Omnivory and food chain length in zooplankton food webs. *Ecology*, 69:418–426.
- Thompson, R., Brose, U., Dunne, J., Hall Jr, R., Hladyz, S., Kitching, R., Martinez, N., Rantala, H., Romanuk, T., Stouffer, D., and Tylianakis, J. (2012). Food webs: reconciling the structure and function of biodiversity. *Trends Ecol. Evol.*, 27:689–697.
- Thompson, R., Hemberg, M., Starzomski, B. M., and Shurin, J. (2009). The ubiquity of omnivory. *SIL Proceedings, 1922-2010*, 30:761–764.
- Thompson, R. M., Hemberg, M., Starzomski, B. M., and Shurin, J. B. (2007). Trophic levels and trophic tangles: The prevalence of omnivory in real food webs. *Ecology*, 88:612–617.
- Tilman, D. (1994). Competition and biodiversity in spatially structured habitats. *Ecology*, 75:2–16.
- Vasseur, P. L. and Leberg, P. L. (2015). Effects of habitat edges and nest-site characteristics on painted bunting nest success. *J. Field Ornithol.*, 86:27–40.

- Vitousek, P. M., Mooney, H. A., Lubchenco, J., and Melillo, J. M. (1997). Human domination of earth's ecosystems. *Science*, 277:494–499.
- Volterra, V. (1931). *Leçons sur la théorie mathématique de la lutte pour la vie*. Paris: Gauthier-Villars.
- Warren, P. H. (1989). Spatial and temporal variation in the structure of a freshwater food web. *Oikos*, 55:299–311.
- Williams, R. J. and Martinez, N. D. (2004). Limits to trophic levels and omnivory in complex food webs: Theory and data. *Am. Nat.*, 163:458–468.
- Willig, M. R. and Lyons, S. K. (1998). An analytical model of latitudinal gradients of species richness with an empirical test for marsupials and bats in the new world. *Oikos*, 81:93–98.
- Wimp, G. M., Murphy, S. M., Lewis, D., and Ries, L. (2011). Do edge responses cascade up or down a multi-trophic food web? *Ecol. Lett.*, 14:863–870.
- Wimp, G. M., Ries, L., Lewis, D., and Murphy, S. M. (2019). Habitat edge responses of generalist predators are predicted by prey and structural resources. *Ecology*, 00:e02622.
- Worm, B., Lotze, H. K., and A., M. R. (2003). Predator diversity hotspots in the blue ocean. *PNAS*, 17:9884–9888.
- Zhao, Y., Zheng, M., and Liu, Z. (2014). A unified framework of mutual influence between two pathogens in multiplex networks. *Chaos*, 24:043129.

Curriculum vitae

Kai Uwe von Prillwitz

born on November 3rd, 1989
in Kevelaer (Germany)



Academic education and career

- | | |
|-------------|---|
| since 2019 | Scientific assistant in the group “Dynamical Processes in the Life Sciences” of Prof. Dr. Jens Timmer at the Institute of Physics, University of Freiburg |
| 2016 – 2019 | Scientific assistant and PhD student in the Mathematical Modelling group of Prof. Dr. Bernd Blasius at the Institute for Chemistry and Biology of the Marine Environment, University of Oldenburg
dissertation: <i>Spatial patterns in meta-food-webs: a colonization-extinction model approach</i> |
| 2013 – 2015 | M.Sc. Physics at Albert Ludwig University of Freiburg
master thesis: <i>Statistical aspects of inferring Bayesian networks from marginal observations</i> |
| 2009 – 2013 | B.Sc. Physics at RWTH Aachen University and Albert Ludwig University of Freiburg
bachelor thesis: <i>Contrast in multipath interference and quantum coherence</i> |

Publications

- K. von Prillwitz, Ł. Rudnicki and F. Mintert. Contrast in multipath interference and quantum coherence. *Phys. Rev. A* **92**, 052114 (2015)
- A. Kela, K. von Prillwitz, J. Åberg, R. Chaves and D. Gross. Semidefinite tests for latent causal structures. *IEEE Trans. Inf. Theory*, DOI:10.1109/TIT.2019.2935755 (Early Access, 2019)

Danksagung

An erster Stelle bedanke ich mich bei Bernd für das Ermöglichen und Betreuen dieser Arbeit. Ich hatte einerseits die Freiheit, meine Arbeit selbst zu gestalten und habe mich dennoch nie planlos oder alleingelassen gefühlt. Danke dafür! Mein Dank geht auch an Christoph und Alex für ihr Feedback zu einzelnen Kapiteln dieser Arbeit und an Christoph zusätzlich für einen fantastischen IT-Support. Auch bei der restlichen Arbeitsgruppe bedanke ich mich für anregende Diskussionen während der Gruppenseminare und die äußerst angenehme Arbeitsatmosphäre. Weiterhin gilt mein Dank Thilo, der sich bereit erklärt hat, die Zweitbegutachtung meiner Arbeit zu übernehmen. Darüber hinaus bedanke ich mich bei meinen Eltern, die mich nicht nur während der letzten Jahre, sondern auch schon all die Zeit zuvor in vielerlei Hinsicht unterstützt haben. Ohne sie wäre mein gesamtes Studium vermutlich nicht so reibungsfrei verlaufen. Schließlich bedanke ich mich bei Tatjana, die mir in den letzten Jahren auch den nötigen persönlichen Halt gegeben hat.

Erklärung zur Dissertation

Hiermit versichere ich, dass ich die vorliegende Arbeit unter Berücksichtigung der Leitlinien guter wissenschaftlicher Praxis an der Carl von Ossietzky Universität Oldenburg selbstständig angefertigt und keine anderen als die angegebenen Quellen und Hilfsmittel verwendet habe. Zusätzlich erkläre ich, dass diese Dissertation weder in ihrer Gesamtheit noch in Teilen einer anderen wissenschaftlichen Hochschule zur Begutachtung in einem Promotionsvorhaben vorliegt oder vorgelegen hat und dass im Zusammenhang mit dem Promotionsvorhaben keine kommerziellen Vermittlungs- oder Beratungsdienste in Anspruch genommen worden sind.

Kai Uwe von Prillwitz
Freiburg, im September 2019